Distribution Agreement

In presenting this thesis or dissertation as a partial fulfillment of the requirements for an advanced degree from Emory University, I hereby grant to Emory University and its agents the non-exclusive license to archive, make accessible, and display my thesis or dissertation in whole or in part in all forms of media, now or hereafter known, including display on the world wide web. I understand that I may select some access restrictions as part of the online submission of this thesis or dissertation. I retain all ownership rights to the copyright of the thesis or dissertation. I also retain the right to use in future works (such as articles or books) all or part of this thesis or dissertation.

Signature:

_____ _____

Winston Y. Lee Date

Structure Function Analysis of SIRPα-CD47 Interactions

By

Winston Y. Lee

Doctor of Philosophy
Graduate Division of Biological and Biomedical Science
Immunology and Molecular Pathogenesis

Charles A. Parkos, M.D., Ph.D.
Advisor

Max D. Cooper, M.D.

Aron Lukacher, M.D., Ph.D.

Asma Nusrat, M.D.

Periasamy Selvaraj, Ph.D.

Accepted:

Lisa A. Tedesco, Ph.D.
Dean of the Graduate School

Date

Structure Function Analysis of SIRPα-CD47 Interactions

By

Winston Y Lee
B.S., Duke University, 2001

Advisor: Charles A. Parkos, MD, PhD.

An abstract of
A dissertation submitted to the Faculty of the Graduate School of Emory University
in partial fulfillment of the requirements for the degree of Doctor of Philosophy

Graduate Division of Biological and Biomedical Sciences
Immunology and Molecular Patholgenesis
2008

Abstract

Structure Function Analysis of SIRPα-CD47 Interactions

By Winston Y. Lee

Signal regulatory proteins (SIRPs) are important regulators of innate immune functions, such as, leukocyte migration and phagocytosis. SIRPs, as a paired receptor family, include an inhibitory member (SIRPα) and an activating member (SIRPβ). They are highly homologous in their ectodomains, which consist of a membrane distal IgV fold (D1) and two membrane proximal IgC folds (D2D3). Despite their similarities, only SIRPα but not SIRPβ binds CD47. Furthermore, SIRPαD1 alone is sufficient to mediate CD47 binding. Therefore, we hypothesized that the unique residues in SIRPαD1 account for its specificity to recognize CD47. Using site directed mutagenesis and *in vitro* binding assay, we identified residues in SIRPαD1 that were critical in binding CD47. Mapping these critical residues onto the crystal structure of SIRPαD1 revealed a novel region that is required for CD47 binding that is distinct from the known CD47 binding site. On the other hand, the high degree of homology between the non-ligand binding domains (D2D3) of SIRPα and SIRPβ signifies a conserved theme in structure. SIRPβ is present on cell surface as a dimer linked covalently through a disulfide bond at D3. Although lacking the necessary cysteine in D3, SIRPα may still dimerize through noncovalent interactions. Our biochemical analysis revealed that SIRPα on cell surface can form homodimers *in cis* through noncovalent interactions at each of the three extracellular Ig folds. Notably, in tunicamycin treated cells, SIRPα dimerization but not CD47 binding was inhibited, suggesting that a SIRPα dimer may be bivalent and capable of binding CD47 with increased avidity. Lastly, in adherent neutrophils stimulated with bacterial derived products, dimerization of SIRPα was enhanced. Collectively, these data suggest that *cis* dimerization of SIRPα plays an important role in regulating CD47 binding and function in

leukocytes. A better understanding of the structural basis of SIRPα/CD47 interactions may provide insights into therapeutics targeting pathologic inflammation.

Structure Function Analysis of SIRPα-CD47 Interactions

By

Winston Y Lee
B.S., Duke University, 2001

Advisor: Charles A. Parkos, MD, PhD.

A dissertation submitted to the Faculty of the Graduate School of Emory University
in partial fulfillment of the requirements for the degree of Doctor of Philosophy

Graduate Division of Biological and Biomedical Sciences
Immunology and Molecular Patholgenesis
2008

Acknowledgements

First, I would like to thank my mentor, Chuck Parkos, for the opportunity to work in his lab. He has shown me the importance of perseverance. He has also granted me much freedom in pursuing my own interests. Along the way, I have learned a great deal that cannot be taught through didactic means

Next, I want to express my gratitude to Dominique Weber. As a teacher, she has been instrumental in my scientific education with a particular emphasis on “structure function.” As a friend, she has celebrated with me during the good times, and supported me through the bad times. We shared many memories that I will treasure forever.

The past and present members of Parkos and Nusrat labs, especially, Ingrid McCall, Alex Chin, Rakieb Andargachew, Rita Jen, Eric Severson, Porfi Nava, Keli Kolegraff, Oskar Laur, and Michael Schnoor, not only kindly provided their support in lab but also filled me with many fun memories outside the lab.

During my education here, I found two good friends, Andrew Evans and Sean Stowell—and yes we will continue to share our struggle and success. Also, Mary Horton has been the compass that guides us every step of the way. Without her, I am not sure where I would be right now.

I also would like to thank my committee members, Drs Aron Luckacher, Asma Nusrat, Periasamy Selvaraj, and Max Cooper for their support and encouragement.

I would like to acknowledge Bill Parker and Rob Philibert, who inspired me to take on research as a career.

Lastly, I would like to thank my family, especially my parents, for their incessant and relentless support.

December 2008

Table of Contents

List of Figures

Chapter 4

Chapter 1

Introduction

In response to the selection pressure from pathogens, animals have evolved the immune system—a systemic set of molecular and cellular responses to infection. The immune system recognizes and eliminates the dangerous "nonself" and at the same time preserves "self." When the immune system is unable to efficiently recognize and eliminate a pathogen, the immunodeficient host becomes vulnerable and often succumbs to the ensuing pathogens. On the other hand, if the immune system is reactive to "self" or reacts to the pathogens excessively, autoimmune diseases can occur. In order for the immune system to respond appropriately, the cell surface receptors on an immune cell play a critical role in communicating and organizing external information as intricate sets of positive and negative signals. The subsequent signaling cascades integrate the information and eventually lead to a coordinated response.

Through the studies of leukocyte receptors of the c-type lectin family and the immunoglobulin superfamily, many receptors can be divided into groups according to the high degree of homology in their ectodomains. Within such groups, one receptor can signal through immunoreceptor tyrosine based activation motifs (ITAM), and another carries immunoreceptor tyrosine based inhibitory motifs (ITIM). These groups of receptors are termed "paired receptors," and include Fc receptors as well as signal regulatory receptors (SIRPs) (1, 2). ITAM is a stretch of amino acid residues with a conserved pattern of YxxL/I(X_{6-8})YxxL/I, where x denotes any amino acid residues. With its tyrosine

phosphorylated, ITAM can recruit kinases, like syk or fyn kinases, and results in cellular activation. On the other hand, ITIM, characterized as (S/I/V/L)xYxx(I/V/L), with its tyrosines phosphorylated can recruit src2 homology phosphotases or inisitol phosphotases, which can inhibit the activation signals in cells.

The functions of the paired receptors are not only defined by the presence of ITAM/ITIM, but are also dictated by specificity of the interaction between ligands and the highly homologous ectodomains of the receptors. In some cases, the subtle differences in protein sequences allow the receptors to bind entirely different ligands. In other cases, the paired receptors may share the same ligand but bind with different degrees of affinity (1, 3-6). A classic example is the Fc receptor family. The activating Fc receptor (FcγRI), which has high affinity for IgG, is important in the recognition and initiation of effector functions that results in the elimination of antigenic pathogens. On the other hand, the inhibitory receptor (FcγRIIB), which has low affinity for IgG, is important in preventing the unnecessary effector cell activation that may harm the host (6, 7). The FcRγIIB knockout mice develop autoantibody against self antigens such as DNA, and eventually succumb to glomerulonephritis (6). This dichotomy of functions in the paired receptors is elegantly coordinated to form a circuit that allows for functional and effective responses to IgG and the cognate antigens. Therefore, understanding the molecular details of how the paired receptors interact with ligands can provide insights into physiological functions.

As another example of the paired receptor family, SIRPs are known to be important regulators of myeloid cell functions (5, 8). Understanding the

molecular mechanisms of how SIRPs sense the external stimuli through interactions with cognate ligands will provide important insights into the physiological functions of the paired receptors. In particular, I will explore the nature of interaction between the inhibitory member (SIRPα) and its ligand—CD47 and the changes in the configuration of SIRPα on cell surface as a way to modulate interaction with CD47.

The SIRP family

SIRPs are type I transmembrane glycoproteins that belong to IgSF. The genes encoding human SIRPs are located in a ~470Kb cluster flanked at 5' end by NSFL1 cofactor p47 and at 3' end by beta-neoendorphin-dynorphin preproprotein on chromosome 20.p13. Within the cluster, the genes are distributed in the following order: SIRPβ2, SIRPδ, SIRPβ1, SIRPγ, and SIRPα (8). Between SIRPδ and SIRPα, there is the stretch of 232kb that contains a pseudogene similar to SIRPβ. Among the SIRP genes, only SIRPα, SIRPβ1, and SIRPγ are biochemically well characterized. Therefore, subsequent discussion will be restricted to these SIRPs.

The extracellular portions of the SIRPs are conserved in their structural organizations with a high degree of homology in their protein sequences. The ectodomains of the SIRPs are consisted of a membrane distal Ig variable like (IgV) fold (D1), and two membrane proximal Ig constant like (IgC) folds (D2D3) (5, 8). A notable difference in the ectodomain of SIRPβ is the presence of an additional cysteine in the most membrane proximal domain (D3), which allows

the formation of covalently linked SIRPβ homodimers (9). Although it has been shown that SIRPα does not form covalently linked homodimers, it is not known whether it can form homodimers though noncovalent associations. No studies so far have examined the dimerization of SIRPγ.

As members of the paired receptors, the signaling elements of SIRPs differ greatly. The cytoplasmic tail of SIRPα contains 4 ITIMs, which can recruit Src homology 2 phosphatases (SHP) as well as other Src homology 2 binding adaptors (5, 10). In contrast, SIRPβ and SIRPγ have short cytoplasmic tails that are only a few amino acids long (5, 8). SIRPβ associates with DAP12, an ITAM containing adaptor protein, through charge interaction in the transmembrane regions (11, 12). On the other hand, SIRPγ, lacking known signaling motifs, is thought to be a decoy receptor (13). Consistent with the definition of paired receptors, SIRPα is considered the inhibitory receptor, and SIRPβ the activating receptor.

SIRPα are mainly expressed by neurons and myeloid cells. Among the myeloid cells, high levels of expression in neutrophils, macrophage, monocytes, and dendritic cells have been described with important functional implications; whereas, expression in neurons are mostly defined using *in vitro* culture systems (10, 14-23). SIRPα is also expressed in smooth muscle cells with functional roles in growth factor signal transduction (24, 25). Recently the expression of SIRPα in endothelial cells was reported; however, the functional significance is not known (26). In contrast, the profiles for SIRPβ and SIRPγ are not as well studied due to a paucity of reagents. In the myeloid compartment, SIRPβ are expressed

by neutrophils, monocytes, and macrophage; whereas, SIRPγ has only been shown to be expressed by lymphocytes (9, 11-13).

Ligands of SIRPs

The major cellular ligand for SIRPα is CD47, also known as integrin associated protein (IAP); whereas, the ligand for SIRPβ remains unknown (5, 8). CD47 can bind to SIRPγ as well, *albeit* with lower affinity than SIRPα (13, 27). CD47 is a ubiquitously expressed type I glycoprotein, which can be divided into three structural domains: an IgV fold containing ectodomain, a penta-membrane spanning transmembrane region, and a cytoplasmic tail. The 4 known isoforms of CD47 differ in the length of their cytoplasmic tails (28).

In addition to SIRPα, CD47 is also known to associate with thrombospondin *in trans* and integrins αvβ1 and α2β1 *in cis*. In the *trans* interaction with thrombosopondin, CD47 binds specifically to residues “RFYVVM” on the carboxy terminal cell binding domain. The *cis* interaction with integrins is dependent on cholesterol suggesting that clustering of the transmembrane domains of the integrin and CD47 in the lipid raft is important (28). In either case, both the IgV and the transmembrane domains are necessary for association. Interestingly, αvβ1 integrin can also bind to the RGD motif on thrombosopondin (29). It is not clear whether the association of CD47 with integrins requires the interaction with thrombospondin.

Crosslinking CD47 with high concentrations of thrombospondin or antibodies induces mitochondrial dysfunction, which leads to apoptosis in T

lymphocytes (30-35). In native conditions, CD47 associates with Bcl-2 homology 3 (BH3)-only protein 19 kDa interacting protein-3 (BNIP3) through the transmembrane domains. However, after crosslinking CD47 with antibodies or thrombospondins, the translocation of BNIP3 to mitochondria set off a cascade of signaling events that eventually lead to apoptosis (30).

The first cytoplasmic binding partner of CD47 identified is trimeric G protein (31, 36). Signals transmitted by CD47 through the G proteins were thought to modulate integrin function by inducing an “inside-out” conformational change that can affect cell migration (36, 37). The other intracellular binding partner links CD47 to intermediate filaments and is therefore named “proteins linking IAP to cytoskeleton”, or PLICs (38). PLICs are ubiquitin like proteins that are important in stabilizing γ-aminobutyric acid (GABA) receptors in neurons through a role in facilitating insertion into membrane, assistance in assembly, trafficking, and possibly inhibition of poly ubiquitination (39). However, no studies have yet demonstrated that PLICs regulates CD47 the same way for GABA receptors. Lastly, in red blood cells, CD47 have been shown to associate indirectly with the spectrin actin cytoskeleton (40, 41). However, the specific partners that directly anchor CD47 to the cytoskeleton remain unknown.

Surfactant proteins A (SP-A) and D (SP-D) were the other class of ligands that can bind SIRPα (42). SP-A/D are collectins expressed primarily in the lungs. A monomer of SP-A/D is a ~30-40KD polypeptide and consists of four domains: the N-terminal non-collagenous domain, the collagenous domain, α-helical coiled coil, and the carbohydrate recognition domain (CRD) at C teriminal. The

monomers of SP-A/D assemble through interactions at the collagenous domains into trimers, and can further oligomerize into octadecamers as in SP-A and dodecamers in SP-D. The CRD allows binding of carbohydrate moieties in a calcium dependent manner. In terms of binding to simple sugars, the CRDs of SP-A/D bind mannose and glucose but not galactose (43). In the physiological setting, the multivalencies of SP-A and D confer a high degree of avidity and specificity in binding complex sugars on a variety of fungal, bacterial, and viral pathogens (44). Furthermore, once the collagenous tails interact with calreticulin, the complex can then deliver activation signals through receptor CD91 on monocytes/ macrophages (42, 45). As a result, SP-A and D act as soluble pattern recognition receptors that can effectively neutralize, aggregate, and oposonize pathogens.

Contrary to previous observations, SP-A/D can exert an inhibitory effect on monocytes/ macrophages by binding SIRPα (42, 46). The interaction is mediated specifically through CRDs of SP-A/D as demonstrated by antibody and domain truncation studies (42). In the presence of pathogens, CRDs of SP-A/D would disengage from SIRPα, presumably through competitive inhibition, and bind to the complex sugars on the pathogen, thus preventing the interaction between CRDs and SIRPα and allowing leukocytes to achieve full activation (42, 46). However, it remains unknown how SIRPα bind to SP-A/D. One possibility is that SP-A/D interacts in the same fashion as CD47. Alternatively, SP-A/D can also crosslink SIRPα through N linked glycosylation on the receptor.

Functions of SIRPα

Some of the first hints of SIRPα as an inhibitory receptor on leukocyte came from *in vitro* studies of purified primary leukocytes and leukocyte cell lines. In these studies, inhibition of cellular responses to inflammatory stimuli was observed after ligation of SIRPα with monoclonal antibodies or recombinant soluble CD47 proteins. For instance, ligation of SIRPα on monocytes/ macrophages reduces oxidative burst, cytokine secretion, and phagocytosis (18, 47-49). Perturbation of SIRPα-CD47 interaction with antibodies results in the inhibition of neutrophil migration across intestinal epithelial cells and monocyte migration across blood brain barriers (50, 51). These *in vitro* observations are consistent with *in vivo* experiments using CD47 deficient mice. These mice succumbed to acute bacterial peritonitis due to a delay in leukocyte recruitment and defective effector functions (52). In addition, activation of SIRPα on macrophages by pulmonary SP-A/D in particular has been attributed to the maintenance of alveolar macrophages in a quiescent state during homeostasis (42, 46).

SIRPα activation by CD47 can alter the profile of dendritic cell maturation. A subset of human blood dendritic cells marked by the presence of 6-sulfo LacNAc moieties on P-selectin glycoprotein ligand 1 (PSGL1) spontaneously mature into producers of IL12 and TNF-α under *in vitro* culturing condition (22). Inadvertently, it was found that the presence of CD47 provided by the contamination of RBCs in culture can inhibit the maturation process. This inhibition is negated in the presence of anti-CD47 antibodies suggesting the

involvement of SIRPα-CD47 signaling. In a different study, SIRPα signaling not only arrested the maturation of dendritic cells that were elicited with bacterial products, but also caused the cells to revert to a state functionally resembling immature dendritic cells—namely, poor migratory capacity, high rate of endocytosis, and low capacity of costimulation (23). It has been suggested that this process may have a role in keeping dendritic cells inactive during the resolution of an immune response. However, the underlying signaling mechanisms are still unknown. Taking these studies together, SIRPα is an important negative regulator of myeloid cells.

The investigations of interaction between wild type (WT) myeloid cells and CD47 deficient RBCs provided an important physiological context for the functional roles of SIRPα-CD47 interaction *in vivo.* Murine CD47 deficient RBCs that were transfused into a WT mouse had a much shorter half life than WT RBC controls due to excessive uptake by splenic macrophages (53). In *in vitro* settings, macrophages also phagocytosed significantly more CD47 deficient RBCs. This phenomenon can be reverted if SIRPα on macrophages are crosslinked (18, 49). The presence of CD47 on platelets has also been shown to be important for retention in circulation (54). It was subsequently demonstrated that transfused RBCs exhibited a shorter half life in SIRPα dysfunctional hosts than WT mice (55). Consequently, a hypothesis was put forth that CD47-SIRPα interaction provides a mechanism for the body to recognize and dispose of senescent blood cells, perhaps especially for platelets and RBCs that do not undergo conventional apoptosis. However, the corollary evidence that naturally

senescent blood cells have less functional CD47 has never been clearly demonstrated. Regardless whether SIRPα-CD47 signal is involved in monitoring the senescence of RBCs and platelets, it is clear that tissue CD47 can signal through macrophage SIRPα to provide the “do not eat me” signal.

Consistent with the “do not eat me” model, the interspecies incompatibility between the graft CD47 and the host SIRPα was found to be a possible barrier of xenotransplantation. *In vitro*, the lack of interaction between porcine CD47 and human SIRPα resulted in the spontaneous phagocytosis of the porcine cells by human macrophages (56-58). This phenomenon was inhibited by the addition of soluble human CD47 or the surface expression of human CD47 on porcine cells suggesting the therapeutic potential of manipulating the SIRPα-CD47 interaction (56, 57). In a different study, it was found that the NOD-severe combined immunodeficiency (SCID) mice, which spontaneous develop type I diabetes in non SCID background, can maintain engraftment of human islet beta cells better than the WT-SCID counterparts (59). Through positional cloning, the permissive phenotype was linked to a specific change in the amino acid residues of murine SIRPα. This variant of murine SIRPα was capable of recognizing human CD47. It is likely that the maintenance was achieved through the inhibitory interaction between CD47 of the human graft and SIRPα on murine macrophage.

The “do not eat me” signal provided by SIRPα-CD47 interaction is also important in balancing the “eat me” signal transmitted by the calreticulin-CD91 pathway in order to prevent bystander clearance by macrophages (42, 46). As cells undergo apoptosis, specific markers, such as phosphatidylserine (PS) and

calreticulin were expressed to mediate recognition and clearance by macrophages. Specifically, this process can be initiated by the interaction of calreticulin on the surface of the apoptotic cells with CD91 on macrophages (42). Since calreticulin is an important chaperone in ER in all cells, there are always some levels of expression on cell surface. The fact that viable cells do not get ingested by phagocytes suggests that on viable cells there are other signals counterbalancing the “eat me” signal. Gardai et al showed that CD47 on viable cells can provide the countering “do not eat me” signal through SIRPα on macrophages. As these cells undergo apoptosis, CD47 becomes dysfunctional through unknown mechanisms (46), thereby diminishing the “do not eat me signal,” and clearance ensued as “eat me” signals dominated.

Molecular Anatomy of SIRPαD1-CD47IgV interaction

Given that the SIRPα-CD47 interaction mediates such a multitude of functions, understanding the molecular details of the interaction may lead to the development of novel therapies. Since SIRPα and CD47 are highly glycosylated, the role of N-linked glycosylation in the binding interaction was examined. Using pharmacological inhibitors, site-directed mutagenesis approaches, and refolded recombinant proteins produced in bacteria, SIRPα and CD47 lacking N-linked glycosylations was found to interact in a manner comparable to their wild type counter parts, suggesting that N linked glycosylations are not required (58, 60-63). Previously, we and others have demonstrated through studies using domain truncations and monoclonal antibodies that the membrane distal Ig-V like fold

(D1) of SIRPα is necessary and sufficient to bind the extracellular Ig-V like fold of CD47 in a highly specific manner (9, 51, 63-68). This observation implies that all structural elements necessary for binding to CD47 are contained within D1. Therefore, further analyses probing the binding mechanism of SIRPα and CD47 only needs to focus on structural elements within D1.

Characteristic of paired receptors, SIRPαD1 and SIRPβD1 share a high degree of homology (>95%; **Figure 1-1**) in protein sequences. The observation that only SIRPαD1 binds to CD47 led to an important hypothesis: the unique residues of SIRPαD1 determine its structural specificity (9, 51, 63, 65, 67). This hypothesis dictates that mutagenesis of specific residues would confer a dramatic effect on the binding interaction. Our investigation of this hypothesis is discussed in Chapter 2. Indeed, as demonstrated by a number of site-directed mutagenesis studies, mutagenesis of certain single unique residues (critical residues) can completely abrogate binding to CD47 (63, 67, 69). Without knowing the tertiary structure of SIRPαD1, it was impossible to deduce the role of critical residues in binding interactions by simply examining their distributions according to the primary protein sequence of SIRPαD1.

Recently, the solutions of the crystal structures of human and rat SIRPαD1 were reported in detail (66, 67). A few structural features of human SIRPαD1 (**Figure 1-1;** pdb code: 2UV3) pertinent to this dissertation are highlighted below (67). The structure of SIRPαD1 is a typical IgV fold consisted of two covalently linked beta sheets—with strands A, B, E, and D forming one beta sheet, and strands C, C', F, and G forming the other beta sheet. The two sheets are

covalently linked through a disulfide bond between residues C25 on strand B and C91 on strand F. Notably, the C'' strand typically present in an IgV fold is missing. As a result, the C'D loop along with BC loop, GF loop, and the DE loop formed a region that is structurally homologous to the antigen binding region in an IgV. Also, C'D and DE loop are regions of significant flexibility, implying the possibility of conformational changes. The most prominent feature of the crystal structure was the putative transdimerization of SIRPαD1. The two monomers interact in an antiparallel manner at an interface consisted of A1 strand, B strand, BC loop, and DE loop. However, the transdimers, undetectable under physiological conditions, were not considered to be biologically relevant (66, 67). Using site directed mutagenesis based on the crystal structure, Hatherley et al identified residues critical in binding CD47 to be concentrated in the antigen binding region, especially in the loops (67). On the other hand, site directed mutagenesis of residues unique to SIRPαD1 identified critical residues that mapped to the trandimerization interface (**Figure 2-6)** (63, 66). It is unlikely that the two sites are parts of the binding region simply due the extensive size of the area. Mutations of the critical residues can abolish SIRPα-CD47 interaction through two possible mechanisms. First, mutagenesis of a residue contacting CD47 can disrupt binding directly. Second, mutagenesis of a residue in the maintenance of the conformation can change the positioning of the CD47 contacting residues and abrogate binding indirectly. The mutagenesis studies could not differentiate either possibilities. Therefore, a structural study of the

SIRPα-CD47 complex is necessary to formally demonstrate how these critical residues are involved in the binding interactions.

In a landmark study, Hatherley et al provided an extensive dissection of the molecular interaction between SIRPαD1 and CD47IgV through the comparative analysis of crystal structures of CD47IgV, SIRPβD1, SIRPγD1, and the SIRPαD1-CD47IgV complex (68). Notably, the CD47IgV used in this study contained a mutation of cysteine residue (C15) implicated in anchoring the IgV domain to the second transmembrane helix (28), and the protein was crystallized without the removal of N-linked glycans (68). Given that the crystal structure of CD47IgV alone is a biologically irrelevant dimer with significant change in conformation, we will focus on the CD47IgV structure (**Figure 1-2**) from the crystal structure of SIRPα-CD47 complex. The crystal structure of CD47 IgV domain resembles a typical IgV structure with strand D missing. Strands A, B, and E form a beta sheet that is covalently linked to another beta sheet consisted of strands C, C", F, and G through a disulfide linkage between the cysteines in strands B and F. In place of the strand D is a long C"E loop. The N terminal residue of CD47 was found to be a pyroglutamate as described previously (68, 70). The gross inspection of the SIRPαD1-CD47IgV structure revealed several important features (**Figure 1-3**) (68). CD47IgV interacts with SIRPαD1 at the antigen binding region with 1:1 stochiometry ratio. The conformation of SIRPαD1 and CD47IgV as a complex do not deviate significantly from the conformation of the molecules in the unbound state. The extensive contact between SIRPαD1 and CD47IgV is stabilized mainly through salt bridges and hydrogen bonds (68).

In particular, the FG loop of CD47 IgV protrudes into the groove formed by the BC, C'D, and FG loops of SIRPαD1 accounting for more than half of the contact area (**Figure 1-3 & 1-4)**. In addition, as the other region of major interactions, the pyroglutamate residue at the N terminus of CD47IgV forms polar and hydrophobic interactions with residues on C'D and DE loops of SIRPαD1 (68).

Given that SIRPαD1 but not SIRPβD1 binds CD47, the comparative analysis of SIRPαD1-CD47IgV to SIRPβD1 crystal structures allowed Hatherley *et al* to examine the molecular mechanisms that confer the specificities of ligand recognition between the paired receptors (68). Although the conformations of α-carbon backbones of SIRPαD1 bound to CD47IgV and SIRPβD1 are highly similar, subtle differences in the arrangement of sidechains along the backbones are thought to be critical in preventing CD47 binding to SIRPβ. As shown by us and other, mutagenesis of SIRPα residue V27 to the corresponding SIRPβ residue M27 abrogated binding to CD47 (63, 69). Residue V27 locates in the aforementioned "groove," which interacts with residues on the FG loop of CD47 (**Figure 1-4)**. In the crystal structure of SIRPβD1, the presence of residue M27, an amino acid with bulkier side chain, is thought to cause the side chains of other residues in the groove to adopt a different orientation, thereby preventing interaction with CD47 FG loop (68). However, as shown by us and others, mutagenesis of M27 to V27 in SIRPβ was not sufficient to gain binding to CD47, suggesting that there are additional elements on SIRPβ that can prevent binding to CD47 (63, 69). Through structure analysis coupled with clever site directed mutagenesis, Hatherley *et al* demonstrated that the residues on the FG loop of

SIRPβD1 contained bulkier sidechains, which prevented binding of CD47 through steric hindrance (**Figure 1-5**) (68). Therefore, a mutant SIRPβD1 polypeptide that contains V27 as well as less bulky residues on FG loop is now capable of binding CD47. These observations elegantly illustrate how SIRP paired receptor exhibited high degrees of specificity in binding CD47. Furthermore, these structural studies provide a frame work to deduce how a single mutation of the critical residues can abolish CD47 binding.

Other factors influencing SIRPα-CD47 interaction

The requirements of SIRPα-CD47 interaction have been well established through structural studies and mutagenesis studies. Although less comprehensively investigated, additional mechanisms that can regulate the dynamics of the interaction on cell surface have also been reported. Depending on cell types, the number of SIRPα molecules on cell surface can be regulated. In monocytes/ macrophages elicited with toll like receptor (TLR) agonists, surface SIRPα are internalized or shed as cells are becoming fully activated (71, 72). In contrast, cell surface SIRPα can also be increased by translocation of intracellular granules in activated PMN (51). However, the reason for PMN to regulate SIPRα an inhibitory receptor during activation is still not known. In addition to changing receptor density on cell surface, SIRPα-CD47 interaction appears to be constrained by surface mobility. Capping studies of human leukocytes and human RBC with antibodies, leukocyte SIRPα and RBC CD47 appeared to form microclusters on cell surface, suggesting that they could be

tethered to the cytoskeleton or restricted by membrane microdomains (40, 41, 58, 61, 73). CD47 has been shown to be linked to the cytoskeleton in human RBC; whereas the mechanism for SIRPα clustering is still unknown (40). It has also been subsequently shown that CD47 on RBC and SIRPα on the leukocyte concentrate at the interface between the two cells (41, 58, 73). Intracellularly, SHP1 recruited by SIRPα results in the inhibition of myosin based phagocytosis (73). The increased local receptor and/or ligand densities in microclusters imply a potential avidity effect that can strengthen SIRPα-CD47 interaction at cell-cell contacts. Therefore, it is conceivable that by redistributing SIRPα and CD47 on cell surface, changes in avidity can affect how the two molecules interact.

In addition to clustering by cytoskeletal redistribution or microdomain compartmentalization, cell surface receptors can also cluster to enhance avidity by forming multimers. In the structural studies, although SIRPαD1 is present as a trans dimer in the crystal structures, these soluble SIRPαD1 proteins were never found to be dimers under native condition (66, 67). To date, no study has ever investigated specifically whether SIRPα is capable of forming dimers on cell surface. The comparative analysis of SIRPα and SIRPβ ectodomains provides correlative evidence that support the idea of SIRPα as a *cis* dimer. In a previous study, SIRPβ but not SIRPα has been shown previously to be a covalently linked dimer (9). Specifically, SIRPβ monomers were linked by a disulfide bond at the most membrane proximal domain (D3). However, it is not known whether SIRPα can form a noncovlantly linked dimer. Comparative analysis revealed that SIRPαD2D3 and SIRPβD2D3 are highly homologous. As demonstrated in the

assembly of heavy chain and light chain during synthesis of an immunoglobulin molecule, the monomers must pair up first noncovalently prior to the formation of covalent linkage (74-76). Given the high degree of homology in D2D3 of SIRPα to SIRPβ, SIRPα may dimerize on cell surface through noncovalent interactions. Therefore, in Chapter 3, we will address the roles of the Ig folds in SIRPα dimerization.

Figure 1-1

A.

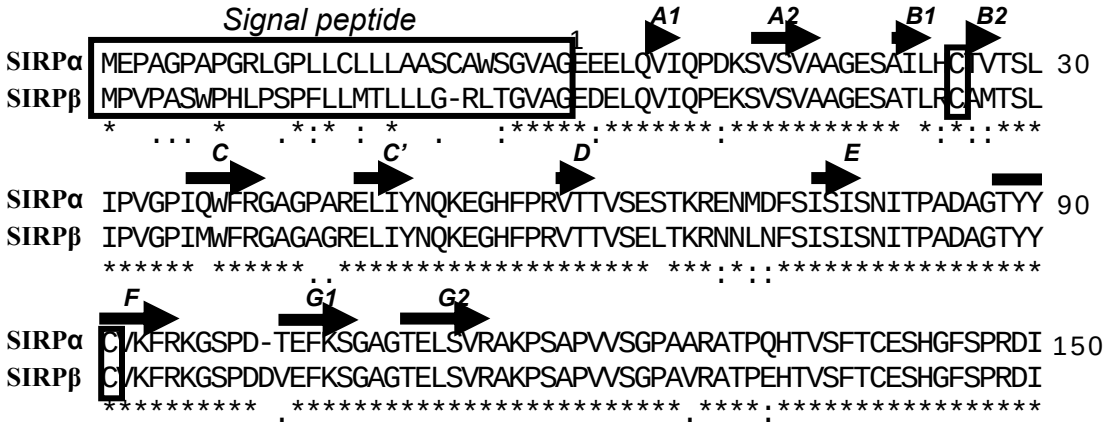
Signal peptide
A1
A2
B1
B2
SIRPα MEPAGPAPGRLGPLLCLLLAASCAWSGVAGEEELQVIQPDKSVSVAAGESAILHCTVTSL 30
SIRPβ MPVPASWPHLPSPFLLMTLLLG-RLTGVAGEDELQVIQPEKSVSVAAGESATLRCAMTSL
C
C'
D
E
SIRPα IPVGPIQWFRGAGPARELIYNQKEGHFPRVTTVSESTKRENMDFSISISNITPADAGTYY 90
SIRPβ IPVGPIMWFRGAGAGRELIYNQKEGHFPRVTTVSELTKRNNLNFSISISNITPADAGTYY
F
G1
G2
SIRPα CVKFRKGSPD-TEFKSGAGTELSVRAKPSAPVVSGPAARATPQHTVSFTCESHGFSPRDI 150
SIRPβ CVKFRKGSPDDVEFKSGAGTELSVRAKPSAPVVSGPAVRATPEHTVSFTCESHGFSPRDI

B.

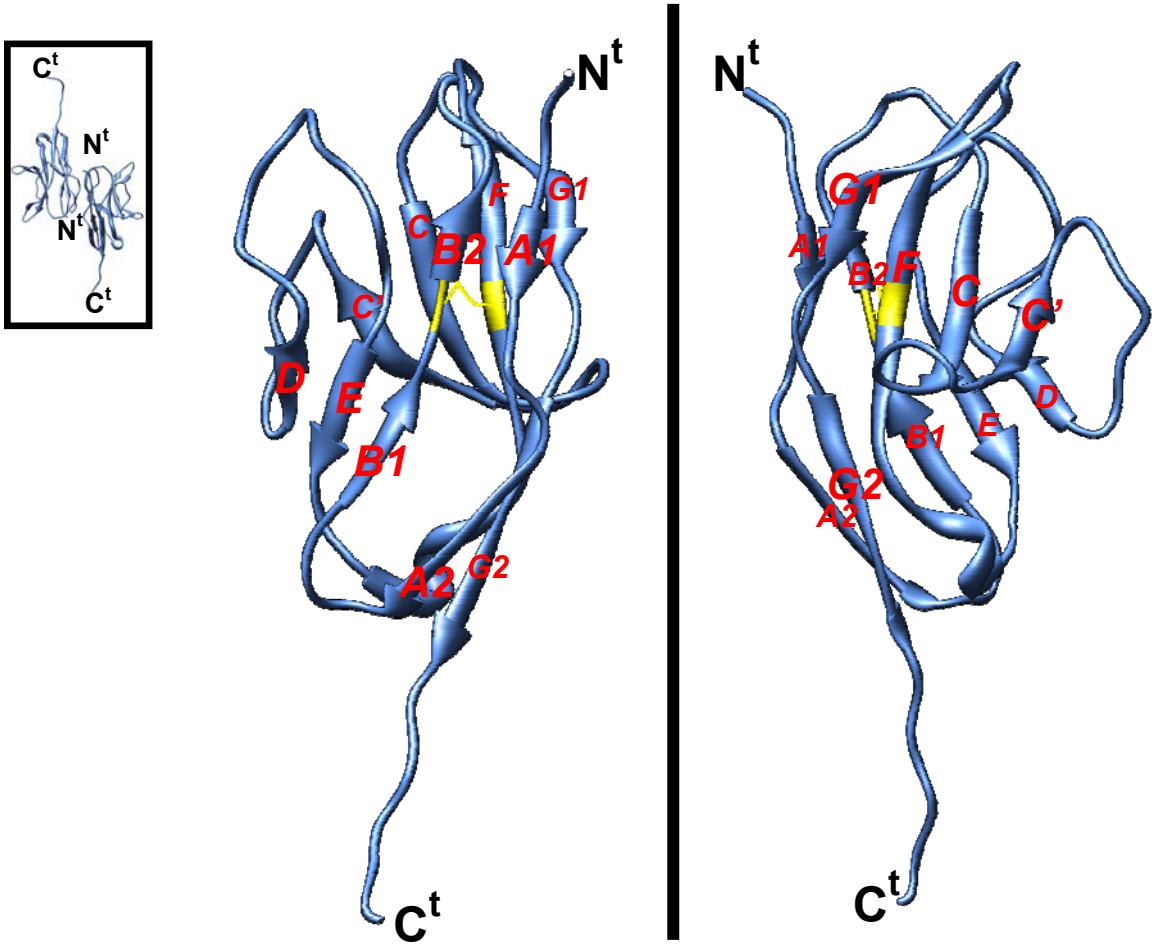
Ct
Nt
Nt
Ct
Nt
F
G1
C
B2
A1
C'
D
E
B1
A2
G2
Ct
Nt
G1
A1
B2
F
C
C'
D
B1
E
G2
A2
Ct

Figure 1-2

A.

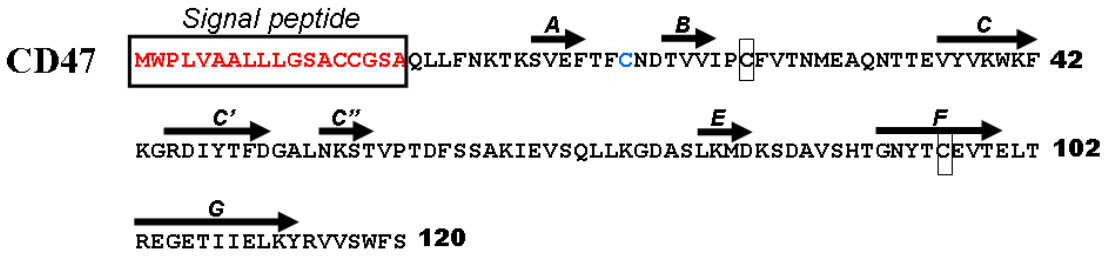
Signal peptide
CD47
MWPLVAALLLGSACCGSAQLLFNKTKSVEFTFCNDTVVIPCFVTNMEAQNTTEVYVKWKF 42
A
B
C
C'
C"
E
F
KGRDIYTFDGALNKSTVPTDFSSAKIEVSQLLKGDASLKMDKSDAVSHTGNYTCEVTELT 102
G
REGETIIELKYRVVSWFS 120

B.

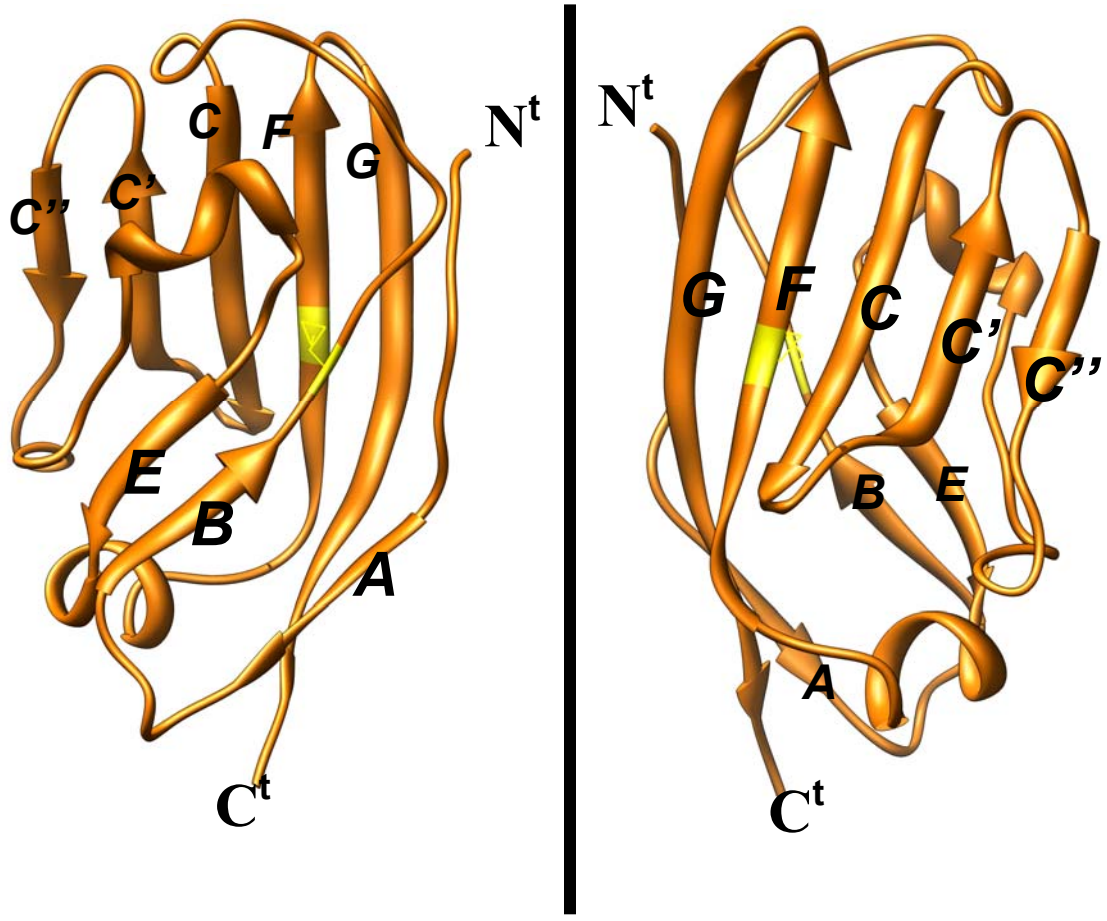
C
F
G
C''
C'
N^t
E
B
A
C^t
N^t
G
F
C
C'
C''
B
E
A
C^t

Figure 1-3
A.

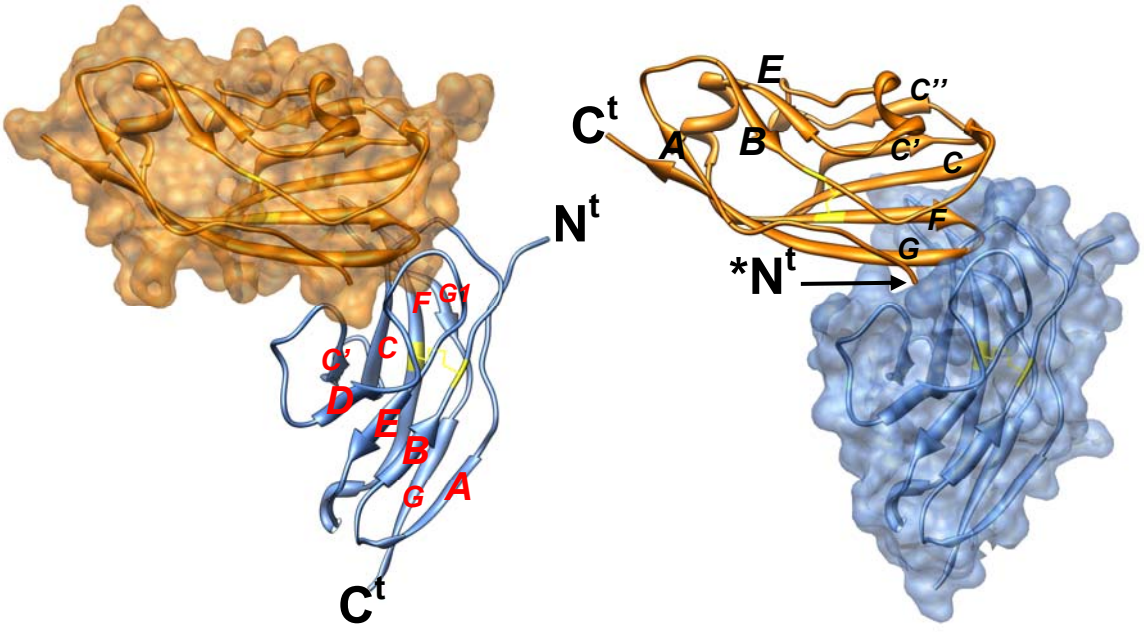

Figure 1-3
B.

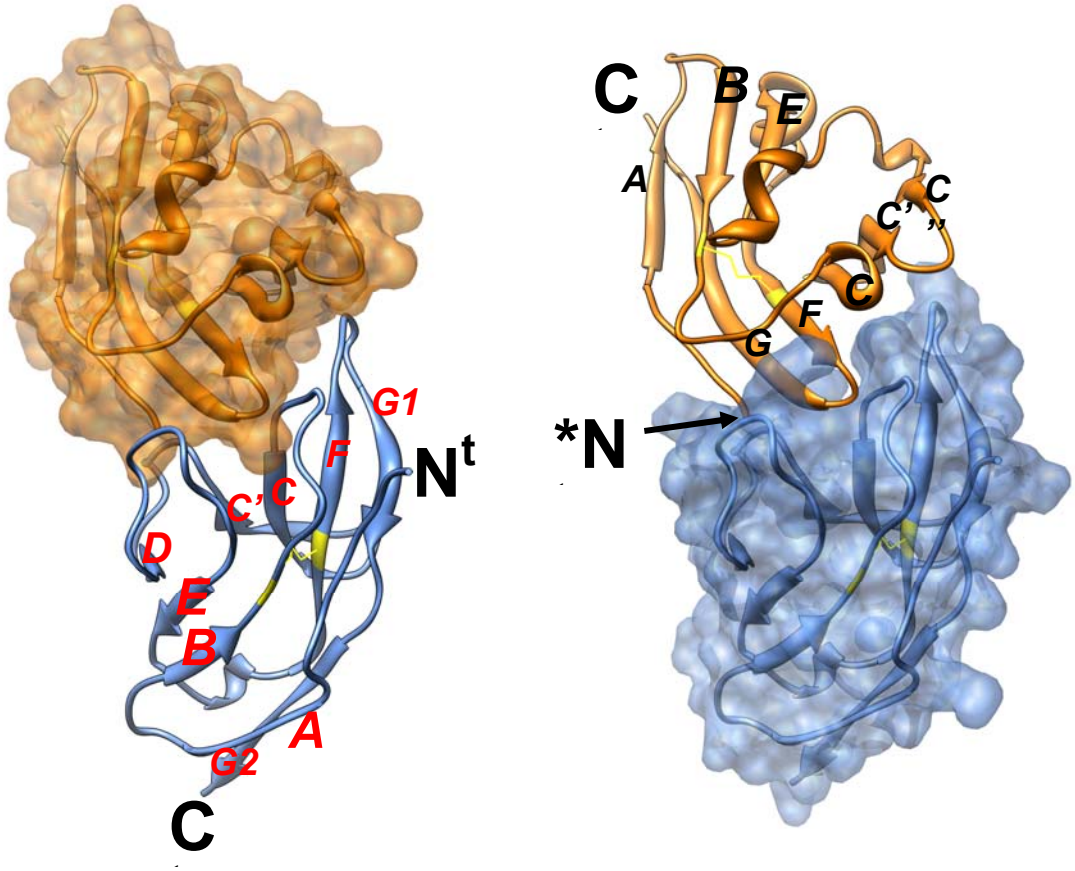

Figure 1-3
C.

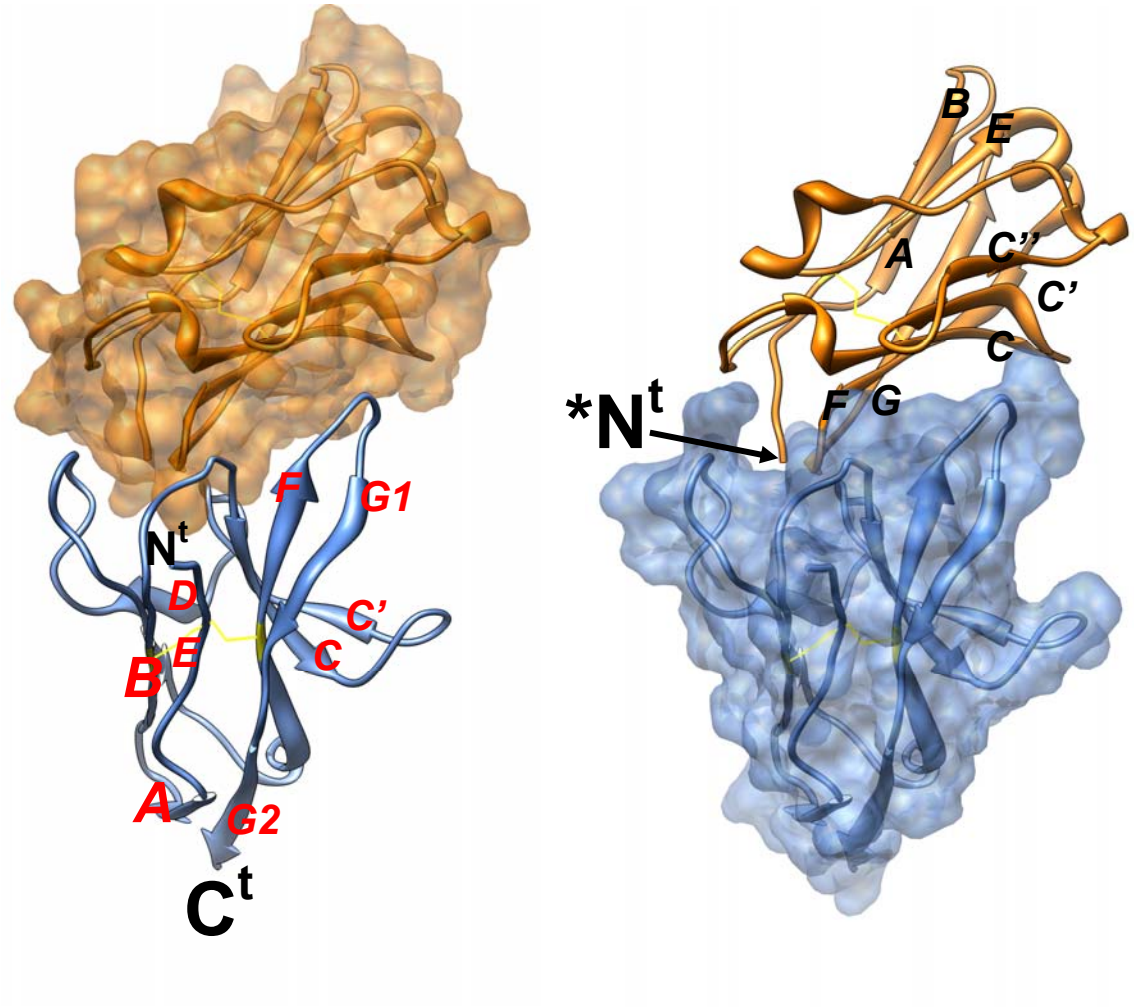

Figure 1-4

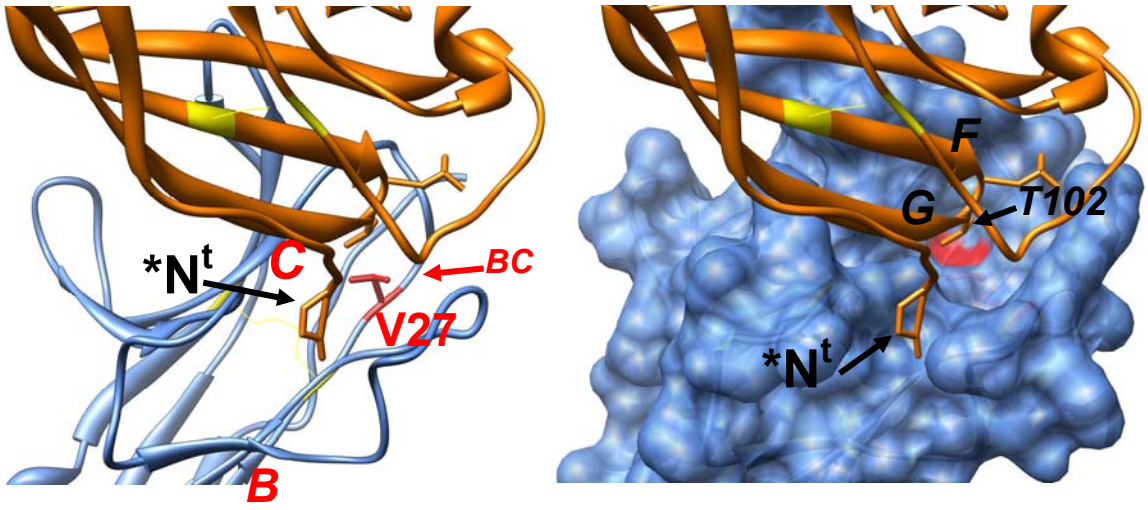

Figure 1-5

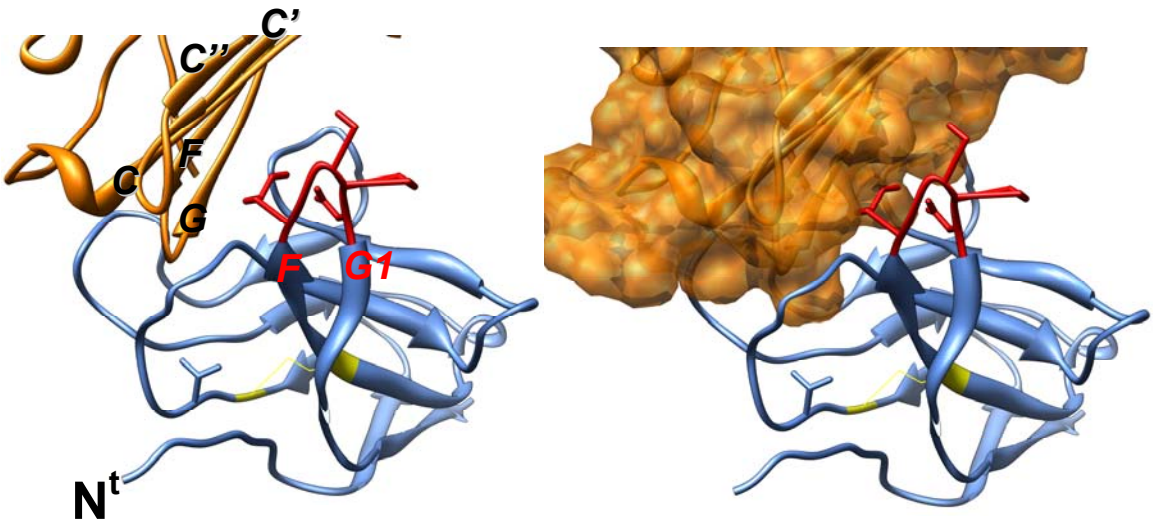

Figure legends

Figure 1-1. The crystal structure of SIRPαD1.

A. Alignment of protein sequences demonstrating the high degree of homology between SIRPαD1 and SIRPβD1. The beta strands are labeled with arrows. Cysteines that form an intramolecular disulfide bond conserved in all Ig structures are boxed. B. The main figures depict two different ribbon diagram views of monomeric SIRPαD1 crystal structure (pdb code: 2UV3). Two beta sheets (strands ABED and strands GFCC') are linked by an intramolecular disulfide bond (yellow). Loops BC, DE, and FG are homologous to an antigen binding region in the variable region of an immunoglobulin. Inset depicts transdimerization of SIRPαD1.

Figure 1-2. The crystal structure of CD47IgV.

A. The protein sequence of CD47IgV is labeled with arrows to indicate beta strands. Cysteines that form an intramolecular disulfide bond conserved in all Ig structures are boxed. The cysteine in blue was mutated in the crystal structure below. B. Two different views of the ribbon diagrams of the CD47IgV crystal structure (pdb code: 2JJT) are displayed. Two beta sheets (strands ABE and strands GFCC'C'') are linked by an intramolecular disulfide bond (yellow). Loops BC, C'C'', and FG are homologous to antigen binding regions in the variable region of an immunoglobulin.

Figure 1-3. The crystal structure of a SIRPαD1-CD47IgV complex.

The structure of a SIRPαD1-CD47IgV complex (pdb code: 2JJT) is displayed in three different views (A, B, & C). Surface rendering (accounting for van der waal radii) are displayed for CD47IgV (orange; left panel) and SIRPαD1 (blue; right panel); otherwise, the left and right panels depicts a SIRPαD1-CD47 complex at the same angle. CD47IgV forms an extensive contact with SIRPαD1 at the region homologous to an antigen binding site in an immunoglobulin. Notice CD47IgV FG loop protrudes into a "groove" like structure that is outline by loop BC, strand C, strand C', loop C'D, and loop DE) SIRPαD1. The N-terminus of CD47IgV is a pyroglutamate residue (*). Disulfide bonds are colored in yellow.

Figure 1-4. The contact between CD47IgV FG loop and the "groove" on SIRPαD1 is a major site of interactions.

The CD47IgV FG loop (orange) protrudes into the groove of SIRPαD1 (blue) as outline by loop BC, strand C, strand C', loop C'D, and loop DE. Mutation of V27 (red) in SIRPαD1 into the corresponding residue M27 in SIRPβ can interfere with residue T102 on the CD47 IgV FG loop and abolish binding with CD47. The left and right panels are identical except for surface rending of SIRPαD1. The difference in the conformation of the "groove," especially the depression in the groove (red) is thought to be one of the mechanisms that prevent SIRPβ from binding CD47. The pyroglutamate (*) at the N terminus of CD47IgV is also a contacting residue.

Figure 1-5. The contact between SIRPαD1 FG loop with the beta sheet (strands GFCC'C") is permissible for binding.

The comparative analysis of a SIRPαD1-CD47IgV complex structure with a SIRPβD1 structure by Hatherley et al revealed the FG loop (orange) of SIRPαD1 (blue) contains less bulky residues than the FG loop of SIRPβD1, thereby avoiding steric hindrance that prevents binding of SIRPβD1 with CD47IgV.

Chapter 2

Novel structural determinants on SIRPα that mediate binding to CD47

Abstract

Signal regulatory proteins (SIRP-α, -β, and -γ) are important regulators of several innate immune functions that include leukocyte migration. Membrane distal (D1) domains of SIRPα and SIRPγ, but not SIRPβ, mediate binding to a cellular ligand termed CD47. Since the extracellular domains of all SIRPs are highly homologous, we hypothesized that some of the 16 residues unique to SIRPα.D1 mediate binding to CD47. By site-directed mutagenesis, we determined that SIRPα binding to CD47 is independent of N-glycosylation. We also identified three residues critical for CD47 binding by exchanging residues on SIRPα with corresponding residues from SIRPβ. Cumulative substitutions of the critical residues into SIRPβ resulted in *de novo* binding of the mutant protein to CD47. Homology modeling of SIRPα.D1 revealed topological relationships among critical residues and allowed the identification of critical residues common to SIRPα and SIRPβ. Mapping these critical residues onto the recently reported crystal structure of SIRPα.D1 revealed a novel region that is required for CD47 binding that is distinct and lateral to another putative CD47 binding site described on that crystal structure. The importance of this lateral region in mediating SIRPα.D1 binding to CD47 was confirmed by epitope mapping analyses of anti-SIRP antibodies. These observations highlight a complex nature of the ligand

binding requirements for SIRPα that appear to be dependent on two distinct but adjacent regions on the membrane distal Ig loop. A better understanding of the structural basis of SIRPα/CD47 interactions may provide insights into therapeutics targeting pathologic inflammation.

Introduction

Neutrophil (PMN) migration across mucosal surfaces, while necessary for host defense, is a central component of disease pathophysiology in many inflammatory conditions. For example, severity of patient symptoms in conditions such as ulcerative colitis and bronchitis/cystitis correlates with the degree of PMN infiltration across mucosal epithelium (77). Previous studies have established that PMN migration across intestinal epithelial monolayers is a complex process involving sequential receptor ligand interactions between PMN and epithelial cells (16). CD47, an ubiquitous transmembrane protein, has been shown to regulate the rate of PMN transmigration across cell monolayer and matrix. The physiological importance of CD47 is apparent from studies employing knockout mice which rapidly succumb to *E. coli* peritonitis due to delayed recruitment of PMN at the site of infection (52). These *in vivo* observations are consistent with *in vitro* studies demonstrating a delayed PMN transepithelial migration in the presence of anti-CD47 antibodies (78, 79). New insights into the function of CD47 came with the identification of its cellular ligand SIRPα.

SIRPα is a transmembrane glycoprotein belonging to the immunoglobulin superfamily (IgSF). Other members of the SIRP family include SIRPβ and SIRPγ. The extracellular regions of the SIRPs are highly homologous and consist of three Ig-like loops (5, 8). The most membrane distal loop contains an IgV domain, whereas the two membrane proximal loops contain IgC domains. Interestingly, an isoform of SIRPα that lacks the two membrane proximal IgC domains has been described in monocytes (21). In contrast to CD47, the expression of SIRPα

is restricted to leukocytes, neurons, and muscle cells (10, 14, 80). Recently, our laboratory has demonstrated that SIRPβ is expressed as a homodimer with a disulfide link between the most membrane proximal Ig loops (9).

In addition to a role in regulating PMN migration, SIRPα-CD47 interactions also mediate negative regulation of several monocyte/macrophage functions. For example, CD47 deficient RBCs are rapidly phagocytosed by splenic macrophages when infused into normal mice due to the absence of CD47-SIRPα generated inhibitory signals that serve to dampen phagocytosis (53). Similar mechanisms are presumed to mediate autoimmune haemolytic anemia (81, 82). The SIRPα-CD47 interaction has also been shown to play a similar role in platelet homeostasis (54, 83). Additional evidence comes from *in vitro* studies demonstrating that ligation of SIRPα with CD47 fusion proteins or anti-SIRPα antibodies results in inhibition of macrophage/monocyte phagocytosis and oxidative burst (18, 49, 54, 57). Furthermore, SIRPα-CD47 interactions have been shown to be crucial in regulating macrophage-mediated clearance of apoptotic cells (42, 46). As highlighted above, several studies have demonstrated that SIRPα has negative regulatory properties, and such inhibitory signals are mediated by immunoreceptor tyrosine inhibitory motifs (ITIM) present in the cytoplasmic domain. In contrast, SIRPβ has been shown to have positive regulatory functions by virtue of the ability to recruit immunoreceptor tyrosine activating motif (ITAM) binding adaptors. SIRPγ is unable to recruit any signaling adaptors and may act as a decoy receptor (5, 8).

A number of studies have provided clues to the structural requirements of SIRPα binding to CD47. Previously, we and others demonstrated that the membrane distal Ig loop of SIRPα binds to the Ig-like extracellular loop of CD47 in a specific manner (51, 64, 65). Importantly, the highly homologous SIRPβ, does not bind to CD47 (51). Several other reports suggest that glycosylation plays a role in regulation of the affinity of binding of SIRPα to CD47, however the conclusions have been contradictory (58, 60-62).

In an attempt to define the CD47 binding site on SIRPα, we took advantage of the high degree of homology between SIRPα and SIRPβ. Through mutagenesis of residues in SIRPα followed by analyses of mutant proteins binding to CD47, structural modeling and additional mutagenesis, we have defined a region on the membrane distal Ig loop of SIRPα that mediates binding to CD47. By mapping critical residues identified in this study on the recently reported crystal structure, we delineate a CD47-binding region on the lateral surface of the membrane distal domain of SIRPα that is distinct from the CD47 binding site recently deduced by Hatherley et al (67). The importance of this region in mediating binding to CD47 is further supported by epitope mapping analyses of anti-SIRP monoclonal antibodies. The significance of these findings with respect to the recently reported crystal structure is discussed.

Materials and Methods

Antibodies

SIRPα and SIRPβ binding monoclonal antibodies SE7C2 and B4B6 (BD Biosciences), affinity purified goat polyclonal anti-GST antibodies (GE-Amersham), horseradish peroxidase (HRP) conjugated goat anti-mouse IgG, HRP conjugated anti Rabbit Fc and HRP conjugated donkey anti-goat IgG (Jackson Immunolab) are all commercially available. J10.1 is a murine monoclonal antibody against Jam-A, and was used as an IgG1 isotype control (84). SAF10.1 is a murine monoclonal antibody produced in our laboratory against human SIRPα, crossreacts with other SIRPs and recognizes an epitope in the membrane most distal domain (D1). SAF10.1 (IgG1) was generated by immunizing female BALB/c mice intraperitoneally with an eukaryotically expressed SIRPα-Fc fusion protein consisting of the extracellular domain and emulsified with complete Freund's adjuvant (Sigma), and followed by 2 subsequent boosts of SIRPα-Fc fusion protein emulsified with incomplete Freund's adjuvant (Sigma). The mouse with the highest antibody titer was given a final intravenous boost with SIRPα-Fc and splenocytes were harvested and fused with P3U1 myeloma cells four days later. Fused cells were then cultured in selection media containing DBA-2 feeder thymocytes as described previously (78). Supernatants of hybridoma colonies were screened by ELISA. Positive colonies were subcloned by limiting dilution and weaned from selection media. The antibody was purified using Protein A-Sepharose (Sigma) from culture supernatant. The protocol used in mouse experiments in this study is approved

by Institutional Animal Care and Use Committee (IACUC) at Emory University, Atlanta GA.

Generation and mutagenesis of GST/ Fc tagged full-length and truncated SIRP plasmid constructs

The generation of constructs encoding rabbit Fc, GST tagged full-length and truncated extracellular regions of SIRP have been described previously (51). The cDNA sequence of SIRPα used in this study corresponds to GeneBank entry BC 029662.1, and the cDNA sequence of SIRPβ corresponds to NM 006065. To simplify the fusion of GST tags, we made a modified pcDNA3 (Invitrogen) vector by inserting GST from pGEX4T1 (Invitrogen) into a multicloning site leaving HindIII and BamHI (New England Biolab) restriction sites available for subsequent insertions of DNA fragments (pcDNA3GSTmod). Site-directed mutations were introduced by overlap extension using PCR and complementary primers carrying the mutation (85). Forward and reverse end primers contained HindIII and BamHI restriction sites respectively, so that the resultant products could be inserted into pcDNA3GSTmod. All constructs were fully sequenced.

Production of recombinant SIRPs

COS 7.2 cells (ATCC) were cultured in DMEM high glucose supplemented with 10% heat inactivated fetal bovine serum and supplements in 5% CO_2 at 37°C. Transient transfections of COS 7.2 with SIRP plasmids were performed by a DEAE-Dextran (GE-Amersham)-based method (86). Briefly, the day before

transfection, COS 7.2 cells were seeded onto a 60 mm Petri dishes (Costar; $0.4x10^6$ cells per dish). The following day, after washing cells in serum free medium, 2 ml of serum free DMEM containing 500µg DEAE-Dextran, 2µg of DNA, and 0.1mM chloroquine was added and incubated for 4 hours in 5% CO_2 at 37°C. Cells were shocked with 2ml of 10%DMSO (Sigma) in serum free DMEM for 2 minutes at room temperature (RT) and further cultured in 4ml of DMEM 10% FCS for 3-4 days. Protein production was assessed by dot blot and ELISA. For dot blots, 5 µl of cell culture supernatants from each transfection were spotted onto a nitrocellulose membrane and allowed to air dry. The nitrocellulose membrane was blocked with a 5% milk/TBS solution for 1 hour, incubated with anti-GST, followed by incubation with donkey anti-goat-IgG HRP. Washed blots were developed using a peroxidase chemiluminescence kit from Roche.

To assess recombinant protein in cell culture supernatants, ELISAs were also performed. Microtiter wells (Immulon II) were coated with goat anti-GST or anti-Rabbit Fc, each at 10µg/ml in PBS overnight at 4°C. After blocking with 1% BSA/TBS and washing in TTBS, supernatants from transfectant cultures were added for 1 hour at RT to capture recombinant proteins. After washing, an anti-pan SIRPα mAb SAF10.1 was added for 1 hour, followed by washing and addition of goat anti mouse IgG-HRP. Color was developed with 2,2'-azino-bis(3-ethylbenzthiazoline-6-sulphonic acid (ABTS, Sigma) and absorbance measured at 405nm.

Immunoblotting of recombinant proteins

Ten microliters of media containing recombinant proteins were boiled in 1x sample buffer under reducing conditions and separated using SDS-polyacrylamide gel electrophoresis (SDS-PAGE) followed by transfer to PVDF membranes (BioRad). Nonspecific binding was blocked in 5% milk in TBS. Rabbit-Fc tagged proteins were detected with HRP conjugated polyclonal anti rabbit IgG antibodies, and GST tagged proteins were detected with affinity purified polyclonal goat anti-GST followed by HRP conjugated polyclonal donkey anti-goat IgG antibodies. Blots were developed using a chemiluminescence kit from Roche.

In vitro binding assay of SIRP and CD47

A modified version of a previously described assay (51) was used in this study. Briefly, affinity-purified polyclonal goat anti-GST antibody or goat-anti-rabbit-Fc was added to microtiter wells (Immulon II) and incubated overnight at 4°C. After blocking with 1% BSA in PBS and washing with TTBS, cell culture supernatants of COS 7.2 transfectants were added to the plates to allow the capture of recombinant proteins for 1hour at RT. Wells were washed with TTBS and cell culture supernatant containing CD47-AP was added for 1 hour. After washing, binding to SIRP proteins was assessed colorimetrically using *p*-nitrophenyl phosphate (PNPP, Sigma) at 405nm.

For antibody inhibition assays, following capture of recombinant SIRP proteins in microtiter wells as above, 10µg/ml of SE7C2 or B4B6 in 1%BSA/PBS was added

for 1 hour at RT. After washing, CD47-AP was added and binding assessed as described as above.

Homology Modeling of SIRPα

A comparative analysis of the membrane distal domain of SIRPα to a database of known protein crystal structures was performed using the Reverse Position Specific Basic Local Alignment Search Tool (RPS-BLAST) search engine (87). An Fv fragment of an antibody (protein data base code 1MFA; (88)) identified to be most homologous to SIRPα.D1 (16% identical residues and 49% conserved residues) was chosen as the template for homology modeling. An alignment of SIRPα.D1 to 1MFA generated by RPS-BLAST was used by MODELLER (89) to obtain a preliminary homology model. The model was then visually inspected and optimized using Sybyl (Tripos). For each step of optimization, the alignment of the protein sequences was first adjusted followed by generation of a new homology model. Improvement in the modeled structure was assessed through a decrease in Discrete Optimized Protein Energy (DOPE) as evaluated by MODELLER (90). Molecular graphics images were produced using the UCSF Chimera package from the Resource for Biocomputing, Visualization, and Informatics at the University of California, San Francisco (supported by NIH P41 RR-01081(91).

Structural alignment of SIRPs

The SIRPα crystal structure (pdb id: 2uv3) and the SIRPβ NMR structure (pdb id: 2d9c) were obtained from the RCSB Protein Data Base (www.pdb.org). The structures were aligned using the MatchMaker function in Chimera (92). Matching was iterated by pruning long atom pairs until no pairs exceeded 1 angstrom. The matching alignment between SIRPα crystal structure and SIRPβ NMR structure (conformation #0.1) is shown in **Figure 2-8**.

Results

The most membrane-distal Ig loop (D1) of SIRPα binds to CD47.

Using an *in vitro* binding assay, we and others have shown previously that the extracellular region of SIRPα specifically interacts with the Ig loop of CD47 (51, 64, 65). The extracellular region of SIRPα consists of three domains with classic Ig folds. In this study, we have modified our *in vitro* binding assay (see Materials and Methods). The recombinant SIRPs were captured onto a plate coated with anti-GST or anti-Fc antibodies instead of coating the microtiter plates with purified recombinant proteins. To validate the modified *in vitro* binding assay, we verified the previous findings that the most membrane distal loop of SIRPα mediates the binding to CD47 (64, 65, 69). We produced tagged fusion proteins containing full-length and truncated extracellular regions of SIRPα. Specifically, we produced soluble rabbit Fc tagged fusion proteins containing only the most membrane-distal loop (**SIRPα.D1-Fc;** residues 1 to 133), the two membrane-proximal loops (**SIRPα.D2D3-Fc;** residues 1 to 33 fused with residues 131 to 366), or the most membrane-proximal loop (**SIRPα.D3-Fc;** residues 1 to 33 fused with residues 227 to 336), as well as the full-length extracellular region of SIRPα (**SIRPα.D1D2D3-Fc;** residues 1 to 366) (**Figure 2-1A**). Using the *in vitro* binding assay, only **SIRPα.D1D2D3-Fc** and **SIRPα.D1-Fc** bound to CD47 (**Figure 2-1C**). We also produced the following GST fusion proteins: **SIRPα.D1D2D3-GST** and **SIRPα.D1-GST**. Given that SIRPβ does not bind to CD47 (51, 65), we generated **SIRPβ.D1D2D3-GST** and **SIRPβ.D1-GST** to be used as negative controls (**Figure 2-1B**). Consistent with the results obtained using Fc-tagged proteins,

only fusion proteins containing SIRPα.D1 bound to CD47 (**Figure 2-1D)**. As detailed in the Materials and Methods section, all cell culture supernatants were assessed both by dot blots and capture ELISAs to ensure that a lack of CD47 binding was not due the absence of recombinant SIRPs (data not shown). As shown in **Figure 2-1**, our modified assay was able to confirm that the most membrane distal Ig loop of SIRPα contains the domain that interacts with CD47. Therefore, we conclude that the assay modification does not alter our binding measurements.

Comparative analysis of protein sequences of SIRPα.D1 and SIRPβ.D1.

As shown in **Figure 2-1D**, CD47 interacts with SIRPα.D1 but not with SIRPβ.D1, despite the fact that SIRPα and SIRPβ are highly homologous (10, 65, 69). In an attempt to characterize the CD47 binding site on SIRPα, we aligned the protein sequences of SIRPα.D1 and SIRPβ.D1 using CLUSTALW to investigate the differences between the two molecules (93). As illustrated in **Figure 2-2**, the two sequences are highly homologous IgV loops that share 89% identity and differ only at 16 positions, of which 12 are conservative substitutions and 4 are non-conservative substitutions. As defined by the N-X-S/T motifs, there are two potential glycosylation sites at positions N73 and N80 in SIRPβ.D1; whereas there is only one potential glycosylation site at N80 in SIRPα.D1 (**Figure 2-2**). We reasoned that the presence of a carbohydrate moiety at N73 in SIRPβ may introduce a spatially bulky domain that might interfere with the binding to CD47. We substituted N73D in SIRPβ to eliminate the putative carbohydrate

moiety at that position. As shown in **Figure 2-3**, the resultant SIRPβ mutant did not bind to CD47. Conversely, the lack of the carbohydrate moiety at D73 in SIRPα could have allowed binding to CD47. We substituted D73N to introduce a potential neoglyclosylation site in SIRPα and observed that the SIRPα mutant still bound to CD47 (**Figure 2-3**). It has been reported that SIRPα can be differentially glycosylated in tissues and the degree of glycosylation may affect its affinity to CD47 suggesting that the sugar moiety at N80 in SIRPα may also play a role in the interaction (60, 62). Therefore, we generated a SIRPα mutant (N80A) and a SIRPβ double mutant (N73D/N80A) in order to eliminate all potential N-linked glycosylation sites. As shown in **Figure 2-3**, the SIRPα mutant did not lose binding to CD47 and the SIRPβ mutant did not gain the ability to bind CD47. Taken together, these data suggest that N-linked glycosylation of SIRPα is not required for binding to CD47.

Analyses of the role of disparate residues between SIRPα.D1 and SIRPβ.D1 in mediating binding to CD47

Since we did not observe a role of glycosylation in binding of SIRPα.D1 to CD47, we reasoned that residues of SIRPα.D1 not present in SIRPβ.D1 must be important for binding to CD47. To test this hypothesis, we swapped the disparate residues in SIPRα.D1 with the corresponding residues in SIRPβ.D1 one at a time through site-directed mutagenesis. These SIRP residues are boxed with solid lines in **Figure 2-2**. Mutations: V27M, Q37M, and P44A/A45G were first introduced into the SIRPα.D1.Fc construct; and later the mutations: S66L, E70N,

M72L, and +D101 (insertion of Asp at position 101) were introduced into SIRPα.D1.GST (**Figure 2-2**). Among the SIRPα-Fc mutants, substitutions at V27M and Q37M completely abolished binding to CD47; whereas the substitutions at P44A/A45G had no effect (**Figure 2-4A**). Among the SIRPα-GST mutants, substitutions at S66L eliminated binding to CD47; whereas at M72L retained binding to CD47. Insertion of Asp at position 101 (+D101) in SIRPα.D1-GST had no effect (**Figure 2-4B**). CD47 binding experiments using full-length wild type and mutant SIRPα proteins expressed on the surface of transfected CHO cells yielded similar results (data not shown). These data suggest that residues V27, Q37, and S66 play important roles in binding SIRPα to CD47 and will be referred to as “critical residues.” Conversely, we will refer to amino acids that can be substituted without altering binding as “non-critical residues.”

The data in **Figure 2-4** demonstrate that substitution of a single critical residue in SIRPα can abolish binding to CD47. In a complementary fashion, SIRPβ mutants carrying incomplete sets of reverse substitutions of SIRPα critical residues could be viewed as equivalent to a SIRPα mutant carrying one or more critical mutations. We reasoned that in order for SIRPβ to gain the ability to bind to CD47, it would be necessary to replace cumulatively all residues that correspond to the critical residues in SIRPα. Indeed as shown in **Figure 2-4C**, when these mutations were introduced singly and in combinations, no binding to CD47 was observed except for the recombinant protein carrying all the critical mutations. Thus, these data serve to identify all of the nonconserved residues that are necessary for SIRPα binding to CD47.

Homology modeling of SIPRa.D1 reveals the topological relationships of critical residues and identifies a region critical for CD47 binding.

Changes in critical residues that abrogated the interaction with CD47 could result from two mechanisms. First, such residues could participate in direct binding interactions with CD47. Second, some of these residues could be necessary for maintaining structural integrity of SIRPs by affecting tertiary structures. In this latter possibility, amino acid substitutions would indirectly alter SIRP binding with CD47. To explore these possibilities, we performed detailed structural modeling studies in order to gain insight into the localization of critical residues in the tertiary structure of SIRPα. At the time of this study the crystal structure had not been solved, and we proceeded to construct a structural model of SIRPα.D1 using homology modeling techniques. Using the RPS-BLAST search engine (87), the structure of SIRPα.D1 was identified to be homologous to a pre-clustered IgV family (CD00099; PSSMID 28982). Members of this family that share homology to SIRPα.D1 can be broadly divided into immunoglobulins (1MFA, 1ADQ, 1NFD, and 1C5D) and T cell receptors (1J8H, 1FYT, 1AO7, and 1BWM). Among these structures, 1MFA was identified to be most similar to SIRPα.D1. 1MFA is a crystal structure of the Fv fragment of an antibody in a complex with a carbohydrate antigen (88). The alignment of SIRPα.D1 and 1MFA by MODELLER demonstrates that 16% of the residues are identical and 49% are conserved. A model was constructed using MODELLER and visually optimized using SYBYL for aberrant folding or unusual residue interactions.

The modeling studies predict that the SIRPα.D1 IgV fold begins at residue E1 and ends at P118 with a disulfide linkage occurring between C25 and C91. Interestingly, the model predicts that critical residue Q37 is located within the hydrophobic core adjacent to the disulfide bond, whereas the other two critical residues V27 and S66 are positioned near each other on a protein surface opposite to the plane containing Q37 (**Figure 2-5A**). The model also predicts that non-critical residues P44/A45 and +D101 are distant to the critical residues, while residues M72 and E70 are positioned close to the critical residues. Taken together, these mutagenesis and modeling data suggest that critical residues V27 and S66 form part of a region that may play an important role in the interaction with CD47.

Identification of critical residues that are common to SIRPα and SIRPβ

Since our model predicted that several critical residues were clustered into a distinct region, we tested the possibility that additional residues in the region containing V27 and S66 may be involved in the interaction with CD47. The selected residues (Q8, H24, T26, S75, S66, R69, E70, and V27) are marked with * on our homology model (**Figure 2-5A**), and are also highlighted in the primary sequence using boxes with dashed and solid borders (**Figure 2-2**). Among these residues, we have already shown that V27 and S66 are critical residues (colored in red in Figure5A), and E70 is a non-critical residue (colored in green in Figure 5A). Since the substitution of M72L is highly conserved, the replacement of M72 with nonconserved residues, such as arginine and alanine, might help define the

role of M72. Neither M72L (**Figure 2-4B**) nor M72R (**Figure 2-5B**) abrogated the binding to CD47. In contrast, the substitution of M72 with alanine abolished the binding to CD47 (**Figure 2-5B**). These data suggest that the physical presence of a medium sized sidechain at residue 72 has an important role in the interaction with CD47.

We applied a similar approach to test whether other candidate residues are important for binding by replacing them with residues not conserved in size, polarity or charge. Using SIRPα.D1.GST as a template, the following mutants were made: Q8L, H24N, H24L, T26A, R69A, R69E, and S75L (**Figure 2-5B)**. Nonconserved substitutions Q8L, T26A, R69A, and, S75L completely abrogated binding to CD47. Conversely, mutations H24L or H24N had no effect on SIRPα binding to CD47. These results lend strong support to the idea that the region on SIRPα.D1 containing Q8, T26, V27, S66, R69, M72, and S75 plays an important role in binding CD47.

The lateral surface of SIRPα.D1 is important in binding CD47.

Recently Hatherley et al reported the solution of a SIRPα.D1 crystal structure and the identification of a CD47 binding site deduced through homology comparison, site directed mutagenesis, and antibody studies (67). Since only two of our critical mutations overlap with their findings (S66 and R69), we proceeded to map our critical and non-critical residues onto their reported crystal structure (**Figure 2-6**). In this figure, we highlighted the CD47 binding site deduced by Hatherley et al in cyan. Interestingly, our critical residues: Q8, T26, V27, S66,

M72, and S75 (colored in red) are clustered in a region on the lateral surface of the crystal structure that is distinct from the binding site deduced by Hatherley et al. Thus, our mutagenesis results in **Figures 2-3** and **2-4** indicate that a lateral surface of SIRPα plays an important role in binding CD47. The lateral region we describe overlaps greatly with a putative "transdimerization region" proposed by Hatherley et al. However, there is no published evidence that transdimerization of SIRPα occurs under physiological conditions. Thus, in this report, we refer to this region as the "lateral surface" of the crystal structure.

A monoclonal antibody that binds to a residue adjacent to the lateral surface of SIRPα.D1 blocks binding of CD47.

We performed an antibody epitope mapping study to investigate the hypothesis that the lateral surface of SIRPα.D1 is involved in binding to CD47. It has been previously published that mAb SE7C2 binds specifically to SIRPα and blocks CD47 binding, whereas mAb B4B6 binds specifically to SIRPβ (9, 51, 65). We reasoned that identifying epitopes of such SIRP-specific antibodies would provide additional insight into the nature SIRPα/CD47 interactions. We screened these two antibodies for the ability to bind to our SIRPα.D1 mutants. As shown in **Figure 2-7A**, SE7C2 bound to all mutants of SIRPα.D1 except SIRPα.D1-E70N. Therefore, SE7C2 binding to SIRPα seemed to be dependent on the presence of E at position 70, suggesting that the epitope of SE7C2 includes E70 on SIRPα. Furthermore SE7C2 was shown to consistently inhibit CD47 binding to wildtype SIRPα.D1 as well as SIRPα.D1-P44A/A45G (**Figure 2-7A and B**). In the

SIRPα.D1crystal structure, residue E70 is immediately adjacent to the cluster of critical residues that we have identified on the lateral surface (**Figure 2-7C**).

On the other hand, B4B6, a monoclonal antibody specific for SIRPβ, did not bind to any of the SIRPα.D1 mutants except to SIRPα.D1-P44A/A45G (**Figure 2-7B**). This result suggests that the epitope of B4B6 contains A44/G45 on SIRPβ. As shown in **Figure 2-4A**, the substitutions P44A/A45G in SIRPα create a SIRPα mutant that not only is still capable of binding to CD47 but also contains a neoepitope of B4B6. On the crystal structure of SIRPα.D1, this epitope is positioned in a region distant from both the CD47 binding site deduced by Hatherley et al and from the lateral surface (**Figure 2-7D)**. Indeed, consistent with our results and those reported by Hatherley, B4B6 did not inhibit the mutant protein SIRPα.D1-P44A/A45G binding to CD47 (**Figure 2-7D**).

Discussion

Given that SIRPα.D1 but not SIRPβ.D1 is a ligand for CD47 (51, 64, 65), our comparative analysis of the primary sequences of the two proteins revealed several key differences that may be important in defining the interaction of SIRPα and CD47. One of the first important distinctions was the different patterns of potential N-linked glycosylation sites. It has been reported that SIRPα in different tissues exhibit differential galactosylation, which can affect its binding specificity to cellular targets (60). However, a recent report demonstrated that recombinant SIRPα proteins produced from tunicamycin treated cells could bind to CD47 as well as the glycosylated SIRPα (58). These conflicting reports prompted us to explore the role of glycosylation in defining the ligand specificity of SIRPs through the use of site-directed mutagenesis. By eliminating the glycosylation concensus motifs in the SIRP proteins, we could address the question unequivocally. We found that glycosylation neither plays a role in facilitating binding of CD47 to SIRPα, nor in preventing binding of CD47 to SIRPβ.

The second major consideration is the presence of a relatively small number of disparate residues between SIRPα and SIRPβ. Substitutions of seven candidate residues in SIRPα with the corresponding residues in SIRPβ revealed that three residues (V27, Q37, and S66) are crucial in the ability of SIRPα to bind CD47. The distribution of the residues in the primary sequence provided no direct clues as to the nature of the binding site. Furthermore, when this study was performed, the crystal structure was not available. Therefore, we constructed a computational model of SIRPα.D1 in order to gain insights into the role of these

critical residues in binding CD47. The model revealed that V27 and S66 are located on the flexible loops at the edge of a β sheet, whereas residue Q37 is in on the opposing β sheet in the interior, proximal to the disulfide bond and a hydrophobic tryptophan that are present in the conserved hydrophobic structural core of IgVs. Since the region containing V27 and S66 is more surface accessible than the region containing Q37, we hypothesized that other residues adjacent to V27 and S66 in that region might also have major effects on ligand binding. Along this line of reasoning, our model predicted that residues Q8, H24, T26, R69, M72, and S75 should influence ligand binding. Among these residues, Q8, H24, R69, and S75 are conserved between SIRPα and SIRPβ. When we replaced these residues in SIRPα.D1 with leucine, a medium sized non-polar amino acid, both Q8L and S75L mutants lost their ability to bind CD47. However, after replacing H24, a large positively charged residue, with leucine or a medium sized polar residue (N), there was no inhibitory effect. On the other hand, when we exchanged a small polar residue such as T26 for a small non-polar residue (A), or a medium sized non polar residue (L), the CD47 binding capacity of the mutant was abrogated. It is interesting to note that T26 is conserved in all SIRPs except for SIRPβ and is identified here as being critical for CD47 binding. When the other residue (R69) that is common between SIRPα and SIRPβ was mutagenized into a small non-polar residue (A), or a large negatively charged residue (E), binding was obliterated. These results lead us to classify Q8, T26, R69, and S75 as critical residues. Finally, when we exchanged M72 in SIRPα.D1 for the corresponding leucine of SIRPβ.D1, the mutant M72L retained

binding to CD47, although the level of binding was consistently lower than wildtype. Since M72L is a fairly conservative substitution, we replaced M72 with nonconserved residues consisting of either a small hydrophobic residue (A), or a large positively charged residue (R). Interestingly, only the mutant M72A lost its ability to bind CD47, suggesting that the physical presence of a sidechain at residue 72 in SIRPα is important in binding to CD47. From these results, it is clear that M72 is also a critical residue in mediating binding interactions with CD47.

Our mutational studies identifying M72 as a critical residue revealed that our initial comparison of primary sequences between SIRPα and SIRPβ was only useful in determining critical residues that have become sufficiently divergent. There is a widely held view that ITAM/ ITIM protein pairs, such as SIRPα and SIRPβ, sharing a highly homologous extracellular region, probably arose from gene duplication and other mechanisms (94, 95). It is conceivable that, as SIRPβ evolved from the duplication of SIRPα, binding to CD47 was lost. However, this does not imply that all residues important in binding to CD47 have become divergent. As demonstrated by our study, one mutation at a critical residue in SIRPα is all that is necessary to abolish binding to CD47. Consequently, the comparative analyses of the primary sequences only reveal nonconserved changes in residues and do not provide any information regarding the significance of conserved residues. Therefore, homology modeling was useful in predicting additional critical candidate residues. As is further discussed below, our model identified residues that, when mapped onto the recently published

crystal structure, confirm the importance of a novel region involved in binding of SIRPα to CD47.

Recently, another group adopted a similar approach comparing various members of SIRPs to identify residues important in interaction with CD47 (69). They concluded that V27 and Q37 were critical residues necessary for interaction, whereas M72 “assisted” the interaction. Although the observation that V27 and Q37 are critical residues is consistent with our findings, no data exploring the role of conserved residues in SIRPα binding interactions with CD47 was presented. Furthermore, two mutually exclusive homology models proposed in this study are inconsistent with the recently reported crystal structure.

Recently Hatherley et al reported the solution of a SIRPα.D1 crystal structure (67). These authors described two major domains on the crystal structure consisting of transdimerization and putative CD47 binding sites. The proposed transdimerization site consists of a region of close contact between two SIRPα.D1 molecules *in trans* at loop DE (residues 60-78), strand B1B2 (residues 20-27), and strand A1 (residues 6 and 7). Despite this observation in the crystal structure, it was acknowledged that no biochemical or functional evidence exists indicating that SIRPα.D1 forms transdimers under physiological conditions (67). Because of the lack of evidence for transdimerization, we refer to this region on SIRPα as the “lateral surface.”

Through homology comparison, site-directed mutagenesis, and an antibody epitope study, a CD47 binding region was deduced by Hatherley et al consisting of residues I31, V33, R69, K96, and D100. As shown in that study, the

epitope of the SIRPα and SIRPβ-binding mAb SE5A5 appears to be conformationally dependent as it spans two different loops (K96 on loop G1F and V33 and I31 on loop B2C) on the top of SIRPα. Interestingly, this epitope also overlays much of the region on SIRPα.D1 proposed by these authors as a CD47 binding site on SIRPα.D1. However, because SE5A5 also binds to SIRPβ, it can be inferred that the conformation of Hatherley's proposed binding site is highly similar to the corresponding region in SIRPβ. This inference is further corroborated by the alignment of the SIRPα crystal structure to the recently available NMR structure of SIRPβ (**Figure 2-8**). The structurally based alignment demonstrates that the 3 dimensional conformations of SIRPα.D1 and SIRPβ.D1 are highly conserved at the five critical residues that are reported by Hatherley to constitute the CD47 binding domain. Given these observations and the fact that the critical residues reported by these authors as well as the amino acids adjacent to these critical residues are identical between SIRPα and SIRPβ, it is hard to envision how this region can alone be sufficient to mediate binding to CD47.

When we mapped the critical residues identified in our study onto the crystal structure of SIRPα, most of them (Q8, T26, V27, S66, R69, M72, and S75), are located in a cluster on the lateral surface of SIRPα.D1. As highlighted in **Figure 2-6**, this region on the lateral surface is distinct from Hatherley's binding site. Interestingly, these authors excluded the possibility that the lateral surface is a CD47 binding site although it was reported that S66D and R69E were critical mutations, whereas E70K and M72R were not (67). However, these

authors only examined residues in the DE loop, but none were examined in the B1B2 and A1 strands, which are also parts of the lateral surface. Residue R69 is actually positioned on the edge of the lateral surface, but it was considered part of their reported CD47 binding site on the top of the molecule. Because of its distance from the putative CD47 binding site, it was also indicated that residue S66 is important in maintaining the structural integrity perhaps through the formation of a potential intramolecular hydrogen bond, that is absent in SIRPβ, to the main peptide chain. However, the high degree of similarity between the 3-dimensional conformations of SIRPα.D1 and SIRPβ.D1 would argue that an intramolecular hydrogen bond at S66 is not essential in maintaining the structural integrity. From their results, Hatherley et al proposed that the lateral surface does not have a role in binding CD47. In this study, we probed the lateral region of SIRPα.D1 in a more comprehensive fashion based on our structural model. We identified 6 additional critical residues on the lateral surface (Q8, T26, V27, S66, and S75) including M72 since M72A, but not M72L or M72R, abolished binding to CD47. These critical residues identified in our study are present in the B1B2 and A1 strands as well as the DE loop. In further support of involvement of this region in binding to CD47, we demonstrated *de novo* binding of SIRPβ to CD47 by exchanging four SIRPβ specific residues with corresponding SIRPα unique residues (A26T, M27V, M37Q, and L66S). Among these residues, three of them are located on the lateral surface. Lastly, involvement of the lateral surface of SIRPα.D1 in binding to CD47 is also supported by our epitope mapping experiments with the SIRPα –specific mAb SE7C2 that inhibits binding

to CD47. The epitope of SE7C2 contains E70, a residue that is immediately adjacent to the critical domain on the lateral surface.

Our site-directed mutagenesis findings coupled with recent crystal structure data strongly suggest that the lateral surface of SIRPα.D1 plays a key role in binding to CD47. We believe that functional effects of the critical residues in the lateral surface of SIRPα.D1 are predominantly mediated through sidechains. As shown in **Figure 2-8**, the conformations of the main peptide chains of the lateral surface of SIRPα.D1 and the corresponding region in SIRPβ.D1 are highly similar. However, the lateral surface of SIRPα.D1 contains 4 unique critical residues (T26, V27, S66 and M72). Therefore, it is reasonable to assume that differences in sidechains of these unique critical residues must dictate the specificity of interaction between SIRP proteins and CD47. It is thus possible that the lateral surface of SIRPα.D1 represents a CD47 binding site. Alternatively, residues in the lateral surface could be necessary for maintenance of the conformational integrity of the binding site proposed by Hatherley, thus indirectly modulating binding interactions with CD47. In order to distinguish between these possibilities, co-crystallization of SIRPα.D1 bound to CD47 will be necessary.

Figure 2-1

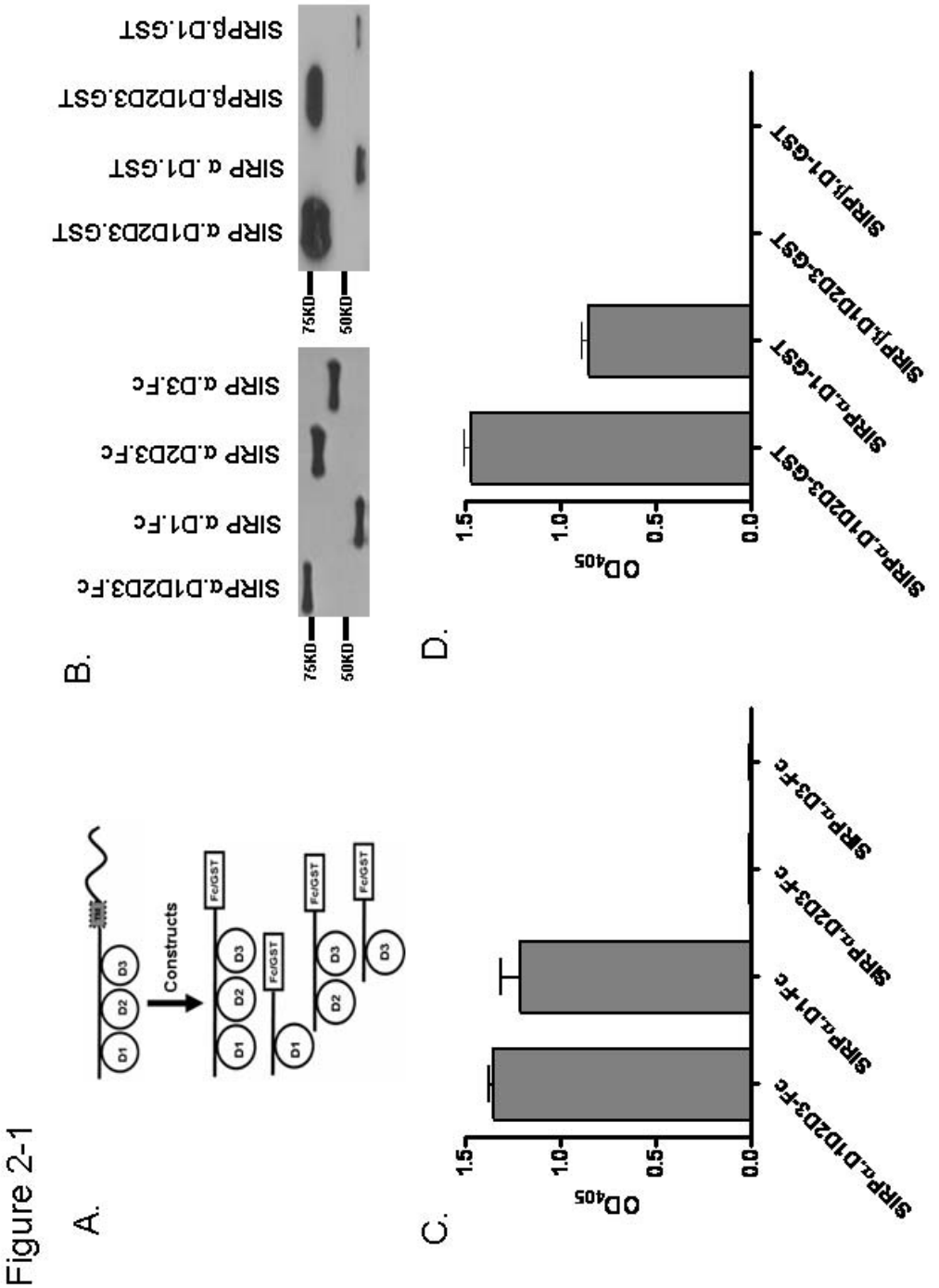
A.
Constructs
D1
D2
D3
Fc/GST
B.
SIRPα.D1D2D3.Fc
SIRP α.D1.Fc
SIRP α.D2D3.Fc
SIRP α.D3.Fc
75KD
50KD
SIRP α.D1D2D3.GST
SIRP α .D1.GST
SIRPβ.D1D2D3.GST
SIRPβ.D1.GST
C.
OD405
1.5
1.0
0.5
0.0
SIRPα.D1D2D3-Fc
SIRPα.D1+Fc
SIRPα.D2D3+Fc
SRPα.D3+Fc
D.
OD405
1.5
1.0
0.5
0.0
SIRPα.D1D2D3-GST
SIRPα.D1-GST
SIRPβ.D1D2D3-GST
SIRPβ.D1-GST

Figure 2-2

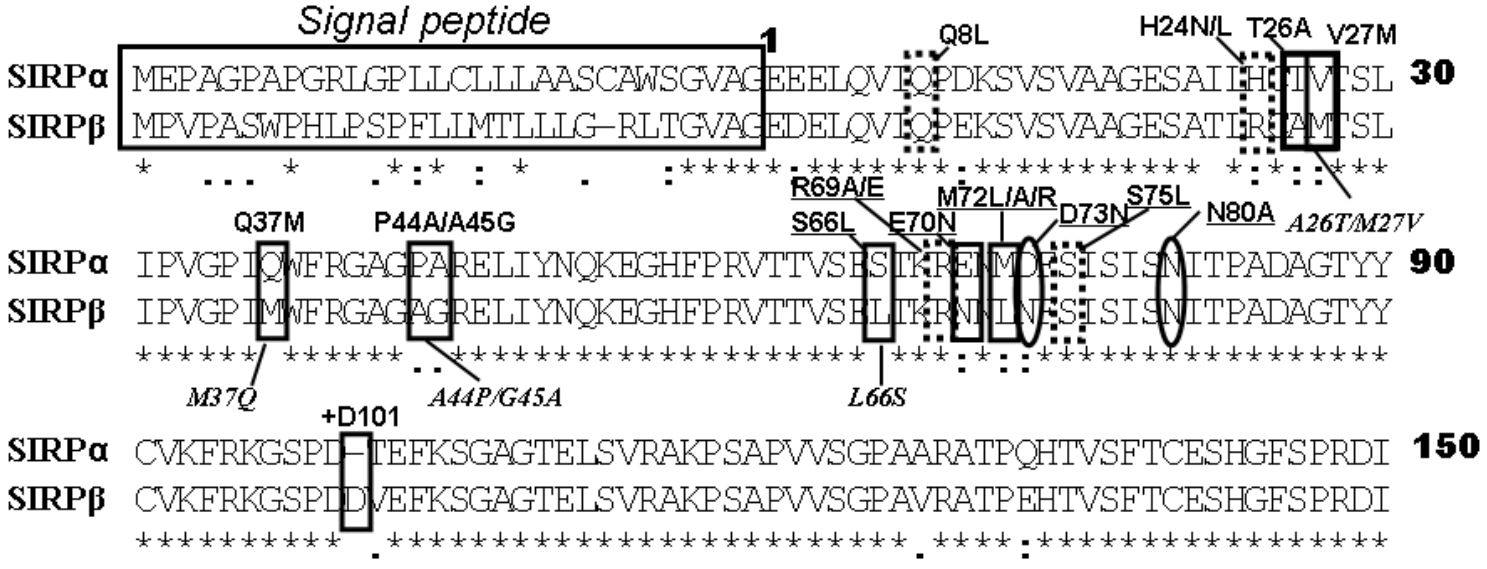
Signal peptide
1
Q8L
H24N/L
T26A
V27M
SIRPα MEPAGPAPGRLGPLLCLLLAASCAWSGVAGEEELQVIQPDKSVSVAAGESAILHCTVTSL 30
SIRPβ MPVPASWPHLPSPFLLMTLLLG-RLTGVAGEDELQVIQPEKSVSVAAGESATLRCAMTSL
R69A/E
S66L
E70N
M72L/A/R
D73N
S75L
N80A
A26T/M27V
Q37M
P44A/A45G
SIRPα IPVGPIQWFRGAGPARELIYNQKEGHFPRVTTVSESTKRENMDFSISISNITPADAGTYY 90
SIRPβ IPVGPIMWFRGAGAGRELIYNQKEGHFPRVTTVSELTKRNNLNFSISISNITPADAGTYY
M37Q
A44P/G45A
L66S
+D101
SIRPα CVKFRKGSPDTEFKSGAGTELSVRAKPSAPVVSGPAARATPQHTVSFTCESHGFSPRDI 150
SIRPβ CVKFRKGSPDDVEFKSGAGTELSVRAKPSAPVVSGPAVRATPEHTVSFTCESHGFSPRDI

Figure 2-3

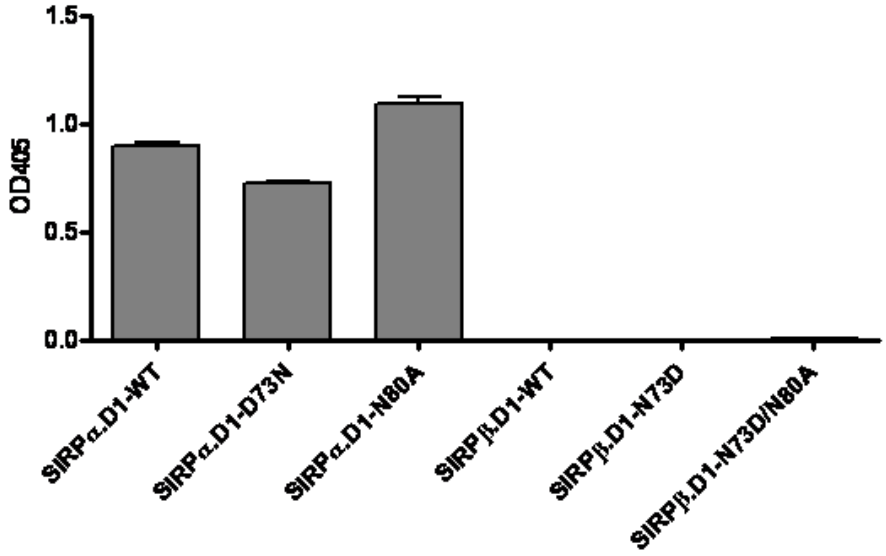
1.5
1.0
0.5
0.0
OD405
SIRPα.D1-WT
SIRPα.D1-D73N
SIRPα.D1-N80A
SIRPβ.D1-WT
SIRPβ.D1-N73D
SIRPβ.D1-N73D/N80A

Figure 2-4

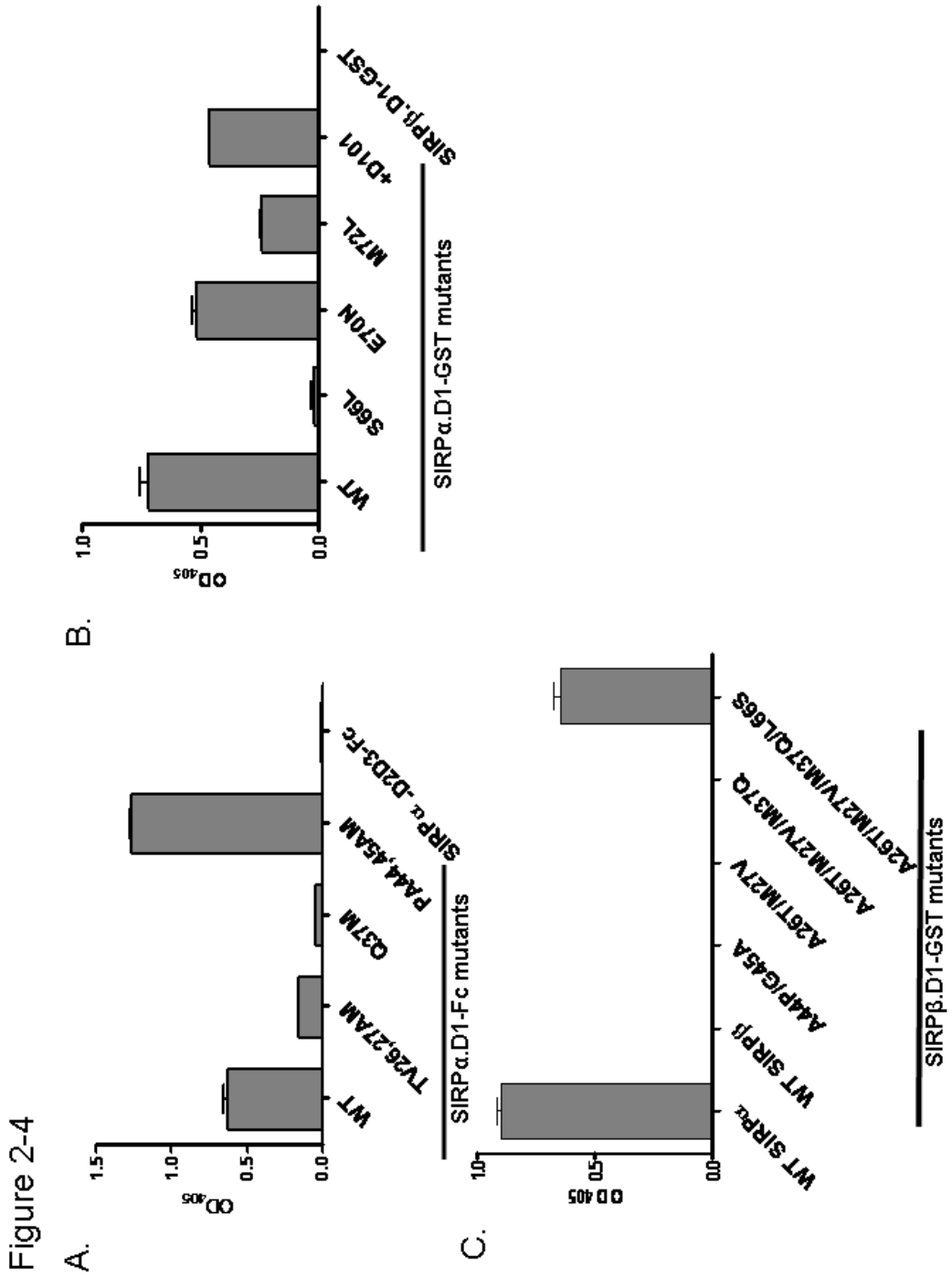
A.
OD405
1.5
1.0
0.5
0.0
WT
TV26,27AM
Q37M
P44,45AM
SIRPα.D2D3-Fc
SIRPα.D1-Fc mutants
B.
OD405
1.0
0.5
0.0
WT
S66L
E70N
M72L
+D101
SIRPβ.D1-GST
SIRPα.D1-GST mutants
C.
OD 405
1.0
0.5
0.0
WT SIRPα
WT SIRPβ
A44P/G45A
A26T/M27V
A26T/M27V/M37Q
A26T/M27V/M37Q/L66S
SIRPβ.D1-GST mutants

Figure 2-5

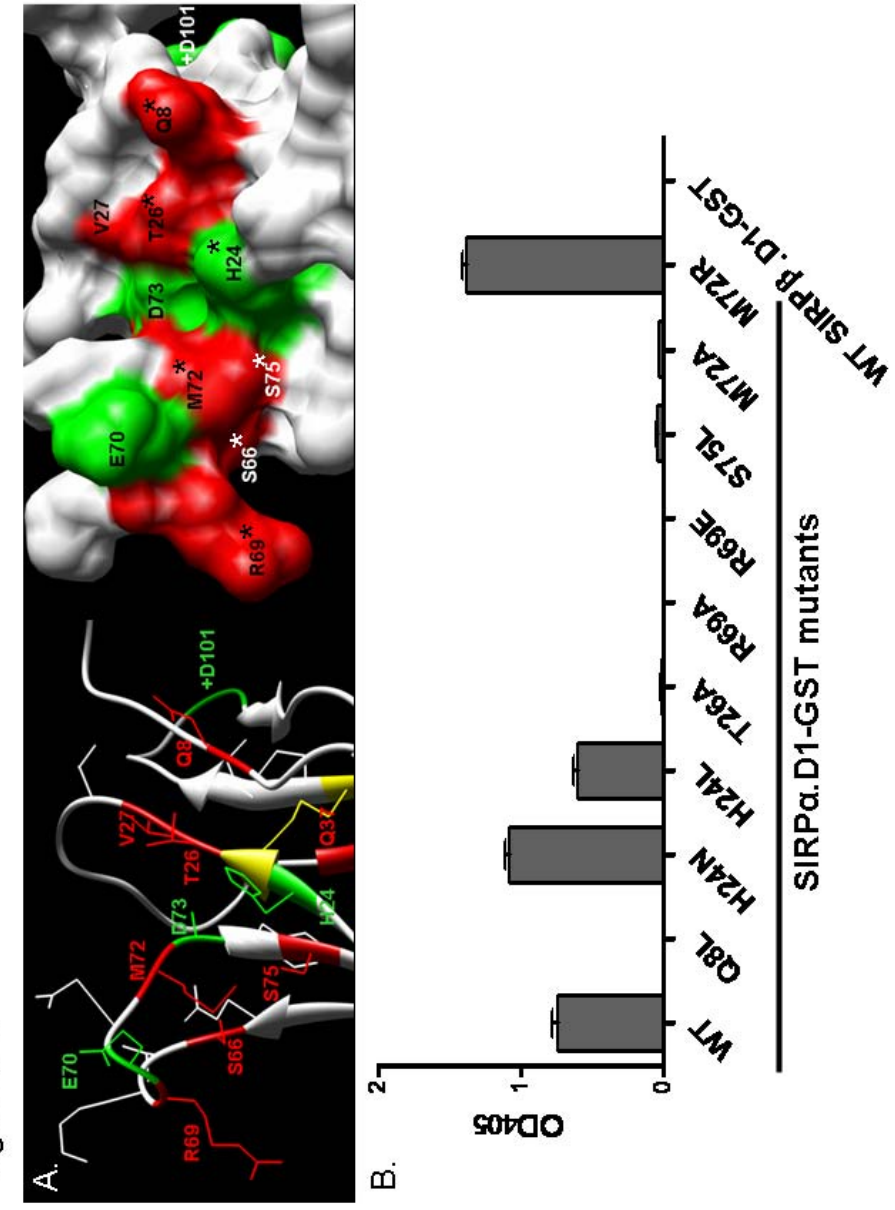
A.
E70
R69
S66
M72
D73
V27
T26
Q8
+D101
H24
Q3
S75
B.
OD405
0
1
2
WT
Q8L
H24N
H24L
T26A
R69A
R69E
S75L
M72A
M72R
WT SIRPβ.D1-GST
SIRPα.D1-GST mutants

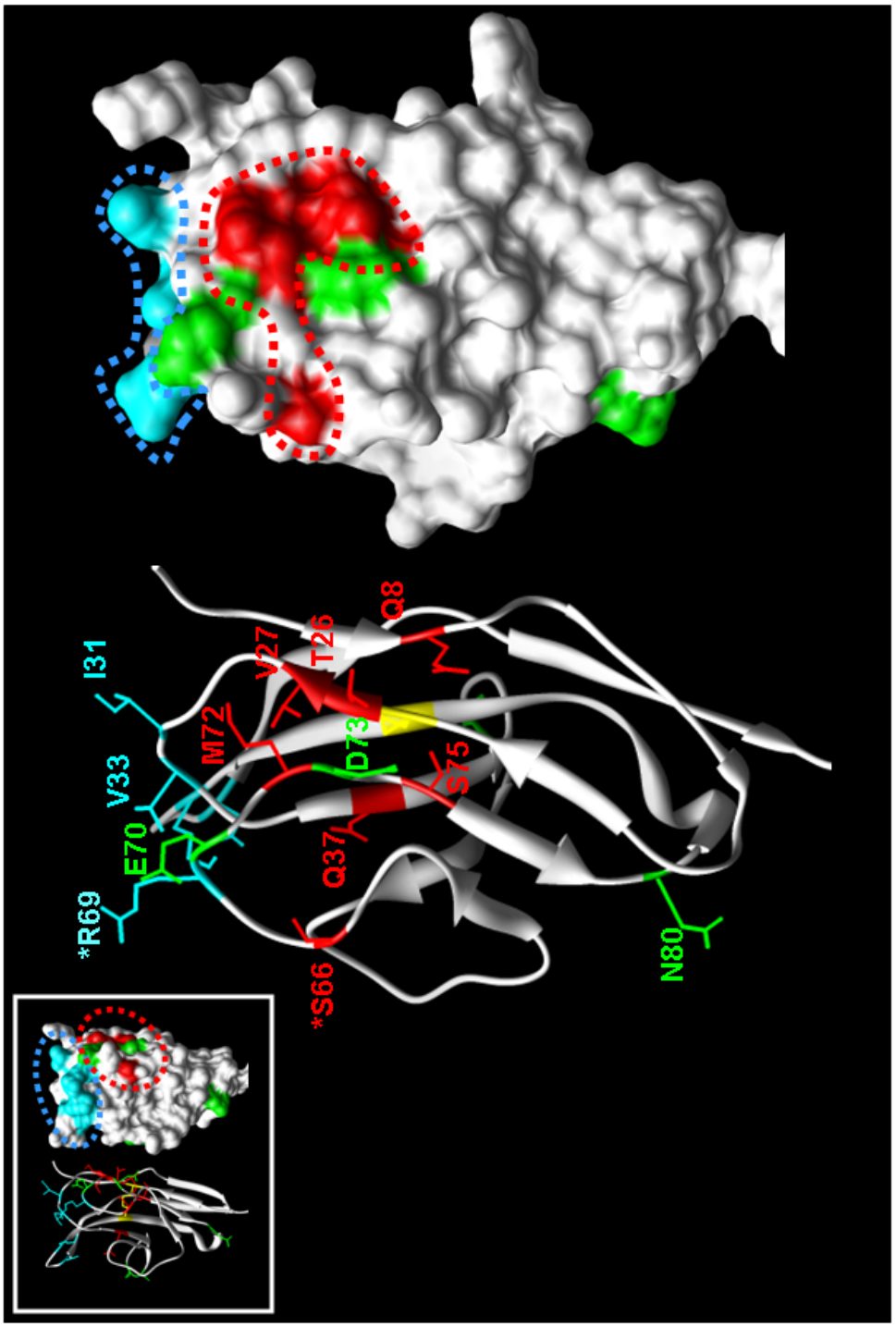

Figure 2-6

Figure 2-7

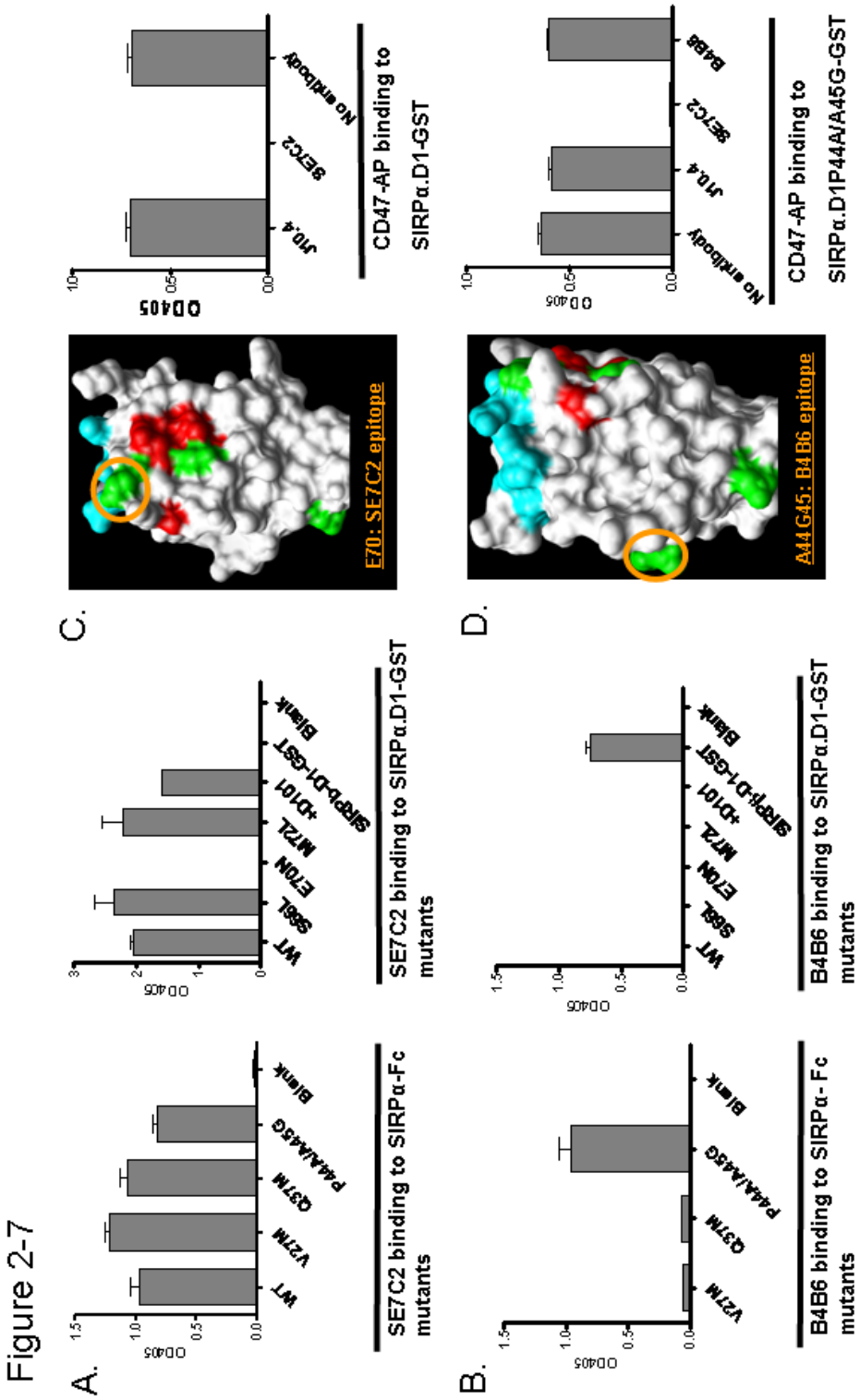
A.
OD405
WT
V27M
Q37M
P44A/A45G
Blank
SE7C2 binding to SIRPα-Fc mutants
B.
OD405
V27M
Q37M
P44A/A45G
Blank
B4B6 binding to SIRPα- Fc mutants
C.
E70: SE7C2 epitope
OD405
J10.4
SE7C2
No antibody
CD47-AP binding to SIRPα.D1-GST
D.
A44 G45: B4B6 epitope
OD405
No antibody
J10.4
SE7C2
B4B6
CD47-AP binding to SIRPα.D1P44A/A45G-GST
SE7C2 binding to SIRPα.D1-GST mutants
WT
S66L
E70N
M72L
+D101
SIRPb-D1-GST
Blank
B4B6 binding to SIRPα.D1-GST mutants
WT
S66L
E70N
M72L
+D101
SIRPb-D1-GST
Blank

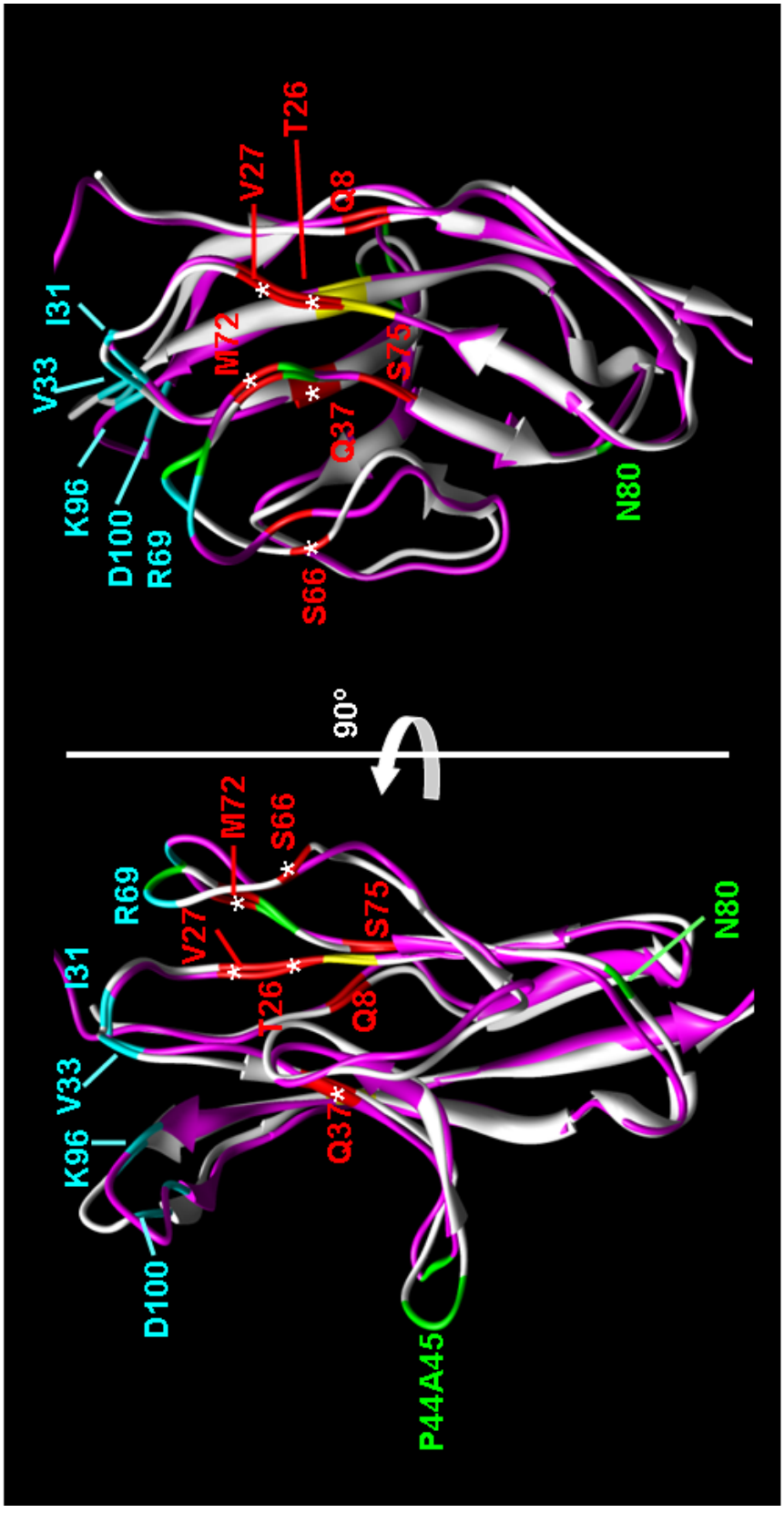

Figure 2-8

Figure Legends:

Figure 2-1. CD47 binds to SIRPα.D1 but not SIRPβ. **A.** Schematic illustration of soluble tagged SIRPα fusion proteins containing various Ig domains. **B.** Western blot confirming production of soluble SIRP fusion proteins by transfected COS7.2 cells analyzed with murine monoclonal anti-pan-SIRP antibody SAF10.1 and goat anti- mouse IgG-HRP. **C.** and **D.** *In vitro* binding assay assessing binding of SIRPα fusion proteins with CD47: CD47-AP containing culture supernatant was added to immobilized recombinant protein and binding assessed colorimetrically using PNPP.

Figure 2-2. Alignment of protein sequences demonstrating that SIRPα.D1 and SIRPβ.D1 are highly homologous. The circled residues are potential N-glycosylation sites in SIRPα or SIRPβ. Boxed residues represent candidate amino acids in this study that may be important in the interaction with CD47. Residues boxed in solid lines are disparate between SIRPα and SIRPβ; residues boxed in dashed lines are identified as potential critical residues through homology modeling. Substitutions of SIRPα residues with either corresponding SIRPβ residues or other non-conserved residues are indicated on top of the boxed amino acids; the corresponding reverse substitutions into SIRPβ are labeled with italicized font under the respective boxed residues.

Figure 2-3. N-Glycosylation does not play a role in the interaction of SIRPα with CD47 nor does it prevent binding of SIRPβ to CD47. Binding of CD47-AP to

SIRP glycosylation mutants was measured as described in Materials and methods. SIRPα.D1-WT contains 1 N-glycosylation motif at N80. The mutant D73N contains 2 motifs, and the mutant N80A contains none. In contrast, SIRPβ.D1-WT contains 2 potential sites (N73/N80). The mutant N73D contains one site, and the double mutant N73D/N80A does not contain any glycosylation sites.

Figure 2-4. Identification of critical residues mediating SIRPα binding to CD47 through substitution of disparate SIRPα residues with corresponding amino acids on SIRPβ. The substitution of a non-conserved SIRPα residue with a corresponding SIRPβ residue or vice versa was achieved using site-directed mutagenesis. Using the CD47-AP *in vitro* binding assay, we analyzed binding to: **A**) SIRPα.D1 Fc mutants **B)** SIRPα.D1-GST mutants and **C**) SIRPβ.D1-GST mutants carrying single or cumulative substitutions of SIRPα residues.

Figure 2-5. A computational homology model of SIRPα.D1 reveals additional critical residues common to SIRPα and SIRPβ that mediate binding to CD47. Critical residues V27 and S66 are located in close proximity; whereas critical residue Q37 is away from both V27 and S66 and is near the hydrophobic core and disulfide bond (yellow). **A.** The left panel is a ribbon diagram with sidechains depicting a front view of the SIRPα.D1 model. The right panel is the space-filled configuration of the model. Based on the assumption that V27 and S66 are involved in binding of SIRPα to CD47, the model predicts other residues (labeled

with *) surrounding V27 and S66 that may also be important in binding to CD47. Critical residues (Q8, T26, V27, Q37, S66, R69, S75, and M72) are labeled in red, and non-critical residues (H24, P44, A45, E70, and +D101) are labeled in green. Yellow residues represent cysteines that form a disulfide bond. **C.** Results of CD47-AP binding to SIRPα.D1 mutants with nonconserved mutations of candidate residues predicted by the homology model.

Figure 2-6. The lateral surface of SIRPα.D1 mediates binding to CD47. Critical residues (red) and non-critical residues (green) are mapped onto the recently reported SIRPα.D1 crystal structure (30). Residues in the putative CD47 binding site deduced by Hatherley *et al* (cyan) are completely conserved between SIRPα and SIRPβ. Two critical residues labeled with * were identified by us and Hatherley et al. Critical residues identified by us are clustered at a surface (circled in red) that is distinct and lateral from the binding site proposed by Hatherley (circled in cyan). The main figure represents an en face view of the lateral surface of SIRPα.D1 whereas the inset represents the structure rotated counterclockwise 90 degrees.

Figure 2-7. CD47 binding is inhibited by a monoclonal antibody that maps to the SIRPa.D1 lateral surface. **A** . mAb SE7C2, specific for human SIRPα, but not SIRPβ, and **B.** mAb B4B6, specific for human SIRPβ, but not SIRPα, were screened for binding to SIRPα mutants by ELISA as described in the Materials and Methods (10μg/ml of mAb in 1%BSA/PBS buffer). **C.** The protein structure

shows the epitope of SE7C2 (circled in orange) contains E100, which is at the upper edge of the lateral surface. The graph shows that CD47-AP binding to SIRPα.D1 is blocked by SE7C2 in an *in vitro* binding assay but not by control mAb J10.4. **D.** The protein structure shows the neoepitope of B4B6 (circled in orange) introduced into SIRPα.D1 with the non-critical mutation P44A/A45G is distant from the lateral surface. The graph shows no inhibition of CD47-AP binding to SIRPα.D1.P44A/A45G in the presence of B4B6.

Figure 2-8. SIRPαD1 and SIRPβD1 exhibit highly similar structural conformations. Alignment of SIRPαD1 crystal structure (2uv3; white) with SIRPβD1 NMR structure (2d9c; magenta) reveals a high degree of similarity between the two structures in the region of the putative CD47 binding site (cyan) proposed by Hatherley et al. Note, the residues in this region are identical between both molecules, thus it is unclear how this domain by itself can confer specificity of binding to CD47. Critical residues reported by us are highlighted in red and cluster on the lateral surface (non-critical residues are in green). Although the conformations of main peptide chains in the lateral surfaces of both proteins are similar between SIRPαD1 and SIRPβD1, four critical residues (labeled with *****) in the lateral surface are unique to SIRPα and presumably confer binding specificity through sidechain interactions.

CHAPTER 3

The role of *Cis* dimerization of SIRPα in binding to CD47.

Abstract

Interaction of SIRPα with its ligand, CD47, regulates leukocyte functions including transmigration, phagocytosis, oxidative burst, and cytokine secretion. However, the molecular details of how this transmembrane glycoprotein interacts with CD47 on the cell surface are incomplete. Here we report that SIRPα forms noncovalently linked *cis*-homodimers and present evidence to suggest that homodimerization may facilitate binding to CD47. Treatment of SIRPα expressing cells with a membrane impermeable crosslinker resulted in the formation of SIRPα dimers and oligomers on western blots. Biochemical analyses of soluble recombinant extracellular regions of SIRPα, including domain-truncation mutants, revealed that each of the three extracellular immunoglobulin loops of SIRPα formed dimers in solution. Co-immunoprecipitation experiments using cells transfected with different affinity-tagged SIRPα molecules revealed that SIRPα forms *cis* dimers. Notably, in cell treated with tunicamycin, SIRPα dimerization but not CD47 binding was inhibited, suggesting that a SIRPα dimer may be bivalent and capable of binding CD47 with increased avidity. Lastly, in adherent neutrophils, stimulation with LPS or fMLP resulted in enhanced dimerization of SIRPα. Collectively, these data suggest that *cis* dimerization of SIRPα likely plays an important role in regulating CD47 binding and function in leukocytes.

Introduction

Signal regulatory proteins (SIRPs) are immunoglobulin superfamily members (IgSF) that include SIRPα, SIRPβ, and SIRPγ (5, 8). Expression of SIRPs is largely restricted to leukocytes, where SIRPα and SIRPβ are expressed in myeloid lineages, and SIRPγ in lymphocytes (5, 8). Interestingly, SIRPα is also expressed in smooth muscle cells and neurons and has important signaling properties (24, 25, 96). The extracellular domains of SIRPs consist of a membrane distal Ig variable-like (IgV) fold (D1), and two membrane proximal Ig constant-like (IgC) folds (D2D3). The ectodomains of the various SIRP family members share a high degree of homology between their respective protein sequences. In contrast, the cytoplasmic signaling elements of different SIRPs differ greatly. For instance, the cytoplasmic tail of SIRPα contains 4 immunoreceptor tyrosine-based inhibitory motifs, that recruit src homology 2 phosphatases upon phosphorylation (10). In contrast, SIRPβ and SIRPγ have short cytoplasmic tails that are only a few amino acids long. SIRPβ associates with the immunoreceptor tyrosine-based activating motif containing adaptor protein DAP12 through charge interactions in the transmembrane regions (11, 12). On the other hand, SIRPγ, lacking known signaling motifs, has been presumed to be a decoy receptor (13). However, a recent report suggests that SIRPγ on T cells may be able to transmit signals that can regulate transendothelial migration (27). The major cellular ligand of SIRPα and SIRPγ is CD47, a ubiquitously expressed transmembrane IgSF protein; whereas, the ligand of SIRPβ remains unknown (5, 8). CD47 consists of an extracellular IgV

fold, a penta-membrane-spanning transmembrane domain, and a cytoplasmic tail (28). Binding interactions between SIRPα and CD47 have been implicated in regulating many aspects of leukocyte function.

SIRPα has emerged as an important inhibitory receptor that regulates a number of leukocyte functions. For example, SIRPα-CD47 interactions have been shown to regulate neutrophil migration across epithelial monolayers and monocyte migration across the blood brain barrier (50, 51, 78, 79). These *in vitro* observations are consistent with *in vivo* experiments with CD47 deficient mice. In these experiments, CD47 deficient mice succumbed to acute bacterial peritonitis due to a delay in leukocyte recruitment (52). In other reports, activation of SIRPα has been shown to negatively regulate toll-like-receptor signaling, inflammatory cytokine secretion and leukocyte respiratory burst (47, 48, 56, 97). SIRPα has also been shown play a role in regulation of phagocytosis in macrophages (18, 49). Specifically, CD47 binding to macrophage SIRPα results in inhibition of phagocytosis (53, 55). Conversely, CD47 expression on apoptotic cells has been shown to cluster resulting in altered SIRPα signaling that allows subsequent clearance by macrophages (42, 46). Recently, it was reported that the inhibition of phagocytosis by tissue resident macrophages through SIRPα-CD47 interactions is essential for successful engraftment of hematopoietic stem cells (56, 57, 59) .

Given the multitude of functions attributed to SIRPα binding to CD47, understanding the molecular details of this interaction has become an important topic that might provide novel therapeutic approaches. It has been shown that

binding of SIRPα to CD47 is mediated through SIRPαD1 and the IgV domain of CD47. Recently, a series of mutagenesis studies using soluble, recombinant proteins and comparative analyses of crystal structures of SIRPD1s, CD47, and SIRPαD1-CD47 complexes have provided important insight into the molecular mechanisms of the binding interaction between SIRPαD1 and CD47 (63, 66-69). However, the majority of these reports have relied on soluble, recombinant truncated proteins and focused on the D1 domain of SIRPs. Little is known about potential contributions of the membrane proximal immunoglobulin loops of SIRPα to the binding to CD47 and how native SIRPα molecules interact within the cell membrane. Previously, we demonstrated that SIRPβ is present on the cell surface as a *cis* homodimer that is covalently linked through a disulfide bond on the most membrane proximal domain (D3) (9). Interestingly, the entire ectodomain, including the membrane proximal domains (D2D3), of SIRPα exhibits a high degree of protein sequence homology to SIRPβ, however SIRPα does not form covalently linked dimers due to the lack of corresponding cysteine residue in SIRPβ. However, given the similarities in protein sequences between the two proteins, we hypothesized that SIPRα might form a noncovalently linked *cis* homodimer on cell surface.

Using full length or truncated SIRPα proteins expressed on cell surface and in solution along with the use of a chemical crosslinker, we explored potential contributions of each of the three Ig folds in dimerization of SIRPα. Immunoprecipitation analyses of differentially tagged SIRPα molecules indicated that SIRPα dimerizes *in cis*. Lastly, we report that dimerization of SIRPα is

enhanced in stimulated adherent human PMN. These results have important implications in the understanding of SIRPα interactions with its ligands.

Methods

Antibodies

Rabbit polyclonal antibody against the cytoplasmic tail of SIRPα and a rabbit polyclonal antibody against GFP are commercially available (Prosci, Abcam). A hybridoma that secretes a murine monoclonal antibody against myc (9E10) was obtained from ATCC. Rabbit polyclonal antiserum against recombinant SIRPα ectodomain produced as previously described (63) was generated by Covance. Murine monoclonal antibody against SIRPα.D1 (SAF17.2) and murine monoclonal antibody against SIRPα.D3 (SAF4.2) were generated in house as previously described (63).

Cell line and tissue culture

A human promyelocytic leukemia cell line (HL60), human embryonic kidney cell line with T antigen (HEK293T), and wild type Chinese hamster ovary cell line (CHO), as well as mutant CHO cell lines with defective N-glycosylations (Lec1, Lec2, and Lec8) were purchased from ATCC. HL60 cells were passaged in RPMI supplemented with 20% heat inactivated FBS and supplements in 5% CO_2 at 37ºC. CHO and HEK293T cells were passaged in DMEM high glucose supplemented with 10% heat inactivated FBS and supplements in 5% CO_2 at 37ºC.

Transfection of CHO cells

$5x10^5$ CHO cells per well were seeded onto a 6 well tissue culture plate (Corning). The next day, cells were transfected with plasmid constructs (2μg/well) using lipofectamine (Invitrogen) according to the manufacturer's instruction. Cells were harvested 24 to 48 hours after transfection. To generate stable transfectants, 3 days after transfection, the cells were transferred to a T25 tissue culture flask. The cells were selected in the presence of 500μg/ml of either G418 or hygromycin for 10 days. Single cell clones were generated by limiting dilution. Expression of recombinant proteins on cell surface was assessed by flow cytometry.

Chemical crosslinking with BS3 of SIRPα on cell surface and in solution

To crosslink cell surface SIRPα, cells were grown to confluency in 6 well plates, washed twice with cold Hank's balanced salt solution with calcium and magnesium (HBSS+; Sigma) followed by crosslinking by addition of 2ml per well of 1mM Bis [Sulfosuccinimidyl] suberate (BS3; Pierce) in HBSS+ at 4ºC for 30 minutes. After two washes with cold HBSS+ , 2ml of cold 40mM Tris-HCl in HBSS+ at pH8 was added for 20 minutes at 4ºC in order to quench the unreacted crosslinkers. The same procedure was used to crosslink cells in suspension after adjusting the cell concentration to $0.5x10^6$ per ml. A different protocol is used to crosslink soluble SIRPα proteins. To purified soluble proteins (see purification methods below) at a concentration of 10μM in PBS was added one tenth volume of freshly prepared 10mM BS3 solution in PBS Followed by

incubation at room temperature for 30 minutes. The crosslinking reaction was quenched with 40mM Tris-HCl at pH8.

Immunoblotting SIRPα

After crosslinking, washing, and quenching, adherent cells were harvested from tissue culture wells in cold RIPA buffer supplemented with protease and phosphatase inhibitors (Sigma). Harvested Cells were lysed by sonication (Sonic dismembranator, Fischer Scientific) for 15 seconds, followed by incubation on ice for 30 minutes. Cell lysates were cleared by centrifugation at 14,000rpm at 4ºC and supernatants boiled in an equal volume of SDS sample buffer under reducing or nonreducing (as needed) conditions. Samples were analyzed using SDS-PAGE followed by transfer to polyvinylidene difluoride membranes (Bio-Rad). For transient transfection samples, the amount of cell lysate added per lane was normalized to protein expression as determined by flow cytometry. For PMNs and HL60 cells, which express SIRPα natively, 10^5 cell equivalents were loaded per lane. For soluble proteins, 1-10ng of protein was loaded per lane.

Flow cytometry

Cell suspensions were prepared from adherent cultures by trypsinization (Trypsin/ EDTA; Sigma). After washing, cells were resuspended at 10^6/ml in serum containing medium. Approximately $2x10^5$ cells per staining condition were incubated with 5μg/ml primary antibody for 1 hr at 4ºC followed by washing and staining with 1μg/ml secondary antibody conjugated with Alexa 488 dyes

(Invitrogen). After a final wash, cells were analyzed using FACS Calibur (BD biosciences) and FlowJo software (Treestar).

Generation of full length and truncated SIRP plasmid constructs

To express full-length wild type SIRPα on the cell surface, SIRPα cDNA corresponding to GenBank entry BC 029662.1 (WTSIRPα) was cloned into pcDNA3 (Invitrogen Life Technologies). In order to study the contribution of specific Ig folds to SIRPα dimerization on cell surface, constructs encoding SIRPα with deletions of specific Ig folds were generated. A truncated SIRPα mutant containing only the membrane distal fold (D1) was made by deletion of residues S140-G338 and a 6xmyc tag was added at the C terminus of the cytoplasmic tail (SIRPαD1-6xmyc). A truncated SIRPα mutant with two membrane distal loops (SIRPαD1D2) was generated by deleting residues V257-Q355. A truncated SIRPα mutant with two membrane proximal domains (SIRPαD2D3) was also made by deletion of residues V1-S116. In each construct, the native signal peptide, transmembrane region, and the cytoplasmic tail were included. Soluble ectodomain counterparts of WTSIRPα, SIRPαD1-6xmyc, and SIRPαD2D3 were also generated by truncation of residues distal to residue S340—thereby excluding the transmembrane domain and the cytoplasmic tail, and included the addition of a 10x histidine tag after S340. These plasmids are defined as solWTSIRPα-His, solSIRPαD1-His, and solSIRPαD2D3-His. Additionally, WTSIRPα fused with EGFP at the C-terminal end (SIRPα-EGFP) was made by cloning SIRPα cDNA into pEGFP (Invitrogen Life Technologies).

WTSIRPα fused with 6xmyc tag (SIRPα-6xmyc) at the C-terminal end was engineered by insertion of 6xmyc sequence into existing WTSIRPα construct before the stop codon. Finally, CD47 cDNA was cloned into pcDNA3.1 that contains a hygromycin resistance cassette (Invitrogen). All constructs were verified by sequencing.

Purification of soluble recombinant histidine tagged SIRPα proteins

HEK293T cells were grown to 80% confluency and transfected with desired plasmid constructs via lipofectamine (Invitrogen) as described above. Dot blots were performed on the cell culture supernatants to ascertain the production of recombinant proteins. Briefly, 5µl aliquots of supernatants were spotted onto a piece of nitrocellulose membrane. After drying, the membrane was blocked with 5% milk in TBS. Proteins were detected with specific primary antibodies and appropriate horse radish peroxidase conjugated secondary antibodies (Jackson Immunoresearch). The blots were developed using a chemiluminescence kit (Roche). Culture supernatants from the transfected cells grown in T162 flasks (Costar) were collected once every four days until cessation of recombinant protein production as determined by dot blot. After each collection, supernatants were cleared by centrifugation at 800xg for 10 minutes followed by adjusting the pH to 8 with Tris. 5 ml of washed Ni-NTA agarose beads (Qiagen) was added to each liter of supernatant followed by incubation at room temperature for 4 hours. Beads were then collected in a column. After washing, first with 150mM NaCl and 50mM NaH_2PO_4 , followed by 300mM NaCl, 50mM NaH_2PO_4, and 10mM

imidazole (Fluka) at pH8, bound SIRPα was eluted sequentially in fractions of 2 bead volumes (10ml) each with increasing concentrations of imidazole (25mM, 50mM, 100mM, and 500mM) in 150mM NaCl, 50mM NaH_2PO_4 at pH 8. Purified proteins were dialyzed in PBS and concentrated using Centricon microconcentrators to 1ml volume. Purity of proteins was assessed by SDS-PAGE and concentrations determined by optical density at 280nm (Nanodrop, Thermo Scientific)

Gel filtration chromatography analysis

Purified protein samples were applied to a Sephacryl S100 (GE Amersham) column on a BioRad DuoFlo Chromatography system. Gel filtration was performed at a flow rate of 1ml/min using a buffer containing 20mM Tris and 150mM NaCl at pH 8. Protein standards consisting of blue dextran (3000KD), conalbumin (75KD), ovalbumin (45KD), chymotrypsinogen (25KD), and cytochrome C (12KD) were used. The logarithmic correlation of the elution peaks of the standard proteins and the molecular weight were calculated using MS Excel. The apparent molecular weights of the protein samples according to their peak elution volumes were calculated from the formula obtained $\mathbf{[MW]=e^{([pev]-538.43)/(-37.497)}}$; R^2=0.984.

MALDI-TOF mass spectrometric analysis

For mass spectrometric analysis, 1 µL of a protein solution of each of the the recombinant domains of SIRPα (D1, D2D3, and D1D2D3) were individually

mixed with sinapinic acid (3-10 mg of sinapinic acid in 1 mL of aqueous solution of 50% (v/v) acetonitrile containing 0.1% (v/v) TFA) as a matrix and spotted onto a MALDI-TOF target. A Bruker Ultraflex II MALDI/TOF Mass Spectrometer was used to analyze all samples. Protein mass was determined using the positive-ion linear mode.

Immunoprecipitation

Cell lysates were precleared with 5µg/ml of nonspecific purified rabbit IgG (JacksonImmunoResearch) and protein A sepharose beads (GE Amersham) for 12 hours at 4ºC. Lysates were incubated with 5µg/ml of affinity purified rabbit polyclonal antiGFP antibody (Abcam) for two hours at 4ºC. Then antigen-antibody complexes were precipitated with protein A sepharose beads at 4ºC for two hours. After washing once with RIPA buffer, then five times with PBS containing 10% RIPA buffer, the beads were boiled in 2x sample buffer under reducing conditions. The samples were subjected to SDS PAGE and immunoblotting analysis.

Inhibition of N-linked glycosylation by tunicamycin and kifunensine.

To inhibit formation of N-linked glycans, confluent CHO cells were incubated with fresh high glucose DMEM supplemented with 10% heat inactivated FBS and 5µg/ml of tunicamycin (Calbiochem) for 18 hours. To arrest maturation of N-linked glycans, CHO cells at 10% confluency were treated with fresh high glucose DMEM-FBS supplemented with 10µg/ml of kifunenesine (Toronto

research). The cells were grown to confluency and were subjected to analyses. Flow cytometry analyses using phytohaemagglutinin type L conjugated with FITC (PHA-L-FITC; Vector Laboratories) were used to assess the reduction in N-linked glycosylation. Alterations in N-linked glycosylation were reflected in protein mobility shifts on immunoblots.

Binding analysis of soluble CD47 to SIRPα on cell surface

Production and purification of soluble CD47 ectodomain fused with alkaline phosphatase (CD47AP) were performed as previously described (51, 63). Given the difficulty involved in obtaining sufficient quantity of purified CD47AP to perform large scale binding assays, soluble CD47AP in cell culture supernatants was used in the binding assay. The concentration of CD47AP in supernatants was calculated by comparing the binding of known quantity of purified CD47AP and CD47AP in supernatants to a murine monoclonal IgG against CD47 (C5D5) in an ELISA assay. Briefly, 100µl of 2µg/ml of C5D5 was coated onto a high binding 96 well plate (Immunolon) at 37ºC for 1.5 hours. After washing, the wells were blocked with 2%BSA (Sigma) in PBS for 1 hour at room temperature. Series of dilutions of CD47AP supernatant or purified CD47AP were added to wells and incubated at room temperature for 1 hour. After washing, binding of CD47AP to C5D5 was assessed colorimetrically using *p*-nitrophenyl phosphate (Sigma-Aldrich) at 405 nm. After measuring the concentration of CD47AP in the supernantant, a series of dilutions of CD47AP supernatants was added to a 96 well plate with confluent CHO-SIRPα at 4ºC for 1 hour. After washing with cold

HBSS+, binding of CD47AP to CHO-SIRPα transfectants was assessed colorimetrically using *p*-nitrophenyl phosphate at 405 nm.

Stimulation of human blood PMNs.

Human PMNs were freshly prepared using the dextran sedimentation method as previously described (98). After isolation, PMNs were resuspended in cold HBSS buffer free of calcium and magnesium (Sigma) at a density of $5x10^7$/ml. $4x10^6$ PMNs in 2ml HBSS+ per well were added to a 6 well tissue culture plate and allowed to settle and adhere at 37ºC for 30 minutes. The cells were then stimulated with 1µg/ml of LPS (Sigma) or 10^{-6} M fMLP (Sigma) for 20 minutes at 37ºC. To stimulate PMNs in suspension, $4x10^6$ PMNs in 1ml of HBSS were prepared and stimulated with 1µg/ml of LPS or 10^{-6} M fMLP for 20 minutes at 37 ºC, followed by crosslinking and analysis as described above.

Results

SIRPα forms noncovalent dimers on cell surfaces.

We have previously reported that SIRPβ but not SIRPα forms a covalent homodimer on cell surface through a disulfide bond at the most membrane proximal domain (D3) (9). The ectodomains of SIRPα and SIRPβ exhibit high degree of homology in protein sequences (**Figure 3-1A**). Since it is generally thought that the monomers of a dimer must pair up noncovalently in a thermodynamically favorable fashion in order to facilitate the formation of intermolecular disulfide bond (74, 75), we hypothesized that SIRPα may form a noncovalent dimer on cell surface. To address this possibility, we analyzed neutrophil lysates by immunoblot for the presence of SIRPα dimers by SDS PAGE. Samples were treated with combinations of boiling, nonboiling, reducing, and nonreducing conditions. Under non-reducing conditions, covalent SIRPβ dimers but not SIRPα dimers were detected. Thus, if SIRPα forms dimers, they are likely non-covalently linked, and unstable in the presence of SDS (**Figure 3-1B**). To stabilize potential non-covalently linked SIRPα dimers, a membrane non-permeable biochemical crosslinker, BS3, was used to covalently crosslink SIRPα on the surface of HL-60 cells. Subsequent immunoblot analyses under reducing conditions using rabbit polyclonal anti-SIRPα cytoplasmic tail antibody revealed three species of SIRPα protein complexes that were consistent with glycosylated monomers at 75-110KD, dimers at 220KD, and oligomers above 250KD (**Figure 3-1C**). Taken together, these results suggested that SIRPα may form noncovalently linked dimers at the cell surface.

CD47 is not a component of crosslinked SIRPα complexes.

Since HL60 cells express CD47 (data not shown), it was important to determine whether the crosslinked SIRPα complexes contain CD47. Our anti-CD47 antibodies on hand did not detect denatured CD47 and inhibit binding to SIRPα (data not shown). Therefore, it was impossible to use these antibodies to determine the presence of CD47 in the crosslinked complexes. To address this issue, we used a recombinant protein expression system in CHO cells. Although CHO cells express CD47, it has been previously shown that hamster CD47 does not interact with human SIRPα (58). CHO cells stably expressing functional human SIRPα (CHO-SIRPα), CD47 (CHO-CD47), or both molecules (CHO-SIRPα/CD47) were then generated. For CD47 to be a component of crosslinked complexes demonstrated in **Figure 3-1C**, crosslinking CHO-SIRPα would be expected to yield a complex of a different molecular weight in the presence of CD47. However, immunoblot analyses under reducing conditions revealed no difference in mobility of the crosslinked species in CHO-SIRPα, CHO-SIRPα/CD47, and CHO-SIRPα cells cocultured with CHO-CD47 (**Figure 3-2**). Furthermore, sequence analyses of the protein bands corresponding to crosslinked complexes revealed the presence of SIRPα protein only (data not shown). Therefore, CD47 is not a component of the crosslinked SIRPα complex.

Soluble ectodomains of SIRPα spontaneously dimerizes in solution.

To determine whether SIRPα dimerizes through its extracellular domains, purified histidine tagged soluble SIRPα containing all three extracellular Ig domains SIRPαD1D2D3His (predicted mw ~40KD) was expressed by human embryonic

kidney 293T (HEK293T) cells and analyzed using gel filtration chromatography on an S100 column. Interestingly, the majority of SIRPαD1D2D3His was eluted at a peak volume corresponding to an apparent molecular weight of 70KD, almost twice that of the predicted molecular weight (**Figure 3-3A**). The eluted sample was further analyzed by MALDI-TOF, and the molecular weight was determined to be 40KD (**Figure 3-3B**). As revealed by the immunoblot analysis with anti-SIRPα mAb SAF17.2, the non-crosslinked SIRPαD1D2D3His had a broad apparent molecular weight in the range of 37-70KD. The shift in gel mobility observed is typical of glycosylation effects. Consistent with the gel filtration analysis, a dimer species (100KD) and an oligomer species (>200KD) were observed after crosslinking (**Figure 3-3C**). These data strongly suggest that under native conditions in solution, SIRPα dimerizes through its extracellular domains.

Interpretation of the recently solved crystal structures of soluble SIRPαD1 suggested the formation of transdimers (66-68). However, subsequent analyses failed to demonstrate dimerization of soluble SIRPαD1 under native condition (66). Given our evidence that the full length ectodomain of SIRPα may dimerize, we tested whether SIRPαD1 also dimerizes under similar conditions. Purified histidine tagged soluble SIRPα membrane distal domain SIRPαD1His with a predicted molecular weight of ~19KD was analyzed using gel filtration chromatography. SIRPαD1His had 4 visible peaks. Two of the peaks were obtained at or near the void volume and contained mostly copurifying contaminants, whereas two other peaks at 158ml (25KD) and 169ml (19KD)

contained the majority of SIRPαD1His (**Figure 3-3A**). Since we could not separate the two peaks completely, they were combined for subsequent analyses. We assumed that the 18KD peak represented monomeric SIRPαD1His and the 25KD peak might represent dimer. In support of this prediction, MALDI-TOF analysis of 18/25KD peaks revealed a single species with a molecular weight of 14KD (**Figure 3-3B**). On immunoblot analysis, the apparent molecular weight of SIRPαD1His ranged from 15-25KD. After crosslinking, a dimer product was apparent at 37KD and oligomers at 55KD (**Figure 3-3C**). Collectively, these data suggest SIRPαD1His forms weak dimers in solution.

We hypothesized that weak dimerization mediated through D1 was not sufficient to account for the robust dimerization observed with the full length ectodomain SIRPαD1D2D3His. This would require significant contributions of SIRPαD2D3 in addition to SIRPαD1 for dimerization. Purified SIRPαD2D3His was thus analyzed using gel filtration chromatography. SIRPαD2D3His eluted as a single peak on gel filtration chromatography with an apparent molecular of 49KD, which is roughly twice the predicted molecular weight (26KD; **Figure 3-3A** and suggests that SIRPαD2D3His is a dimer in solution. In addition, MALDI-TOF analysis revealed a 30KD monomeric species and a 60KD dimeric species **(Figure 3-3B)**. Furthermore, a dimeric species was also detected by immunoblot after crosslinking **(Figure 3-3C)**. These data indicate that the membrane proximal domains of SIRPα also play an important role in mediating dimerization of soluble SIRPα.

Extracellular domains contribute to the dimerization of SIRPα on cell surfaces.

Since soluble ectodomains of SIRPα could form dimers in solution, we performed experiments to verify whether dimerization of full and truncated SIRPα ectodomains could also occur on cell surface. Expression of truncated SIRPα on the surface of transiently transfected CHO cells was verified and followed by crosslinking experiments. Following transfection, surface expression of WTSIRPα, SIRPαD1D2, SIRPαD1, SIRPαD2D3, and SIRPαD3 was assessed by flow cytometry using anti-SIRPαD1 antibody (SAF17.2) and an anti-SIRPαD3 antibody (SAF4.2). All truncated SIRPα proteins were expressed similarly except for SIRPαD16xmyc (**Figure 3-4A**). Immunoblot analyses of crosslinked WTSIRPα, SIRPαD1D2, SIRPαD16xmyc, SIRPαD2D3, and SIRPαD3 on cell surface revealed dimerization and oligomerization (**Figure 3-3B**). However, only a low amount of SIRPαD16xmyc dimers was detected and likely the result of consistently low levels of surface expression after transfection. These data suggest that each domain of SIRPα mediates dimerization, and the collective contribution of individual domains may be important. Furthermore, we hypothesized that if all three domains participate in dimerization, it is likely that the dimers are formed in *cis*.

SIRPα dimerizes in cis on cell surface.

Analyses of the crystal structure have suggested that SIRPαD1 may form dimers *in trans*; however, no studies thus far have confirmed or ruled out this possibility

(66-68). On the other hand, our data on crosslinked SIRPα supports dimerization *in cis* as a more plausible model. Using tagged fusion SIRPα proteins, including SIRPα-GFP and SIRPα-6xmyc, a strategy was devised to test whether dimerization of SIRPa can occur *in trans*. In these experiments, populations of CHO cells expressing individual tagged SIRPa were mixed and cocultured, treated with crosslinker, solubilized and subjected to immunoprecipitation analyses for the presence or absence of individual tagged proteins. In **Figure 3-5A,** it is shown that each of the tags we introduced do not interfere with dimerization in CHO cells that co-express both proteins or in cocultures of cells that express each protein separately. As a positive control, immunoprecipitation was performed with anti-GFP from lysates of CHO cells coexpressing SIRPα-GFP and SIRPα-6xmyc. Both SIRPα-GFP and SIRPα-6xmyc were precipitated with anti-GFP antibody with and without crosslinking suggesting that the SIRPα dimer is stable in the presence of non-denaturing detergent **(Figure 3-5B).** In this scenario, dimers containing both tags could potentially form through either *cis* or *trans* interactions (**Figure 3-5B**). On the other hand, immunoprecipitation with anti-GFP from lysates of co-cultures of CHO cells that separately express each of the tagged proteins precipitated SIRPα-GFP but not SIRPα-6xmyc even after crosslinking (**Figure 3-5B**). The lack of tagged dimers containing both GFP and 6xmyc in this case rules out *trans* interaction. These results further support our data suggesting that SIRPα dimerization occurs through *cis* interaction.

N glycans facilitate SIRPα dimerization.

Previous studies that failed to detect SIRPα dimers utilized only SIRPαD1 and not the full ectodomain (66-68). As shown in figure 3-3B and C above, SIRPαD1 by itself exhibited weak dimerization. However, SIRPαD2D3 forms stronger dimers, as evidenced by the gel-filtration and MALDI -TOF data in figure 3-3B. Furthermore, in one study, SIRPαD1 was produced in *E Coli*, which lacked post translational modifications such as N-linked glycosylation (66). In contrast, the recombinant proteins used in this study were produced in HEK293T cells and retained proper N-linked glycosylation. Thus, we speculated that the discrepancies in SIRPα dimerization may stem from the differences in N-linked glycosylation.

To examine this possibility, SIRPα dimerization was assessed in CHO-SIRPα treated with tunicamycin and kifunensine. Treatment with tunicamycin prevents addition of any polysacharride onto asparagine by inhibiting GlcNAc phosphototransferase (99, 100). On the other hand, treatment with kifunensine arrests the N-glycation at high mannose stage without the addition of terminal structures by inhibiting ER mannosidase (101). To assess the efficacy of the inhibitors, the degree of N-glycation was measured with PHA-L-FITC by flow cytometry (102). In parallel, the surface expression of SIRPα was assessed by flow cytometry to ensure that SIRPα was expressed on the surface and to allow for normalization of protein loading on SDS-PAGE gels for western blots. In CHO-SIRPα treated with tunicamycin, the total amount of N linked glycation was reduced by ~80% as shown by PHA-FITC staining, whereas the expression of

cell surface SIRPα was maintained at ~70% of the levels observed in untreated cells (**Figure 3-6A**). Interestingly, after crosslinking and immunoblot, SIRPα dimerization was greatly inhibited (**Figure 3-6A**). These observations suggest that N-glycans on SIRPα may play an important role in facilitating dimerization.

Several studies recently demonstrated that complex N glycan interactions with lectins may facilitate the formation of higher order molecular complexes (103). Therefore, it is possible that lectin interactions with SIRP□ may be in part responsible for higher order oligomers in the fully glycosylated protein. To test this, we incubated cells with inhibitors of common cell surface carbohydrate-lectin interactions: α-methyl-D-mannoside, which inhibits mannose recognizing C type lectins, and lactose, which effectively blocks galectin interactions (104, 105). However, incubation of CHO cells with either 100mM α-methyl-D-mannoside or 100mM lactose failed to alter SIRPα dimerization **(Figure 3-6B).** Furthermore, incubation of cells with kifunensine, which specifically inhibits the formation of many N glycan modifications required for lectin interactions (101, 106), also failed to alter surface expression or dimerization of SIRPα **(Figure 3-6C)**

Although kifunensine significantly inhibited total cell surface complex N glycan formation, it was not possible to determine whether specific inhibition of complex N glycans on SIRPα also occurred. To further examine the potential role of N glycans in dimerization, we expressed SIRPα in mutant CHO cells that lack enzymes necessary for terminal modification of N-glycans. Specificially, CHO-Lec1 (Mannose rich), CHO-Lec2 (sialic acid deficient), and CHO-Lec8 (galactose deficient) were used (107). However, consistent with kifunensine treated cells,

the dimerization of SIRPα in these CHO cell mutants remained unaffected (**Figure 3-6D**). These results suggest that terminal modifications of N-glycans do not facilitate dimerization even though complete inhibition of the formation of N glycans appears to play an important role in SIRPα dimerization.

SIRPα dimerization is not necessary for binding to soluble CD47.

From these data, we speculated that dimerization of SIRPα may be functionally important in the interaction with CD47. Comparison of the binding affinities of soluble CD47 to monomeric and dimeric SIRPα on cell surface would allow for determination of whether dimeric SIRPα is necessary for CD47 binding. As shown in **Figure 3-6A**, treatment of CHO-SIRPα with tunicamycin resulted in a major reduction in dimerized SIRPα on the cell surface and, by inference, that a majority of SIRPα on the cell surface is in a monomeric state. Binding analyses were then performed on CHO-SIRPα cells grown in the presence or the absence of tunicamycin. Consistent with the flow cytometry analysis (**Figure 3-6A**), the number of SIRPα molecules on the surface of treated CHO-SIRPα was reduced as indicated by the lower Bmax (**Figure 3-7**). More importantly, the binding affinity (Kd) of SIRPα in treated cells was not significantly altered (**Figure 3-7**). Thus, dimerization of SIRPα is not necessary for CD47 binding and does not change affinity of SIRPα for CD47. Furthermore, consistent with the recently published crystal structure of SIRPα.D1 complexed with CD47, the stoichiometry of CD47 binding to SIRPα is one to one (68). By inference, we predict that a

SIRPα dimer can bind to two CD47 molecules suggesting that avidity may have important implications for SIRPα CD47 interactions at the cell surface.

SIRPα dimerization is enhanced in stimulated adherent human PMN.

Given that the majority of our results were obtained using transfected cells, we sought to verify whether SIRPα exists as dimers on cell surface of human PMN that naturally express SIRPα. Human PMNs isolated from normal donors were stimulated with LPS and fMLP, either in suspension or after adhesion to plastic. Stimulation of PMN with LPS and fMLP has previously been shown to alter SIRPα signaling and trafficking (51, 71). We thus assessed SIRPα dimerization by immunoblot from PMN after crosslinking. Interestingly, only traces of dimers were detected on the cell surface of suspended PMNs even under stimulation with LPS or fMLP (data not shown). However, significant dimerization was detected after crosslinking treatment of stimulated adherent PMNs (**Figure 3-8**). These data suggests that dimerization of SIRPα is a regulated physiological event and cellular mechanisms in addition to molecular dimerization may be involved.

Discussion

Recently a series of structural studies and mutagenesis studies reported on molecular mechanisms involved in binding interactions of soluble SIRPα.D1 to CD47 (59, 63, 66-69). Despite these advances, little is known about the mode of interaction between SIRPα and CD47 on cell surface. It was previously shown that SIRPβ is present on the cell surface as a dimer that is covalently linked through a disulfide bond in the most membrane proximal Ig fold. Due to the very high degree of homology between the ectodomains of SIRPα and SIRPβ, we investigated the possibility that SIRPα also dimerizes. SIRPαD1 is an IgV domain, whereas, SIRPαD2 and D3 are categorized by PFAM database as IgC1 domains by virtue of their conservation in protein sequences with other known IgC domains (108). There is only a modest degree of similarity between SIRPαD2 and D3, each only having 57% homologous residues. However, SIRPαD2 and D3 exhibit high degrees of homology to the corresponding domains in SIRPβ and SIRPγ (**Figure 3-1A**). A notable difference in SIRPβD3 is the presence of an extra cysteine residue that forms an intermolecular disulfide bond linking two SIRPβ monomers (9). The formation of such intermolecular disulfide bonds is dependent on intimate noncovalent association between monomers before bond formation. In immunoglobulins, for example, noncovalent association of light chains and heavy chains has been shown to occur before interchain covalent linkage (74-76). The high degree of homology between SIRPα and SIRPβ, led us to hypothesize that SIRPα may form noncovalently linked dimers.

Given that conventional immunoblot analyses require denaturation of proteins in detergents, noncovalently linked protein complexes most often dissociate and thus detection of the dimers is impossible. To circumvent this problem, chemical crosslinkers capable of forming stable covalent linkages between closely associated partners are often used to stabilize dimers under denaturing conditions. BS3, a membrane impermeable homobifunctional crosslinker that reacts specifically with primary amines, has been used extensively for this purpose (109). After crosslinking with BS3, we demonstrate that SIRPα exists as a dimer on cell surface. We excluded the possibility of CD47 as a component of the crosslinked SIRPα complex by demonstrating that the presence or lack of CD47 does not alter the size of crosslinked SIRPa dimers (**Figure 3-2**). Furthermore, mass spectrometry of crosslinked protein did not yield evidence of CD47 in the complex. In support of this hypothesis, the apparent molecular weight of soluble SIRPαD1D2D3 ectodomain estimated by the gel filtration column was approximately twice the predicted molecular weight. Also, the crosslinked dimer of soluble SIRPαD1D2D3 ectodomains was readily detected on immunoblots after resolving by SDS PAGE (**Figure 3-3**). These results strongly suggest that dimerization of SIRPα occurs through the ectodomain under native conditions.

To identify which Ig folds in the ectodomain mediate dimerization, soluble truncated and fully glycosylated ectodomains produced in eukaryotic cells were analyzed by gel filtration chromatography and immunoblots (**Figure 3-3)**. Soluble SIRPαD2D3His eluted from the gel filtration column as a single peak with an

apparent molecular weight that corresponded to a dimer. The presence of SIRPαD2D3 dimers was then verified by immunoblot analysis after crosslinking. Interestingly, soluble SIRPαD1His eluted as two overlapping peaks by the gel filtration column. The species in the lower molecular weight peak approximated the predicted molecular weight; whereas the higher molecular weight species was approximately 10Kd short of the predicted weight of the dimer. Analysis of the pooled protein fractions by MALDI-TOF revealed only the smaller species of SIRPαD1 suggesting that the higher molecular weight species is most likely a weak dimer. Crosslinking studies confirmed the presence of D1 dimers. The fact that SIRPαD1 eluted as both monomer and dimer indicates that dimerization of SIRPαD1 is weak and may account for the lack of others to detect this interaction (66, 67). In our hands, this weak D1 interaction was difficult to detect without stabilization by chemical crosslinkers. In addition, it is worth noting that the preparation of SIRPαD1 used in other studies lacked full N linked glycosylation, which may have also affected the degree of dimerization.

Our findings that both the IgV loop and the IgC loops contribute to the dimerization of SIRPα led us to propose a working model of SIRPα forming *cis* homodimers on the cell surface. This model would predict that in cells that co-express two differently tagged SIRPα, SIRPα dimers containing both tags should be detectable after crosslinking. On the other hand, in a mixture of cells that individually express a single type of tagged SIRPα, crosslinked SIRPα dimers would contain only one type of tag. Indeed, as revealed by our immunoprecipation analysis, SIRPα dimers with two different tags are only

detectable in cells that co-express both tagged SIRPα but not in a mixture of cells that each express a single type of tagged SIRPα (**Figure 3-5**). This finding indicates that dimerization does not occur *in trans*, at least under these conditions. The observation that differentially tagged SIRPα molecules co-precipitated even in the absence of the crosslinker further supports a model of *cis* dimerization.

In our working model, SIRPα dimerizes on cell surface primarily through the IgC folds. A notable precedent that illustrates many modes of *cis* dimerization between IgC folds came from structural studies of immunoglobulins. For example, in IgG there are 4 pairs of IgC folds with 2 identical pairs in the two arms of the Fab2 region, and 2 distinct pairs in the Fc region. The IgC folds in the Fab region pair though noncovalent and covalent linkages. In the Fc region, the residues of one pair of IgC folds (Ch1) do not contact at all. Here, stabilization occurs through weak interactions of glycans and amino acid residues. In contrast, the other pair (Ch2) dimerize though noncovalent interactions between the residues only (110, 111).

It is also possible that the addition of N linked glycans can directly affect the conformation of Ig folds and in turn changes the propensity to dimerize (112, 113). Using pharmacological inhibitors and CHO cell mutants, we found that SIRPα dimerization was inhibited only when all components of N-linked glycosylation were absent (**Figure 3-6**). On the other hand, as maturation of N-linked glycans was arrested in a high mannose stage or terminal modification remained incomplete, dimerization was not affected. These results suggest that

terminal modification of N-linked glycosylation is not likely to facilitate dimerization. In addition, the results of our competitive inhibition assays with soluble disaccharides excluded the possibility that SIRPα dimers are mediated through crosslinking interactions by a third party lectin. Therefore, the most likely role of N linked glycosylation is to maintain a conformation that is favorable for dimerization.

The presence of SIRPα as *cis* dimers on cell surface adds a new dimension of complexity in considering interaction with its ligand CD47. Three mutually exclusive models are possible. First, *cis* dimerization of SIRPα may be independent of CD47 binding. Second, *cis* dimerization of SIRPα may be necessary to form a proper binding site for CD47. Third, *cis* dimerization of SIRPα may block the CD47 binding site thereby inhibiting interaction with CD47. Although the first and second models include dimerized SIRPα binding to CD47, interactions on the cell surface would be considerably different in the first model due to avidity effects from dimerization. In particular, the first model would require one SIRPα to bind to one CD47; whereas the second model would require two SIRPα to bind one CD47. There are several observations from this study and previous studies that strongly support the first model. First, the CD47 binding sites and the sites of *cis* dimerization are compartmentalized structurally. Previous studies have already established that the membrane distal IgV fold of SIRPα is the only site necessary and sufficient in binding CD47 (51, 64-68). In this study, we showed that the membrane proximal IgC folds of SIRPα, that are not important in binding CD47, are important in *cis* dimerization. Furthermore, the

cis dimerization of full length SIRPα occurs despite our extensive mutagenesis of the contacting residues of the SIRPαD1 putative transdimer predicted in the crystal structure, as well as the mutations of the CD47 binding site, or of the "lateral surface" that can indirectly regulate CD47 binding (data not shown). Secondly, the interaction with CD47 and *cis* dimerization are functionally independent. Previous studies have already shown that N-linked glycosylation is not important in SIRPα CD47 binding interactions (58, 61-63, 67). In this report, we show that SIRPα expressed at the cell surface after treatment with tunicamycin is capable of binding CD47 to an extent comparable with controls, even though dimerization was greatly diminished. In other words, the CD47 binding site of membrane bound SIRPα monomers and dimers both appear to exhibit equivalent affinity for CD47. Lastly, the recently published crystal structure of SIRPαD1-CD47 complexes revealed that one SIRPα binds to one CD47 (68). Therefore, it is most likely that SIRPα binding to CD47 and *cis* dimerization both happen independently.

In our attempt to verify our model in primary leukocytes that natively express SIRPα, we observed that the dimerization of SIRPα is likely a regulated process. Specifically, SIRPα dimerization was enhanced in stimulated adherent human PMNs (**Figure 3-8**). In PMNs, SIRPα is present both on cell surface and in the secondary granule fraction (51). It has been proposed that SIRPα is restricted within certain membrane microdomains or possibly tethered to certain cytoskeletal structures, since crosslinking with antibody resulted in the formation of microclusters (41). Interestingly, we did not consistently observe an increase

of SIRPα on cell surface after stimulation of PMNs with LPS or fMLF (data not shown). However, other mechanisms may operate to regulate levels of SIRPα on cell surface. For instance, the ectodomain of SIRPα has been shown to be cleaved by matrix metalloproteases or other means (15, 72). Furthermore, macrophage cell surface SIRPα has been shown to be internalized after stimulation with LPS (71). Additionally, it has been shown that adhesion of leukocytes results in phosphorylation of SIRPα without the engagement of CD47 (114). Therefore, it is more likely that the enhanced dimerization of SIPRα may result from mechanisms such as membrane partitioning or cytoskeletal reorganization. Conversely, the same machinery may also work to prevent dimerizaton in naïve leukocytes.

A major implication of our model of SIRPα *cis* dimerization is the effect of avidity on binding interactions with CD47. A SIRPα *cis* dimer would act as a bivalent receptor, and might enhance signal transduction through more robust interactions with ligands and downstream mediators. Therefore, it is possible that SIRPα interaction with CD47 may work in the same way as B7-1/2 interaction with CD28/CTLA4, in which the interaction of ligand dimers with receptor dimers is enhanced by increased avidity (115). Furthermore, the observation that clustering of SIRPα on human macrophages as well as CD47 on human RBC at the interface between the two cells forming “synapse” like structures regulates inhibition of phagocytosis corroborates with our model (73). However, more investigations are needed to explore the possibility that CD47 is also present as dimers on cell surface. It is possible that CD47 clusters to form local

concentrates on cell membrane through association with other molecules, such as integrins, that are capable of clustering (28, 40).

Our model raises an interesting question: why would activated neutrophils exhibit enhanced sensitivity to CD47 signaling through increased SIRPα dimerization? As PMNs are recruited from circulation, they must traverse tissues to reach sites of injury of pathogen invasion. It is possible that the enhancement of SIRPα dimerization in stimulated PMNs may provide the necessary level of inhibitory signals to keep their activation in check in order to prevent unnecessary damage to tissues.

In conclusion, we demonstrate that soluble SIRPα ectodomains and cell surface SIRPα form noncovalently linked dimers. We provide evidence that SIRPα dimerization is a regulated physiological event that has important implications. Elucidation of molecular mechanisms involved in dimerization of SIRPα will require further detailed structural and mutagenesis studies of the D2D3 domains of SIRPs. Generation of reagents that can manipulate SIRPα dimerization will advance understanding of the functional roles of SIRPα in cells and may facilitate development of novel immunoregulatory therapies.

Figure 3-1.

A.

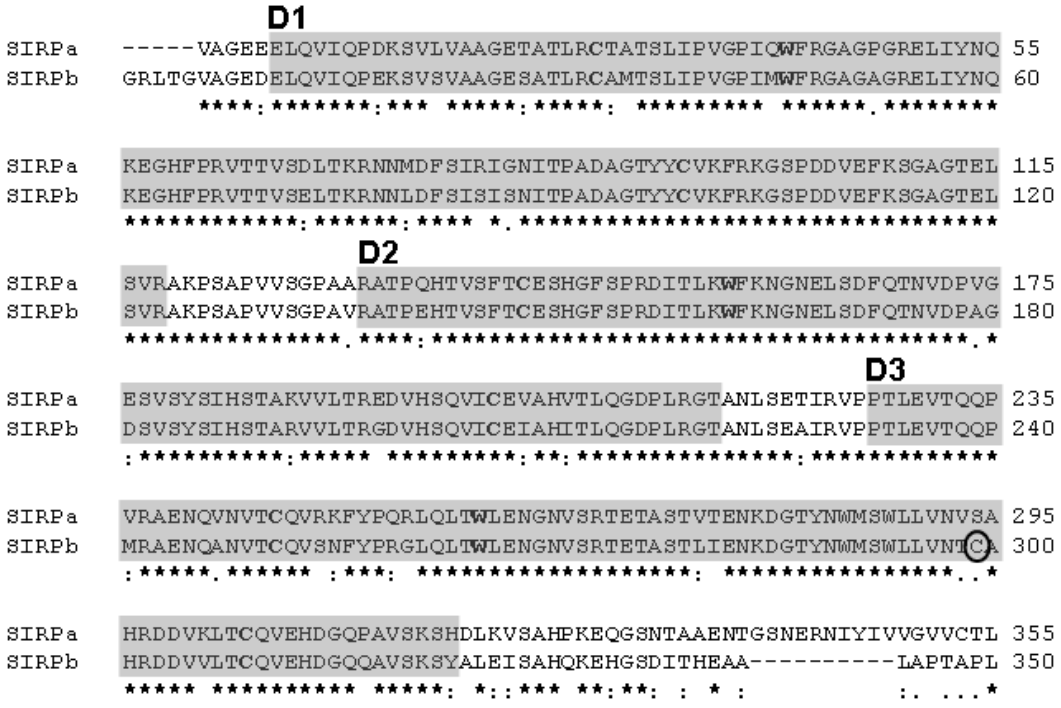

	Identifical (%)	Conserved Changes (%)	Homology (%)
Ectodomain	84.7	8.7	93.4
D1 (IgV)	91.7	5.3	97.0
D2 (IgC)	91.8	7	98.8
D3 (IgC)	83.5	10.2	93.7

Figure 3-1.

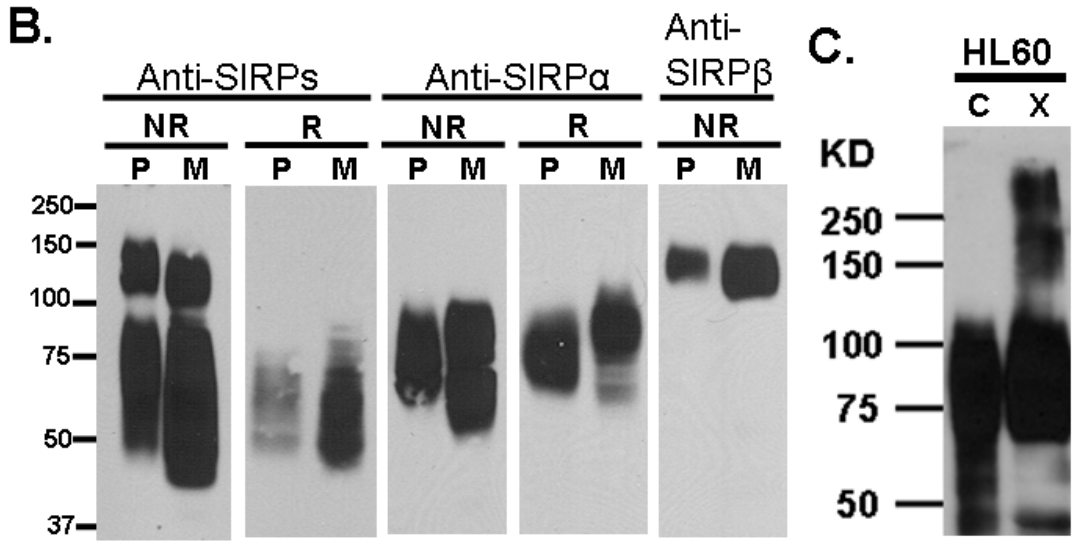
B.
Anti-SIRPs
Anti-SIRPα
Anti-SIRPβ
NR
R
NR
R
NR
P M P M P M P M P M
250
150
100
75
50
37
C.
HL60
C X
KD
250
150
100
75
50

Figure 3-2.

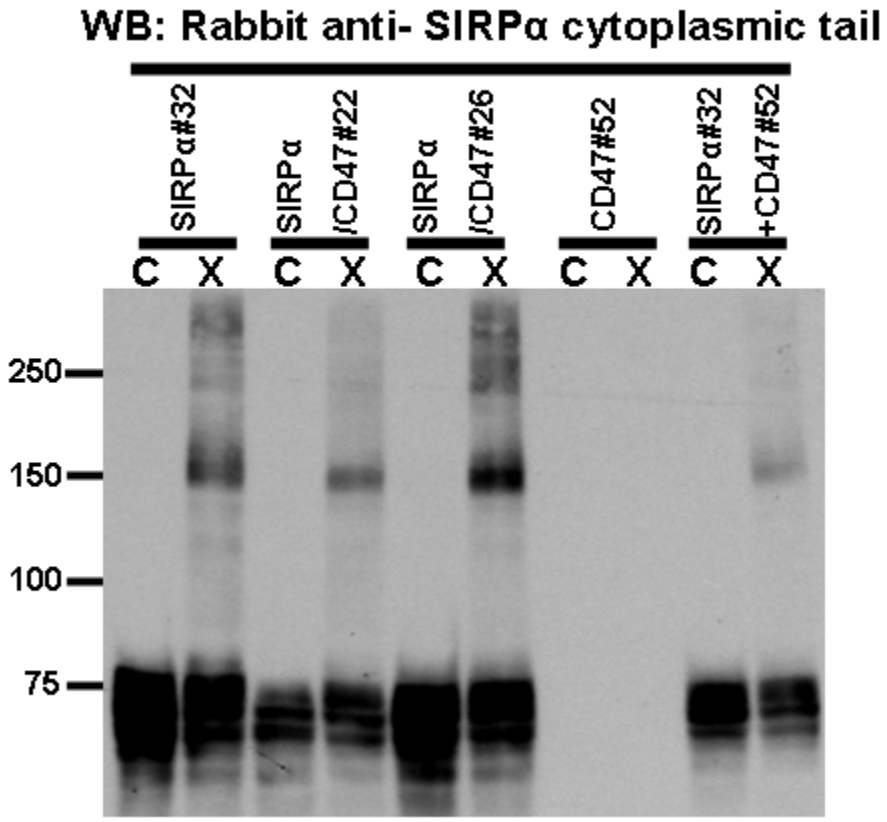
WB: Rabbit anti- SIRPα cytoplasmic tail
SIRPα#32
SIRPα /CD47#22
SIRPα /CD47#26
CD47#52
SIRPα#32 +CD47#52
C X C X C X C X C X
250
150
100
75

Figure 3-3.

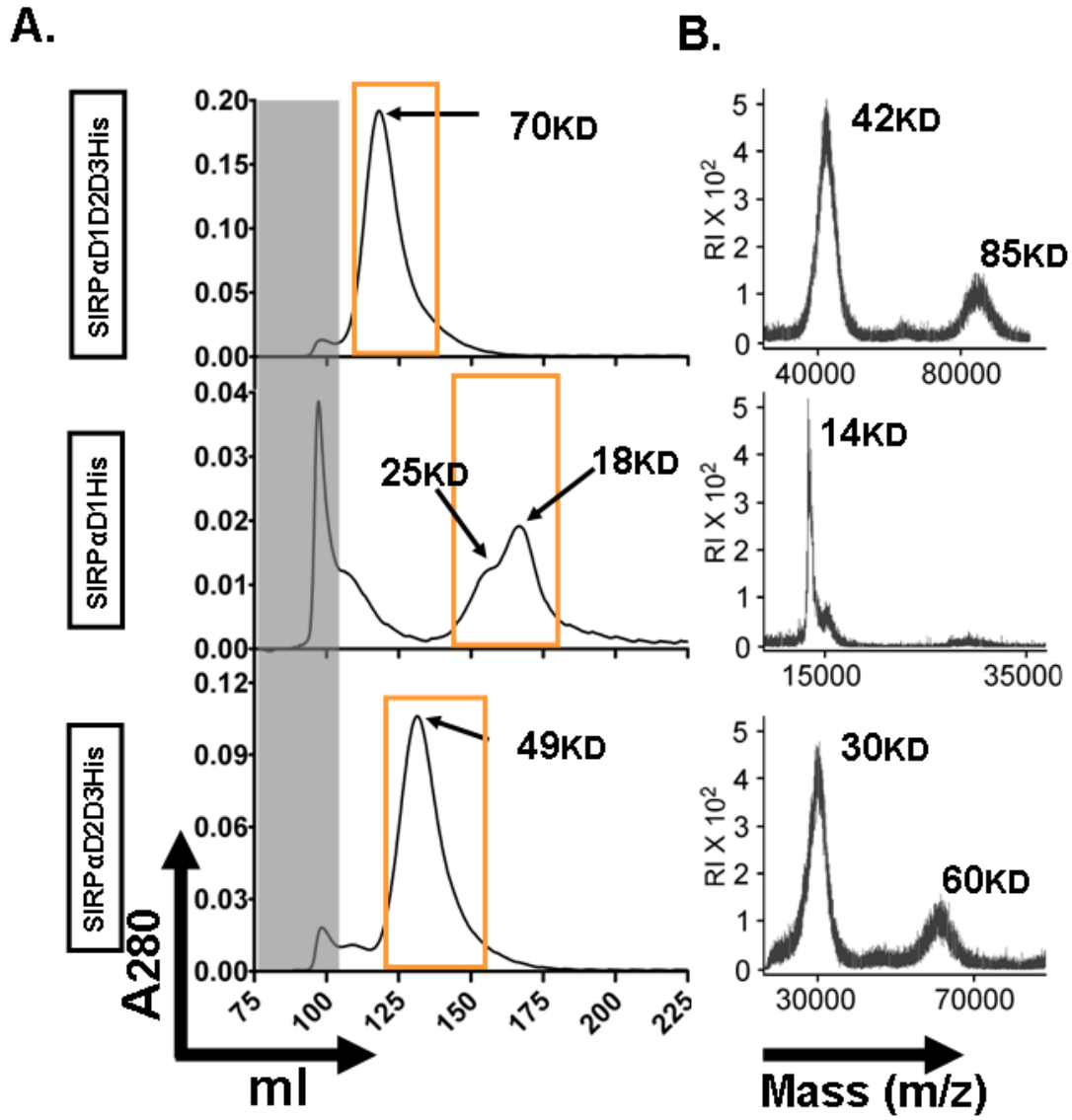
A.
B.
SIRPαD1D2D3His
SIRPαD1His
SIRPαD2D3His
70KD
25KD
18KD
49KD
42KD
85KD
14KD
30KD
60KD
A280
ml
RI X 10²
Mass (m/z)

Figure 3-3.

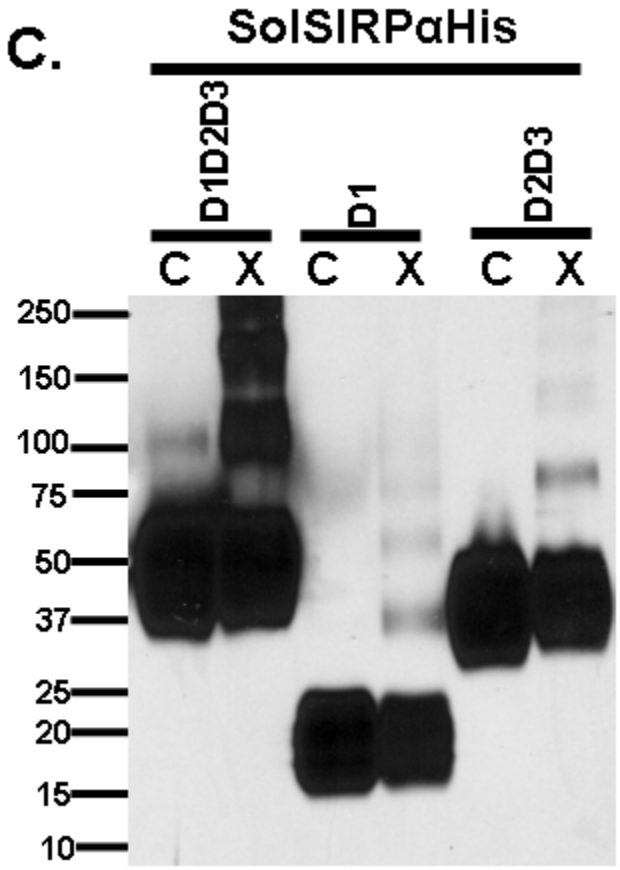
C.
SolSIRPαHis
D1D2D3
D1
D2D3
C
X
C
X
C
X
250
150
100
75
50
37
25
20
15
10

Figure 3-4.

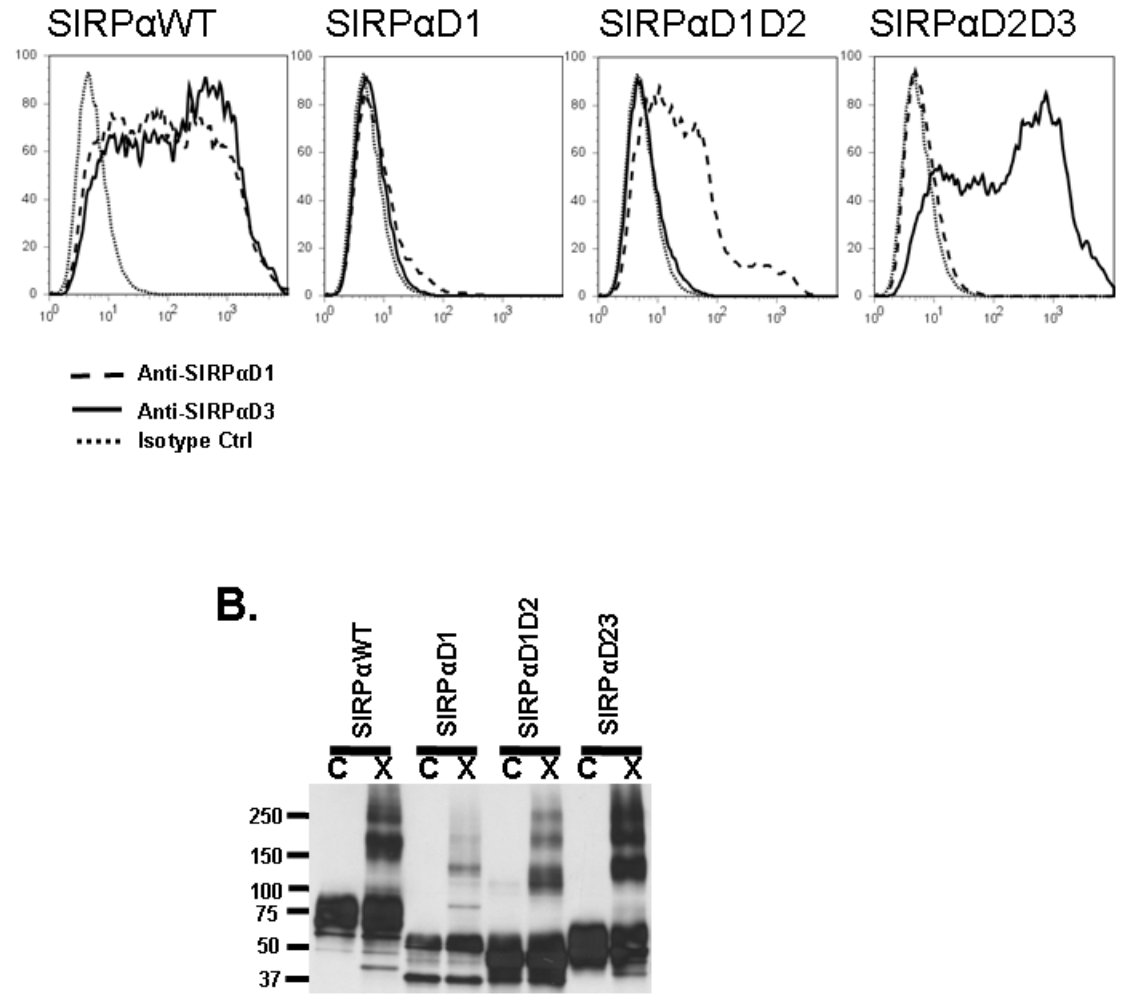
A.
SIRPαWT
SIRPαD1
SIRPαD1D2
SIRPαD2D3
Anti-SIRPαD1
Anti-SIRPαD3
Isotype Ctrl
B.
SIRPαWT
SIRPαD1
SIRPαD1D2
SIRPαD23
C X C X C X C X
250
150
100
75
50
37

Figure 3-5.

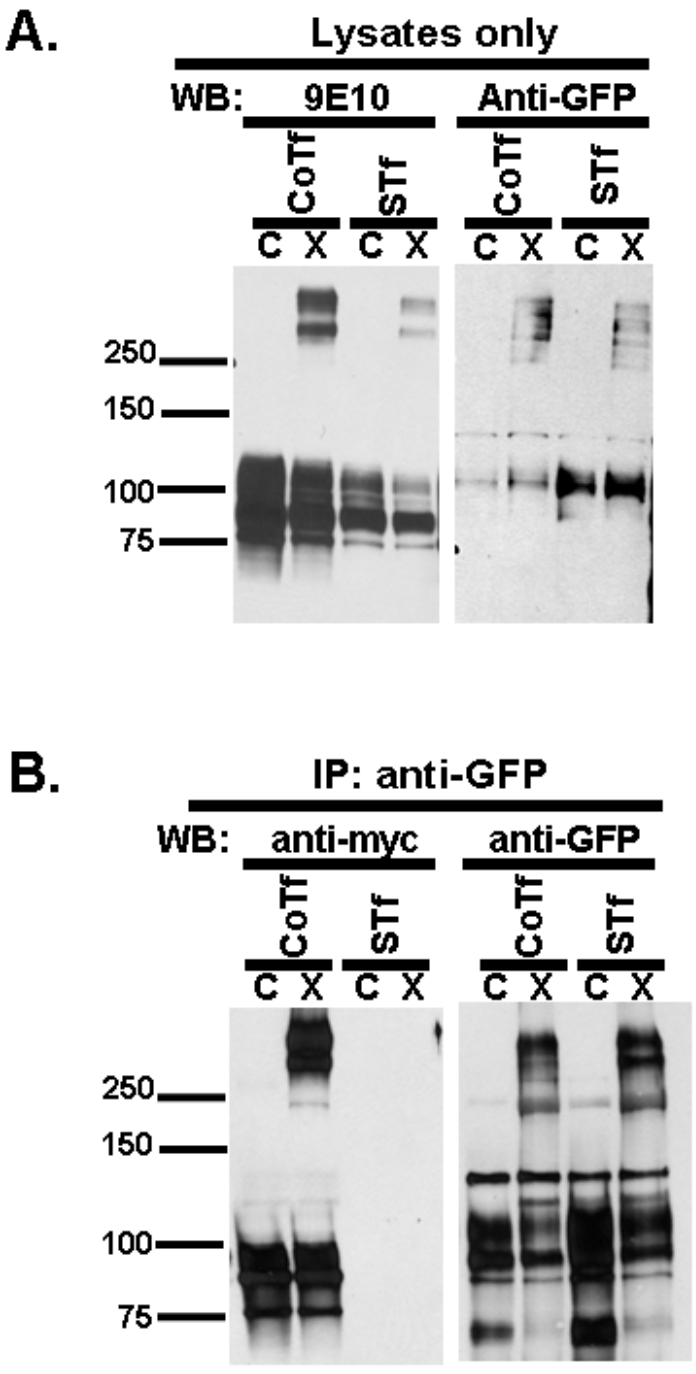
A.
Lysates only
WB:
9E10
Anti-GFP
CoTf
STf
CoTf
STf
C X C X C X C X
250
150
100
75
B.
IP: anti-GFP
WB:
anti-myc
anti-GFP
CoTf
STf
CoTf
STf
C X C X C X C X
250
150
100
75

Figure 3-6.

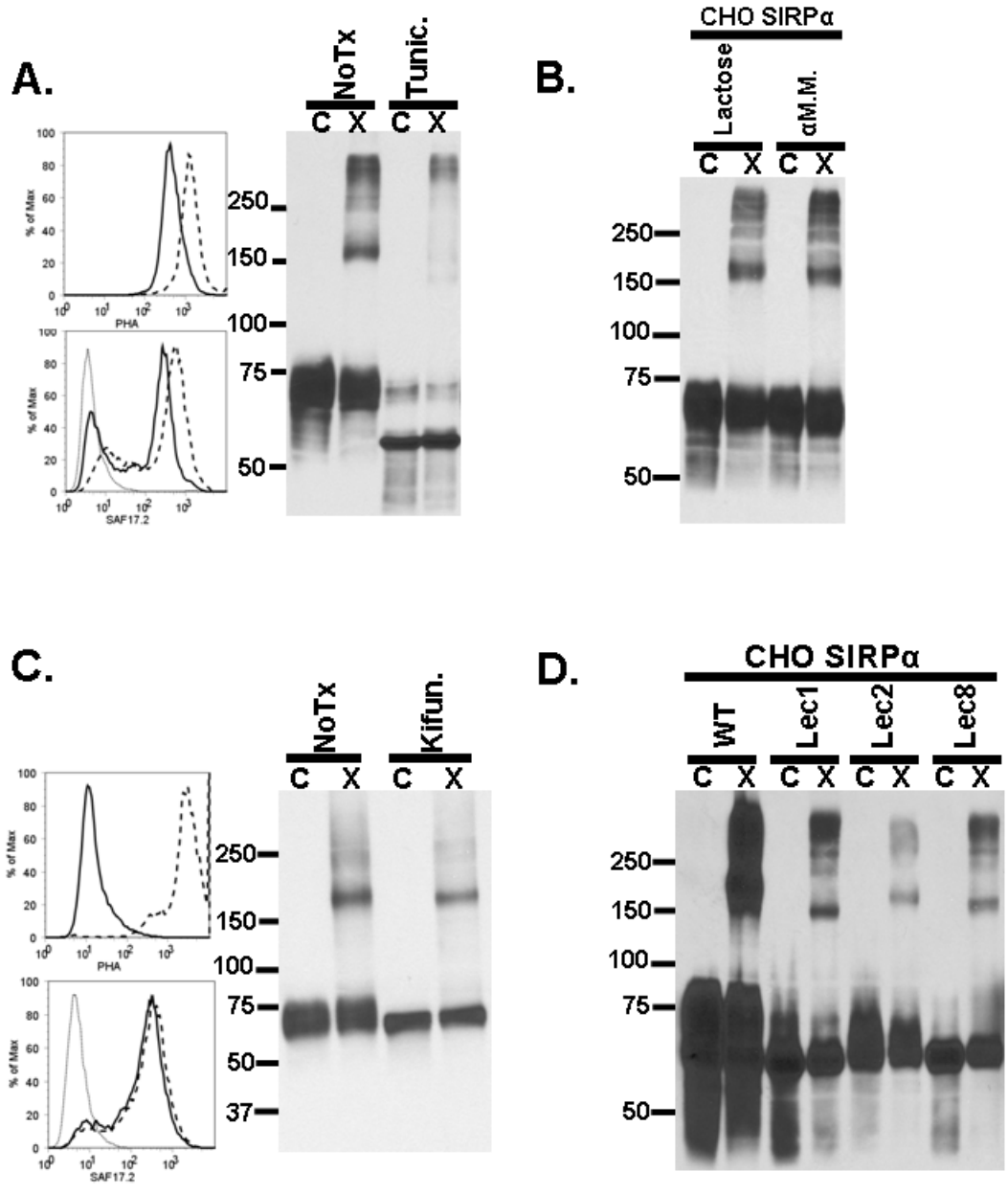
A.
NoTx
Tunic.
C X C X
250
150
100
75
50
% of Max
PHA
SAF17.2
B.
CHO SIRPα
Lactose
αM.M.
C X C X
250
150
100
75
50
C.
NoTx
Kifun.
C X C X
250
150
100
75
50
37
% of Max
PHA
SAF17.2
D.
CHO SIRPα
WT
Lec1
Lec2
Lec8
C X C X C X C X
250
150
100
75
50

Figure 3-7

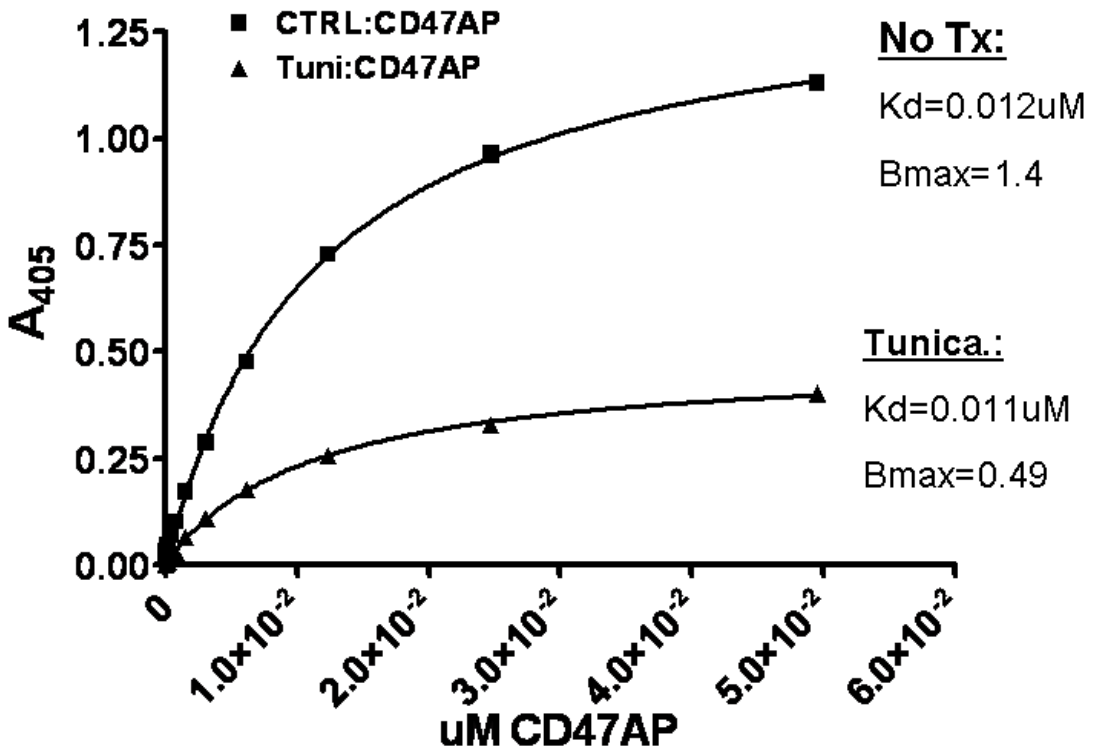
CTRL:CD47AP
Tuni:CD47AP
No Tx:
Kd=0.012uM
Bmax=1.4
Tunica.:
Kd=0.011uM
Bmax=0.49
A405
1.25
1.00
0.75
0.50
0.25
0.00
0
1.0×10-2
2.0×10-2
3.0×10-2
4.0×10-2
5.0×10-2
6.0×10-2
uM CD47AP

Figure 3-8

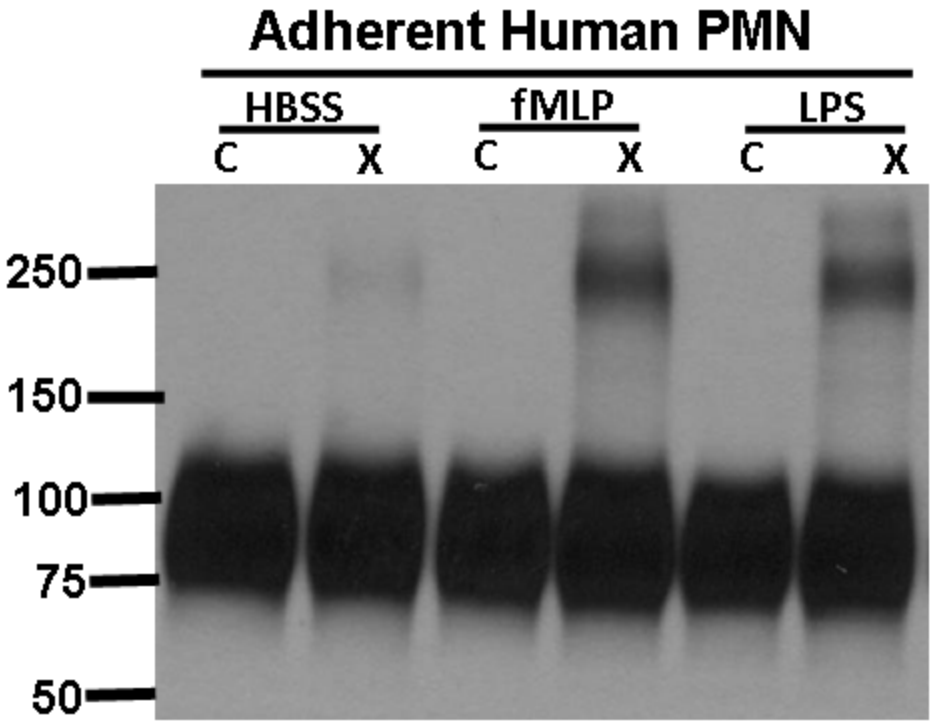

Figure Legends:

Figure 3-1. SIRPα is highly similar to SIRPβ and dimerizes after chemical crosslinking in HL60 cells. **A.** Alignment of SIRPα and SIRPβ ectodomains revealing identical (stars) and conserved (dots) residues. The peptide sequences that represent each of the Ig folds as defined by PFAM databases and the crystallization study are enclosed in gray boxes. The cysteine and tryptophan residues conserved in Ig folds are in bold. SIRPβ dimerization is mediated through a disulfide linkage at cysteine residue C299 (circled) as previously reported. **B.** Immunoblots of human PMN and monocyte lysates under non-reduced (NR) and reduced (R) conditions with murine monoclonal anti pan-SIRPs antibody (SAF10.1), rabbit polyclonal antiserum against SIRPα cytoplasmic tail (anti-SIRPαCT), and murine monoclonal anti-SIRPβ (B4B6). Anti-SIRPβ antibody was unable to detect SIRPβ under reducing conditions (data not shown). **C.** Immunoblot analysis using a rabbit polyclonal antibody against the SIRPα cytoplasmic tail detecting noncovlanetly linked SIRPα dimers after treatment of HL60 cells with a cell membrane impermeable chemical crosslinker BS3.

Figure 3-2. The crosslinked SIRPα complex does not contain CD47. **A.** A flow cytometrric analysis of stable CHO cell transfectants expressing SIRPα, CD47, or both molecules (co-expressing clones #22 and #26) confirmed surface expression of the recombinant proteins after labeling with murine monoclonal anti-SIRPαD1 antibody (SAF17.2) and murine monoclonal anti-CD47 antibody

(C5D5). **B.** An immunoblot analysis of the stable CHO cell transfectants demonstrating that the apparent molecular weight of the crosslinked SIRPα complex does not change in the presence of human CD47.

Figure 3-3. The IgC folds of SIRPα ectodomains are critical for dimerization of SIRPα. Soluble full-length and truncated ectodomains tagged with 10 Histidines were produced in HEK293T cells and purified using Ni-NTA columns. **A.** Gel filtration chromatograpy analysis demonstrating that full-length SIRPα ectodomain (SIRPαD1D2D3His) with a predicted molecular weight of 38kD eluted as a single peak with an apparent MW of 70kD. SIRPαD1His (membrane distal IgV fold) has a predicted MW of 16KD but eluted as two major peaks with apparent MWs of 25KD and 18KD. SIRPαD2D3His, (membrane proximal IgC folds) has a predicted MW of 26KD but eluted as a single peak with an apparent MW of 49KD. Void volume is indicated by the gray shaded area. **B.** MALDITOF analysis of the eluted recombinant SIRP proteins. As can be seen, SIRPαD1D2D3His consisted of monomers at 42KD and dimers at 85KD, and SIRPαD2D3His consisted of monomers at 30KD and dimers at 60KD. In contrast, SIRPαD1His consisted of only monomers at 16KD. **C.** Immunoblot analysis of purified SIRPα proteins using rabbit antiserum against the full length SIRPα ectodomain confirming the presence of noncovalently linked dimers after crosslinking with BS3.

Figure 3-4. All three Ig folds of SIRPα ectodomain participate in dimerizaton on the cell surface. Membrane bound SIRPα with full-length or truncated ectodomains were expressed transiently in CHO cells. **A.** Flow cytometric analysis of surface expression. Each transfectant was probed with murine monoclonal anti-SIRPαD1 (SAF17.2; dashed), anti-SIRPαD3 (SAF4.2; solid), and an isotype control (dotted). **B.** Immunoblot analysis with rabbit antiserum against the full length SIRPα ectodomain demonstrating that membrane bound WTSIRPα, SIRPαD16xmyc, and SIRPαD2D3 dimerize on the cell surface after crosslinking with BS3.

Figure 3-5. SIRPα forms homodimers *in cis* on the cell surface. Crosslinked SIRPα dimers from a mixture of CHO cells that separately expressed SIRPα-EGFP and SIRPα6xmyc (STf) were compared with dimers from a culture of CHO cells that were co-expressing SIRPα-EGFP and SIRPα-6xmyc (CoTf). **A.** Immunoblots of STf and CoTf cell lysates were probed with a murine monoclonal anti-myc antibody (9E10; left blot) and with a rabbit polyclonal anti-EGFP antibody (right blot) after crosslinking, demonstrating that the EGFP and myc tags did not interfere with SIRPα dimerization. **B.** Immunoprecipitation of non-treated and crosslinked cell lysates of STf and CoTf with polyclonal rabbit anti-EGFP antibody and probed with anti-myc antibody in order to determine the presence of SIRPα dimers that contain both 6xmyc and EGFP tags (left blot). As a positive control for immunoprecipitation, proteins precipitated by the rabbit

polyclonal anti-GFP antibody were also probed with the same anti-GFP antibody (right blot).

Figure 3-6. SIRPα dimerization is disrupted after treatment with tunicamycin. (**A**) Flow cytometric analysis of tunicamycin treated CHO-SIRPα transfectants labeled with PHA-L-Fitc (left upper subpanel) to measure the degree of deglycosylation, and with anti-SIRPαD1 (SAF17.2; lower left subpanel) to assess the level of SIRPα expression. After crosslinking, treated cells were analyzed by immunoblots for the presence of SIRPα dimers. (**B**) Immunoblot after crosslinking demonstrating that SIRPα on CHO cells still dimerized in the presence of 100mM α methyl-D-mannoside or 100mM lactose which were added to competitively inhibit potential dimerization by multivalent mannose or galatose binding lectins. (**C**) Flow cytometric analysis of kifunenzine treated CHO-SIRPα transfectants labeled with PHA-L-Fitc (left upper subpanel) to measure the degree of deglycosylation, and with anti-SIRPαD1 (SAF17.2; lower left subpanel) to assess the level of SIRPα expression. After crosslinking, treated cells were analyzed by immunoblots for the presence of SIRPα dimers. (**D**) Immunoblot after crosslinking demonstrating that SIRPα expressed in mutant CHO cells lacking enzymes necessary for terminal modification of N-glycans, such as, Lec1 (mannose rich), Lec2 (sialic acid deficient), and Lec8 (galactose deficient), can still dimerize.

Figure 3-7. Dimerization of SIRPα is not required for binding to CD47. Serial dilutions of cell supernatants containing known concentrations of soluble CD47 fused with alkaline phosphatase (CD47AP) were assessed in binding assays to cell surface-expressed SIRPα in tunicamycin treated or nontreated control CHO-SIRPα cells grown in 96 well tissue culture plates. Analysis of binding curves for affinity constant (Kd) and maximal binding value (Bmax) was performed with PRISM software.

Figure 3-8. SIRPα dimerization is enhanced in stimulated adherent human PMNs. Immuoblot of cell lysates from noncrosslinked and crosslinked human blood PMNs stimulated with vehicle, 10^{-6}M fMLP, or 1μg/ml of LPS for 20 minutes at 37ºC after adhesion to plastic tissue culture wells. The crosslinked dimers were detected with polyclonal rabbit antiserum against SIRPα cytoplasmic tail.

Chapter 4

Discussion and Future Direction

SIRPs, as a paired receptor family, include activating and inhibitory members that are highly similar in their ectodomains. Understanding how the members of the paired receptor family interact with their perspective ligands is critical in elucidating the roles of these receptors in cellular functions. The goal of this work is to further our understanding on how the inhibitory member, SIRPα, interacts with CD47. Despite the high degree of homology in their ectodomains, SIRPα, but not SIRPβ, binds to CD47 (5, 8). Furthermore, SIRPαD1 alone is sufficient to mediate CD47 binding (9, 51, 63-68). Taking these observations together, we hypothesized that the unique residues in SIRPαD1 account for its specificity to recognize CD47. Using site directed mutagenesis and *in vitro* binding assay, we identified residues in SIRPαD1 that were critical in binding CD47. However, it was not possible to discern whether these critical residues directly interact with CD47 or are important in maintaining the conformation of SIRPαD1.

In addition to SIRPαD1, the non-ligand binding domains (D2D3) of SIRPα also exhibited a remarkable degree of homology with corresponding domains in SIRPβ (**Figure 3-1**). The high degree of homology may signify a conserved theme in structure. SIRPβ is known to be present on cell surface as a dimer linked covalently through a disulfide bond at D3 (9). Although SIRPα lacks the

necessary cysteine in D3, it is still possible that SIRPα may be present as a dimer through noncovalent interactions. Through our biochemical analysis, we found that SIRPα on cell surface can dimerize *in cis* through noncovalent interactions at the ectodomains. We also found the SIRPα dimerization on neutrophil surface was enhanced after stimulation with bacterial derived products such as fMLP and LPS. Yet it remains unclear whether the dimerization of the inhibitory receptors SIRPα is enhanced to potentially deliver stronger inhibitory signals in activated PMNs.

The recently published structures of SIRPαD1-CD47IgV complex directly identify the molecular interactions involved in binding CD47, and elucidate mechanisms that confer the specific recognition of CD47 by SIRPαD1 (68). This set of important data also provides us a frame work to examine how mutations of the critical residues in SIRPαD1 abolish binding to CD47, as discussed below. The refined understanding of the SIRPα-CD47 interaction coupled with our novel observations of SIRPα dimerization on cell surface led us to propose a working model of how SIRPα may function in leukocytes in the section below.

Direct and indirect effects of SIRPα critical residues in the recognition of CD47

As described in Chapter 2, we investigated our hypothesis that the unique residues in SIRPαD1 are critical in binding CD47 by substituting them with the corresponding residues in SIRPβD1. At the time of the study, the crystal structure of SIRPαD1 was not available. Homology modeling of SIRPαD1

revealed the topological relationship among the unique residues and allowed the identification of additional critical residues that are common to both SIRPαD1 and SIRPβD1. We identified 8 critical residues: Q8, T26/V27, Q37, R69, S66, M72, and S75. As the solution of the SIRPαD1 crystal structure became available, six (Q8, T26/V27, S66, M72, and S75) of the eight critical residues were mapped to a region bordering the loops and the beta strands of the beta sheets formed by strands ABED—overlapping greatly with the putative transdimerization site. The region identified by us is distinct from the region identified by Hatherley et al, which is located in the flexible loops BC, DE, and FG (63, 67). Mutation of a residue can exert its effect in two possible ways. First, the mutation can eliminate the direct interaction between the residue and the ligand. Alternatively, the mutation can cause a change in the conformation of the protein thereby affect binding of the ligand indirectly. It was impossible to discern how the mutations in the two regions function without the solution of the crystal structure of SIRPαD1-CD47 complex.

The recently published structures of SIRPαD1-CD47 complex provide us a framework to discuss the roles of our critical residues on SIRPαD1 in binding CD47 (68). It was found that CD47 docks at the region containing the flexible loops as previously described by Hatherley et al. Therefore, residues S66, R69, and T26/V27, which directly interacts with CD47, have already been discussed in detail (please see introduction for a brief summary; (68)). However, understanding how the mutations of the remaining critical residues (Q8, Q37, M72, and S75) also abolished binding has not been explored.

Residues Q8, Q37, and S75, are located distal to the CD47 binding site and are likely to be important in maintaining the conformation of SIRPαD1 (**Figure 4-1**). In particular, the sidechain of Q8 points inward and forms contact with W38, which is conserved in all Ig like structures and is important for packing the disulfide bond to allow the formation of the beta sheet sandwich (**Figure 4-2**). Additionally, the sidechain of Q8 also exhibits hydrogen bond potentials with T109 on strand G, and the backbone of Y89 on strand F. Therefore, the mutation of Q8 to leucine will likely change how the beta sheets are stacked and will possibly deviate the relative positions of strands F and G, thereby affecting the conformation of SIRPαD1.

The effect of mutation Q37M can be best explained by comparing the crystal structures of SIRPαD1 (pbd id:2UV3) to SIRPβD1 (2JJU). The sidechains of Q37 in SIRPαD1 and M37 in SIRPβD1 are both situated in a hydrophobic pocket surrounded by the sidechains of P35, F39, L48, and F94 (**Figure 4-3**). However, in SIRPαD1, Q37 can interact with K53 on C'D loop through a hydrogen bond, which is missing in SIRPβD1. Consequently, despite the identical peptide sequences of the C'D loops in SIRPα and SIRPβ, the orientations of the sidechains off C'D loops (especially Q52, K53, and E54) of both proteins are entirely different. As a result, mutation of Q37 to M leads to a disruption of interaction of the C'D loop of SIRPαD1 with the FG loop of CD47, and may represent another mechanism that prevent SIRPβ from binding CD47.

In the case of residue S75, it is less clear as to how mutation to leucine disrupts the conformation of SIRPαD1 and prevents binding of CD47. The

sidechain of S75 may form intramolecular hydrogen bonds with N73 (also on DE loop) or H24 (on strand B). However, the interaction with H24 is probably not important since mutation of H24 to leucine or asparagine did not abolish CD47 binding. Therefore, it is conceivable that the interaction of S75 with N73 is important in keeping the DE loop in the proper orientation for CD47 binding.

In contrast to the aforementioned residues, M72, located on DE loop, is near the CD47 binding site, but does not appear to contact CD47 residues directly. As mentioned in Chapter 2, the effect of M72 mutation is dependent on the sidechain of the mutant residues. Normally, the sidechain of M72 forms intramolecular hydrophobic interactions with the sidechains of L30 and V27, which are CD47 contacting residues on the BC loop and the B strand (**Figure 4-4**). When substituted with alanine, the shortened sidechain was not likely to maintain interaction with the BC loop and thereby abolished binding to CD47. On the other hand, substitution with leucine, which has a longer sidechain capable of maintaining the original hydrophobic interactions, had no effect. Intriguingly, substitution with arginine enhanced binding. The sidechain of arginine contains a chain of aliphatic hydrocarbons that is equivalent in length to the sidechain of leucine and can form stabilizing hydrophobic interactions with the BC loop. Given that the sidechain of arginine is longer than methionine, the extra length may be sufficient to allow its positively charged terminus to directly interact with pyroglutamate at the N terminus or T102 on the FG loop of CD47 through hydrogen bond. These additional interactions may lead to an increased binding to CD47.

Our analyses indicated that mutations of our critical residues disrupt CD47 binding indirectly by altering the conformation of the important elements in the CD47 binding site on SIRPαD1. Therefore, the region containing our critical residues plays an important role in maintaining the conformation of SIRPαD1 permissible for interaction with CD47. It is important to note that in the first crystal structure (pdb code: 2uv3) of SIRPαD1, our critical residues mainly located in the putative transdimerization region (strands ABDE and DE loop)(67), which was thought to be an artifact of crystallization. It was unclear at that time what effect this putative transdimerization site has on the overall conformation of the structure. This question becomes especially important in interpreting the CD47 binding site in the crystal structures of SIRPαD1-CD47 complex. To answer this question, we examined two crystal structures (pdb codes: 2JJS and 2JJT) of SIRPαD1-CD47 complex available through the Protein Database Bank (**Figure 4-5**) (68). In 2JJT, although the SIRPαD1 is present as a dimer, the angles between the monomers and the sites of dimerization (C'D loop and C' strand) are entirely different from 2UV3. Further comparison of 2JJT and 2uv3 revealed that the sites of dimerization in both structures, although extensive, were defined mainly through nonspecific hydrophobic interactions with few directional charged or polar interactions. On the other hand, in 2JJS, the contacts between SIRPαD1 monomers are minimal. Even though the 2JJT structure suggests dimerization of SIRPαD1, the conformation of a single SIRPαD1-CD47 complex in either 2JJS or 2JJT is essentially identical, suggesting that the effect of dimerization on the conformation of the CD47 binding site is minimal.

Implications of SIRPα *cis* dimers in PMN functions

As described in Chapter 3, our biochemical analyses of recombinant SIRPα ectodomains and full length SIRPα expressed on cell surfaces revealed that SIRPα can form cis dimers through interactions of the ectodomains, especially D2 and D3. Interestingly, SIRPα dimers were enhanced on adherent PMNs stimulated with bacterial products, suggesting that SIRPα dimerization can be regulated. Our finding that SIRPα dimers on cell surface bind to CD47 with an affinity comparable to SIRPα monomers indicated two important properties of SIRPα dimers: 1) dimerization of SIRPα does not hinder the access of CD47 to the CD47 binding site on SIRPαD1, and 2) a SIRPα dimer is likely to be able to bind two CD47.

As a model for SIRPα function, the bivalent nature of SIRPα dimer can increase both the avidity in binding CD47 extracelullarly as well as the recruitment of SHP-1 intracellularly, thereby amplifying the strength and duration of the inhibitory signal. In addition, SIRPα dimers may cluster CD47 on the opposing cells and strengthen the signals transmitted by CD47. In support of this model, it was reported that clustering of macrophage SIRPα and RBC CD47 at the contact between the two cells can result in the recruitment of SHP-1, which can effectively dephosphorylate myosin heavy chains to prevent phagocytosis of the RBC (73). Along the same line, we believe that dimerization of SIRPα also function in the same way to amplify the inhibitory signals in neutrophils.

It is tantalizing to think: why is the dimerization of SIRPα—an inhibitory receptor, enhanced in activated adherent PMNs? We believe that the enhancement in inhibitory signals is necessary to minimize damages to self by activated PMNs. In an inflammatory setting, such as bacterial induced colitis, PMNs are recruited from the circulation, and they must traverse a great distance through self tissues, guided by gradients of chemoattractants, before reaching the site of infection (77). The immunopathology of these inflammatory diseases is often focused at the site of infection, suggesting that the effector functions of PMNs such as oxidative burst and release of proteases occurs significantly later after migration across self tissues (116). The chemotaxis of PMNs has been studied extensively *in vitro*. However, under *in vitro* conditions, exposure of PMN to chemoattractants not only induces migration but also elicit significant effector responses (116-119). Comparison of the two scenarios suggests anecdotally that PMNs while in transit through tissues may be able to sense “self” and modulate effector functions to minimize damages to tissues. A similar instance of inhibition by sensing self has been reported in macrophages. Macrophages are highly phagocytic, yet they do not engulf other macrophages even if highly stimulated. The intercellular homophilic interactions of PECAM (CD31), which contains both ITIM and ITAM in its cytoplasmic tail, provides the inhibitory signal to prevent uptake of neighboring macrophages (120). In fact, under homeostatic conditions, the interaction of macrophage SIRPα with ubiquitously expressed tissue CD47 prevents bystander clearance of viable cells (described in Introduction; (18, 42, 53)). In both instances, the inhibitory effects are mediated

through SHP1. Furthermore, PMNs stimulated by chemoattractant not only mobilizes intracellular reservoirs of SIRPα in granules to cell surface, but also enhances the formation of SIRPα dimers. Therefore, we believe that these mechanisms allow SIRPα to transmit the necessary inhibitory signals in activated PMNs to minimize injury to self tissues.

Conclusion and future directions

Our investigations of SIRPα interactions revealed a modular nature of structure and function in the Ig folds of SIRPα ectodomain. SIRPαD1 serves as the ligand binding domain; whereas SIRPαD2D3 contributes strongly to dimer formation. Since the onset of this project, the molecular mechanisms of SIRPαD1-CD47IgV interactions have been explored in details through analyses of the crystal structures of SIRPαD1-CD47IgV complex as well as the mutagenesis studies by us and others. In light of recent advances in elucidating the physiological functions of SIRPα-CD47 interaction *in vivo*, the molecular details of how SIRPαD1 binds CD47 will foster the possibility of developing small compound inhibitors that may have potential therapeutic applications. Formation of SIRPα *cis* dimers through Ig folds, especially D2D3, in the ectodomains is a novel finding that adds a new layer of complexity to SIRPα-CD47 interactions on cell surface. In the model described above, we extrapolated the physiological implications of SIRPα dimerization on cell surface. However, it has not been formally demonstrated that the clustering of SIRPα and CD47 at cellular contact can induce an effect on signaling in a manner similar to

receptors in an immune synapse. To do so, we have to first determine whether clustering of SIRPα at cellular contact is mediated through dimerization. Second, it is unknown if interaction with CD47 on an opposing cell surface can induce SIRPα dimers formation. Third, it is important to know the mechanisms that can enhance SIRPα dimerization, such as phosphorylation of ITIM or cytoskeletal rearrangement. Last but not least, it remains to be determined whether the avidity effect of SIRPα dimers both in binding CD47 and recruitment of SHP1 can enhance inhibitory signals. To answer these questions, Förster resonance energy transfer based microscopy techniques will be needed in order to perform studies in intact cells and to identify dimerization of SIRPα that are tagged with paired donor and acceptor, such as CFP and YFP. We believe that these experiments will provide important insights into the physiological functions of SIRPα dimers.

Understanding the structural basis of SIRPα dimerization is an important topic that will provide us with a more complete picture of the molecular properties of SIRPα. To do so, it would require the solution of glycosylated SIRPα full length ectodomain crystal structures. Such information would allow us to deduce how the non ligand binding domains are influencing the orientation of the ligand binding domain of SIRPα on cell surface. The analysis of the SIRPα dimer structure will also identify the structural elements involved in dimerization and allow us to generate valuable tools, such as nondimerizing SIRPα, that can advance our understanding of the physiological functions of SIRPα dimers.

Figure 4-1.

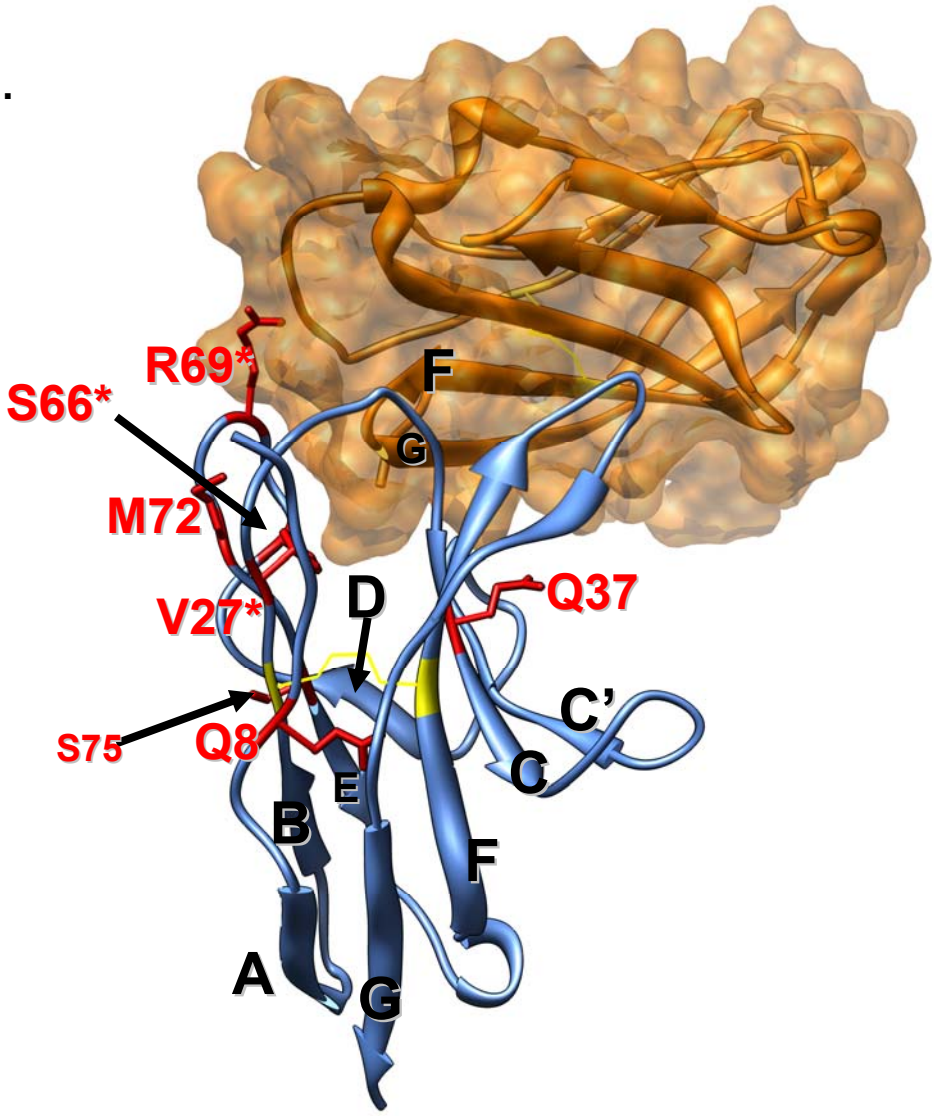

Figure 4-2.

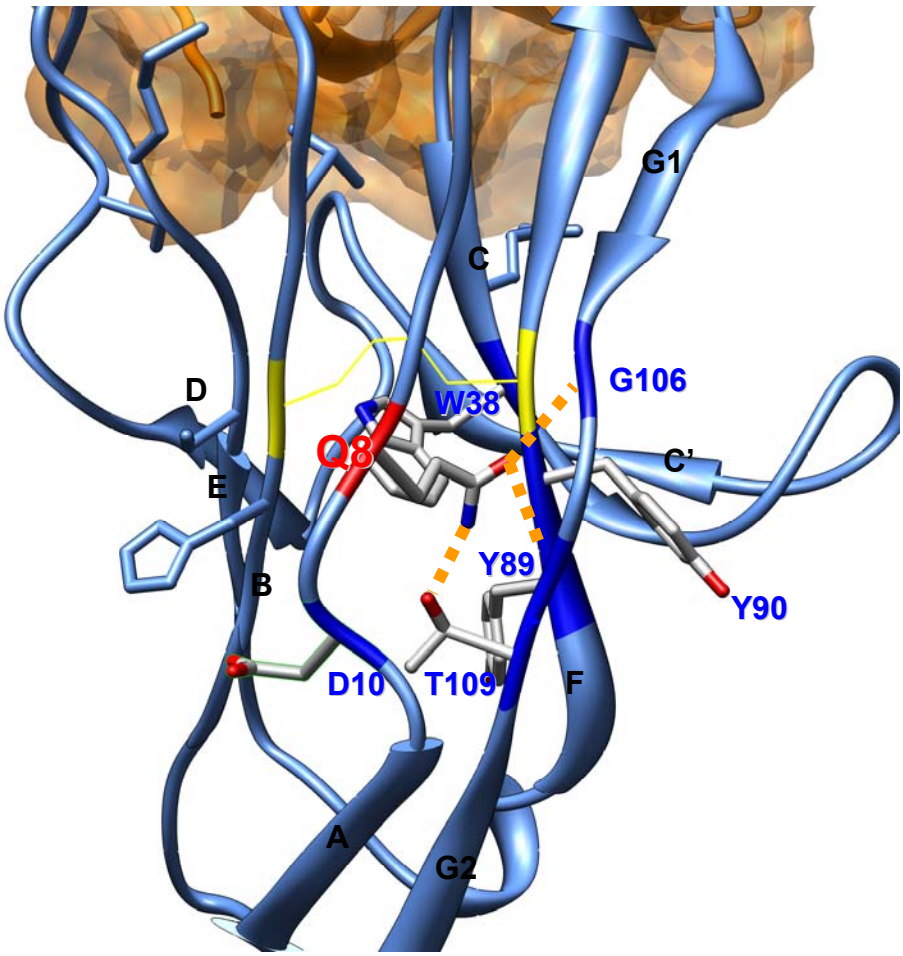

Figure 4-3.

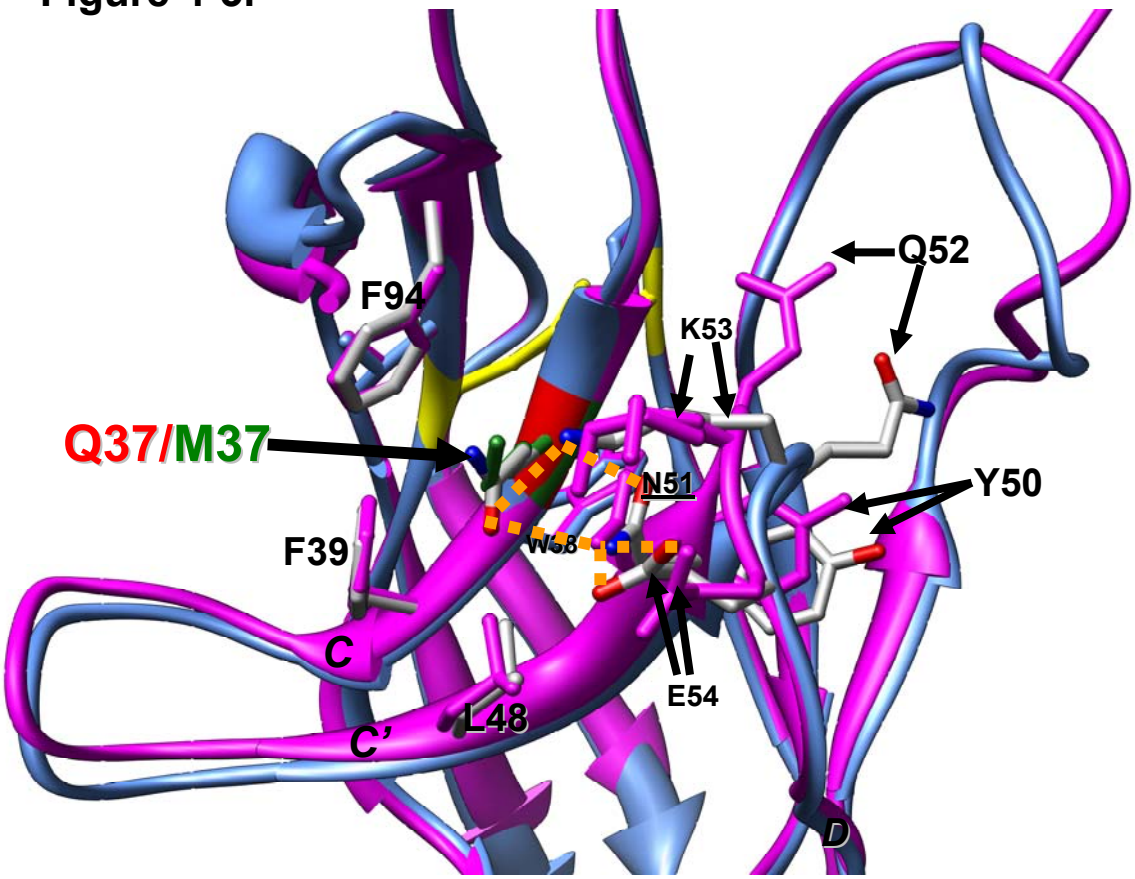

Figure 4-4.

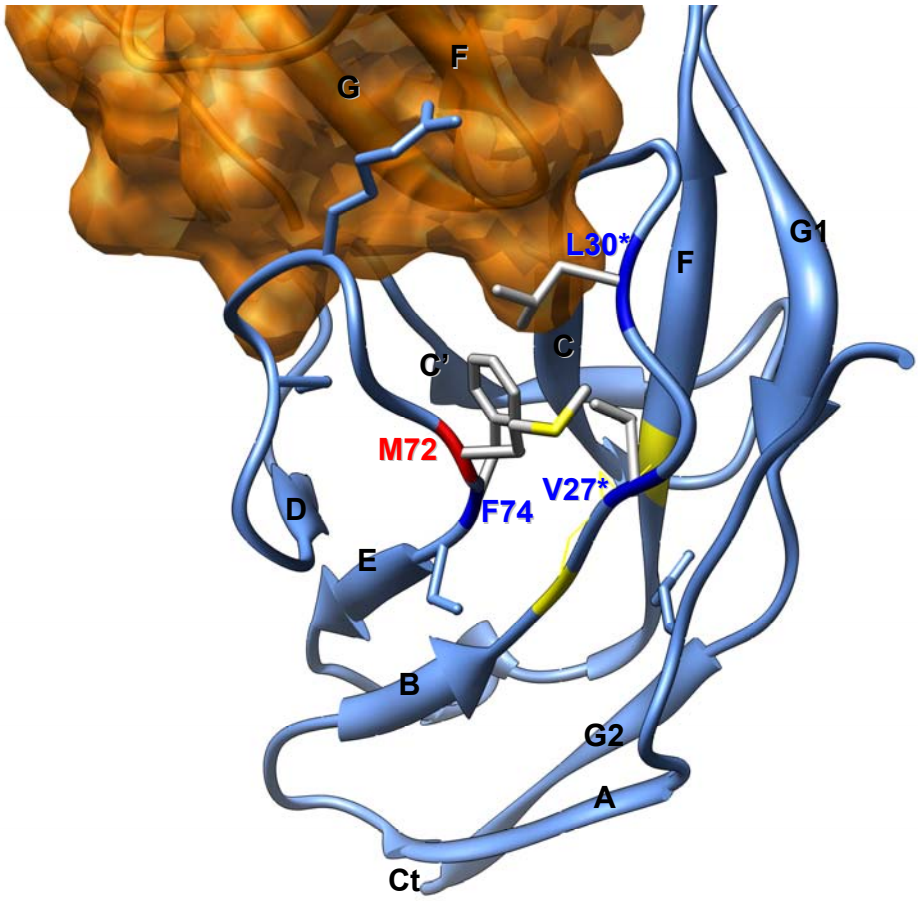

Figure 4-5.

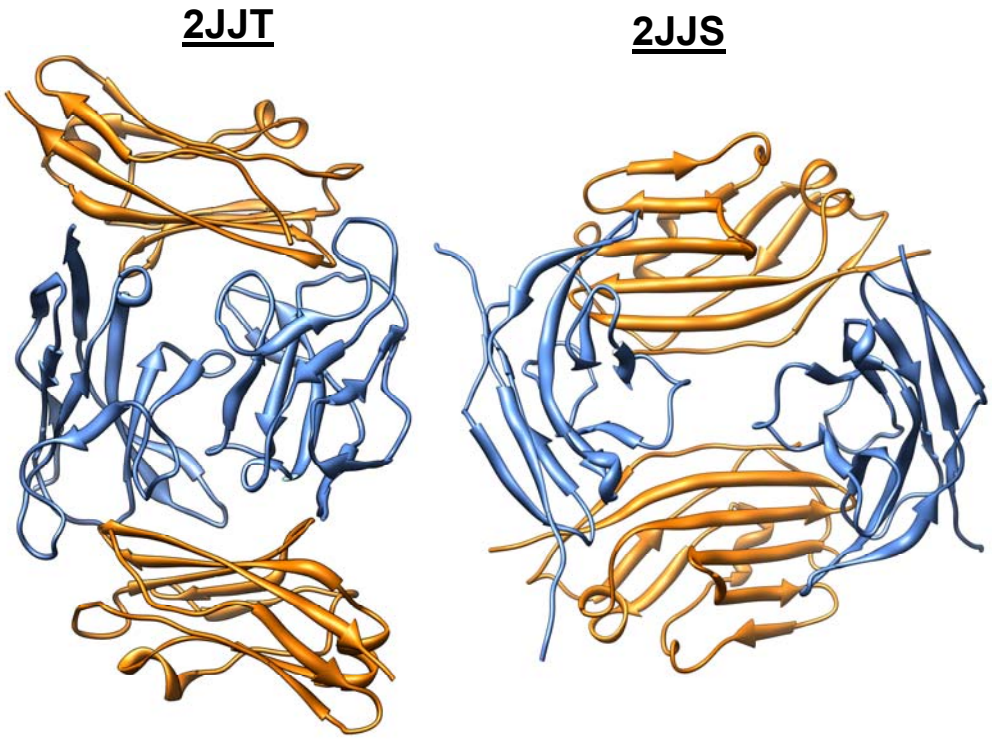

Figure Legends:

Figure 4-1. Our critical residues are distal to the CD47 binding sites on SIRPαD1. Using the crystal structure of SIRPαD1 CD47IgV complex (pdb code: 2JJT), we mapped our critical residues (see Chapter 2) onto SIRPαD1. Except for S66 and R69 and V27, the rest of the critical residues (Q8, Q37, M72, and S75) are not in direct contact with CD47 (orange), suggesting that they are important for the maintenance of conformation. Therefore mutations of these residues abrogate CD47 binding through indirect mechanisms. The residues labeled with * are already discussed in detail by Hatherley et al. The beta strands are denoted in black letters, and the disulfide bonds are colored yellow.

Figure 4-2. Critical residue Q8 is important in maintaining the conformation of strands FG and the packing of the two beta sheets. In this rendering, the critical residue is identified by the red coloring of its peptide backbone, and the residues (blue) that are in direct contact with the critical residues are identified by blue coloring of their peptide backbones. The sidechain of the residues are colored by the elements: oxygen=red, nitrogen=blue, sulfur=yellow, and carbon=white. Potential hydrogen bonds were indicated by dashed lines. The polar groups of Q8 have great potential to form hydrogen with T109 and the backbone of G106 on strand G as well as the backbone of Y89.

Figure 4-3. An alignment of the crystal structures of SIRPαD1 (light blue; pdb code: 2UV3) and SIRPβD1 (magenta; pdb code: 2JJU) to analyze how mutation Q37M in SIRPα abolishes binding to CD47. Q37 (red) on SIRPα and M37 (green) on SIRPβ are essential surround by hydrophobic residues. However, Q37 being charged, can potentially interact with E54, N51, and K53 either through charged or polar interactions (dashed lines). As a result, the conformations of the C'D loops between the two proteins are quite different despite having identical protein sequences. The orientations of sidechains (Y50, Q52, K53) off the C'D loop in SIRPα deviate from SIRPβ. In additional, the analysis by Hatherley et al indicated that the C'D loop contacts CD47 directly.

Figure 4-4. Critical residue M72 interacts with many CD47 contacting residues on SIRPαD1. M72 is in contact with three residues (F74, V27, and L30) through hydrophobic interactions. In particular, the direct interaction of V27 and L30 with the CD47IgV FG loop, a key determinant of the binding interaction, has been described by Hatherley et al. Mutation M72A abolished CD47 binding perhaps by altering the orientation of L30 and V27 due a shortening of the hydrophobic sidechain. This notion is supported by mutation M72L as CD47 binding remains unaffected. Interestingly, mutation M72R enhanced binding to CD47. Arginine although charged at the terminus of its sidechain has sufficient number of aliphatic carbons to maintain the hydrophobic interaction, as well as sufficient length to allow the charged terminus to be sufficiently close to interact with the CD47 N terminal pyroglutamate residue or T102 residues on the FG loop.

Figure 4-5. Transdimerization of SIRPαD1 does not affect the conformation of the CD47IgV binding site on SIRPαD1. Left panel is a crystal structure (2JJT) of SIRPαD1-CD47IgV complex, in which SIRPαD1 is present as a transdimer (with a different configuration of dimerization from SIRPαD1 crystal structure 2uv3). On the right is a different crystal structure of SIRPαD1-CD47IgV complex , in which the SIRPαD1 are not even contacting. Despite the vastly different configuration in dimerization, the conformation of the CD47IgV (orange) and SIRPαD1 (blue) subunits are essential identical, suggesting that dimerization does not affect conformation significantly.

References

1. Taylor, L. S., S. P. Paul, and D. W. McVicar. 2000. Paired inhibitory and activating receptor signals. *Rev Immunogenet* 2:204-219.
2. Lanier, L. L. 2001. Face off--the interplay between activating and inhibitory immune receptors. *Curr Opin Immunol* 13:326-331.
3. Ravetch, J. V., and L. L. Lanier. 2000. Immune inhibitory receptors. *Science* 290:84-89.
4. Lanier, L. L. 2005. NK cell recognition. *Annu Rev Immunol* 23:225-274.
5. Barclay, A. N., and M. H. Brown. 2006. The SIRP family of receptors and immune regulation. *Nat Rev Immunol* 6:457-464.
6. Ravetch, J. V., and S. Bolland. 2001. IgG Fc receptors. *Annu Rev Immunol* 19:275-290.
7. Nimmerjahn, F., and J. V. Ravetch. 2008. Fcgamma receptors as regulators of immune responses. *Nat Rev Immunol* 8:34-47.
8. van Beek, E. M., F. Cochrane, A. N. Barclay, and T. K. van den Berg. 2005. Signal regulatory proteins in the immune system. *J Immunol* 175:7781-7787.
9. Liu, Y., I. Soto, Q. Tong, A. Chin, H. J. Buhring, T. Wu, K. Zen, and C. A. Parkos. 2005. SIRPbeta1 is expressed as a disulfide-linked homodimer in leukocytes and positively regulates neutrophil transepithelial migration. *J Biol Chem* 280:36132-36140.
10. Kharitonenkov, A., Z. Chen, I. Sures, H. Wang, J. Schilling, and A. Ullrich. 1997. A family of proteins that inhibit signalling through tyrosine kinase receptors. *Nature* 386:181-186.
11. Tomasello, E., C. Cant, H. J. Buhring, F. Vely, P. Andre, M. Seiffert, A. Ullrich, and E. Vivier. 2000. Association of signal-regulatory proteins beta with KARAP/DAP-12. *Eur J Immunol* 30:2147-2156.
12. Dietrich, J., M. Cella, M. Seiffert, H. J. Buhring, and M. Colonna. 2000. Cutting edge: signal-regulatory protein beta 1 is a DAP12-associated activating receptor expressed in myeloid cells. *J Immunol* 164:9-12.
13. Brooke, G., J. D. Holbrook, M. H. Brown, and A. N. Barclay. 2004. Human lymphocytes interact directly with CD47 through a novel member of the signal regulatory protein (SIRP) family. *J Immunol* 173:2562-2570.
14. Jiang, P., C. F. Lagenaur, and V. Narayanan. 1999. Integrin-associated protein is a ligand for the P84 neural adhesion molecule. *J Biol Chem* 274:559-562.
15. Umemori, H., and J. R. Sanes. 2008. Signal regulatory proteins (SIRPs) are secreted presynaptic organizing molecules. *J. Biol. Chem.*:M805729200.
16. Liu, Y., S. K. Shaw, S. Ma, L. Yang, F. W. Luscinskas, and C. A. Parkos. 2004. Regulation of leukocyte transmigration: cell surface interactions and signaling events. *J Immunol* 172:7-13.
17. Seiffert, M., C. Cant, Z. Chen, I. Rappold, W. Brugger, L. Kanz, E. J. Brown, A. Ullrich, and H. J. Buhring. 1999. Human signal-regulatory protein is expressed on normal, but not on subsets of leukemic myeloid

cells and mediates cellular adhesion involving its counterreceptor CD47. *Blood* 94:3633-3643.
18. Oldenborg, P. A., H. D. Gresham, and F. P. Lindberg. 2001. CD47-signal regulatory protein alpha (SIRPalpha) regulates Fcgamma and complement receptor-mediated phagocytosis. *J Exp Med* 193:855-862.
19. Miyashita, M., H. Ohnishi, H. Okazawa, H. Tomonaga, A. Hayashi, T. T. Fujimoto, N. Furuya, and T. Matozaki. 2004. Promotion of neurite and filopodium formation by CD47: roles of integrins, Rac, and Cdc42. *Mol Biol Cell* 15:3950-3963.
20. Ohnishi, H., Y. Kaneko, H. Okazawa, M. Miyashita, R. Sato, A. Hayashi, K. Tada, S. Nagata, M. Takahashi, and T. Matozaki. 2005. Differential localization of Src homology 2 domain-containing protein tyrosine phosphatase substrate-1 and CD47 and its molecular mechanisms in cultured hippocampal neurons. *J Neurosci* 25:2702-2711.
21. Veillette, A., E. Thibaudeau, and S. Latour. 1998. High Expression of Inhibitory Receptor SHPS-1 and Its Association with Protein-tyrosine Phosphatase SHP-1 in Macrophages. 22719-22728.
22. Schakel, K., M. von Kietzell, A. Hansel, A. Ebling, L. Schulze, M. Haase, C. Semmler, M. Sarfati, A. N. Barclay, G. J. Randolph, M. Meurer, and E. P. Rieber. 2006. Human 6-sulfo LacNAc-expressing dendritic cells are principal producers of early interleukin-12 and are controlled by erythrocytes. *Immunity* 24:767-777.
23. Braun, D., L. Galibert, T. Nakajima, H. Saito, V. V. Quang, M. Rubio, and M. Sarfati. 2006. Semimature stage: a checkpoint in a dendritic cell maturation program that allows for functional reversion after signal-regulatory protein-alpha ligation and maturation signals. *J Immunol* 177:8550-8559.
24. Ling, Y., L. A. Maile, J. Lieskovska, J. Badley-Clarke, and D. R. Clemmons. 2005. Role of SHPS-1 in the regulation of insulin-like growth factor I-stimulated Shc and mitogen-activated protein kinase activation in vascular smooth muscle cells. *Mol Biol Cell* 16:3353-3364.
25. Maile, L. A., and D. R. Clemmons. 2002. Regulation of insulin-like growth factor I receptor dephosphorylation by SHPS-1 and the tyrosine phosphatase SHP-2. *J Biol Chem* 277:8955-8960.
26. Johansen, M. L., and E. J. Brown. 2007. Dual regulation of SIRPalpha phosphorylation by integrins and CD47. *J Biol Chem* 282:24219-24230.
27. Stefanidakis, M., G. Newton, W. Y. Lee, C. A. Parkos, and F. W. Luscinskas. 2008. Endothelial CD47 interaction with SIRPgamma is required for human T-cell transendothelial migration under shear flow conditions in vitro. *Blood* 112:1280-1289.
28. Brown, E. J., and W. A. Frazier. 2001. Integrin-associated protein (CD47) and its ligands. *Trends Cell Biol* 11:130-135.
29. Hynes, R. O. 2002. Integrins: bidirectional, allosteric signaling machines. *Cell* 110:673-687.
30. Lamy, L., M. Ticchioni, A. K. Rouquette-Jazdanian, M. Samson, M. Deckert, A. H. Greenberg, and A. Bernard. 2003. CD47 and the 19 kDa

interacting protein-3 (BNIP3) in T cell apoptosis. *J Biol Chem* 278:23915-23921.

31. Manna, P. P., and W. A. Frazier. 2003. The mechanism of CD47-dependent killing of T cells: heterotrimeric Gi-dependent inhibition of protein kinase A. *J Immunol* 170:3544-3553.
32. Mateo, V., E. J. Brown, G. Biron, M. Rubio, A. Fischer, F. L. Deist, and M. Sarfati. 2002. Mechanisms of CD47-induced caspase-independent cell death in normal and leukemic cells: link between phosphatidylserine exposure and cytoskeleton organization. *Blood* 100:2882-2890.
33. Mateo, V., L. Lagneaux, D. Bron, G. Biron, M. Armant, G. Delespesse, and M. Sarfati. 1999. CD47 ligation induces caspase-independent cell death in chronic lymphocytic leukemia. *Nat Med* 5:1277-1284.
34. Pettersen, R. D., K. Hestdal, M. K. Olafsen, S. O. Lie, and F. P. Lindberg. 1999. CD47 signals T cell death. *J Immunol* 162:7031-7040.
35. Roue, G., N. Bitton, V. J. Yuste, T. Montange, M. Rubio, F. Dessauge, C. Delettre, H. Merle-Beral, M. Sarfati, and S. A. Susin. 2003. Mitochondrial dysfunction in CD47-mediated caspase-independent cell death: ROS production in the absence of cytochrome c and AIF release. *Biochimie* 85:741-746.
36. Frazier, W. A., A. G. Gao, J. Dimitry, J. Chung, E. J. Brown, F. P. Lindberg, and M. E. Linder. 1999. The thrombospondin receptor integrin-associated protein (CD47) functionally couples to heterotrimeric Gi. *J Biol Chem* 274:8554-8560.
37. Cooper, D., F. P. Lindberg, J. R. Gamble, E. J. Brown, and M. A. Vadas. 1995. Transendothelial migration of neutrophils involves integrin-associated protein (CD47). *Proc Natl Acad Sci U S A* 92:3978-3982.
38. Wu, A. L., J. Wang, A. Zheleznyak, and E. J. Brown. 1999. Ubiquitin-related proteins regulate interaction of vimentin intermediate filaments with the plasma membrane. *Mol Cell* 4:619-625.
39. N'Diaye, E. N., and E. J. Brown. 2003. The ubiquitin-related protein PLIC-1 regulates heterotrimeric G protein function through association with Gbetagamma. *J Cell Biol* 163:1157-1165.
40. Dahl, K. N., C. M. Westhoff, and D. E. Discher. 2003. Fractional attachment of CD47 (IAP) to the erythrocyte cytoskeleton and visual colocalization with Rh protein complexes. *Blood* 101:1194-1199.
41. Subramanian, S., R. Tsai, S. Sen, K. N. Dahl, and D. E. Discher. 2006. Membrane mobility and clustering of Integrin Associated Protein (IAP, CD47)--major differences between mouse and man and implications for signaling. *Blood cells, molecules & diseases* 36:364-372.
42. Gardai, S. J., Y. Q. Xiao, M. Dickinson, J. A. Nick, D. R. Voelker, K. E. Greene, and P. M. Henson. 2003. By binding SIRPalpha or calreticulin/CD91, lung collectins act as dual function surveillance molecules to suppress or enhance inflammation. *Cell* 115:13-23.
43. Wright, J. R. 2005. Immunoregulatory functions of surfactant proteins. *Nat Rev Immunol* 5:58-68.

44. Sano, H., and Y. Kuroki. 2005. The lung collectins, SP-A and SP-D, modulate pulmonary innate immunity. *Mol Immunol* 42:279-287.
45. Vandivier, R. W., C. A. Ogden, V. A. Fadok, P. R. Hoffmann, K. K. Brown, M. Botto, M. J. Walport, J. H. Fisher, P. M. Henson, and K. E. Greene. 2002. Role of surfactant proteins A, D, and C1q in the clearance of apoptotic cells in vivo and in vitro: calreticulin and CD91 as a common collectin receptor complex. *J Immunol* 169:3978-3986.
46. Gardai, S. J., K. A. McPhillips, S. C. Frasch, W. J. Janssen, A. Starefeldt, J. E. Murphy-Ullrich, D. L. Bratton, P. A. Oldenborg, M. Michalak, and P. M. Henson. 2005. Cell-surface calreticulin initiates clearance of viable or apoptotic cells through trans-activation of LRP on the phagocyte. *Cell* 123:321-334.
47. Smith, R. E., V. Patel, S. D. Seatter, M. R. Deehan, M. H. Brown, G. P. Brooke, H. S. Goodridge, C. J. Howard, K. P. Rigley, W. Harnett, and M. M. Harnett. 2003. A novel MyD-1 (SIRP-1alpha) signaling pathway that inhibits LPS-induced TNFalpha production by monocytes. *Blood* 102:2532-2540.
48. Miyake, A., Y. Murata, H. Okazawa, H. Ikeda, Y. Niwayama, H. Ohnishi, Y. Hirata, and T. Matozaki. 2008. Negative regulation by SHPS-1 of Toll-like receptor-dependent proinflammatory cytokine production in macrophages. *Genes Cells* 13:209-219.
49. Okazawa, H., S. Motegi, N. Ohyama, H. Ohnishi, T. Tomizawa, Y. Kaneko, P. A. Oldenborg, O. Ishikawa, and T. Matozaki. 2005. Negative regulation of phagocytosis in macrophages by the CD47-SHPS-1 system. *J Immunol* 174:2004-2011.
50. de Vries, H. E., J. J. Hendriks, H. Honing, C. R. De Lavalette, S. M. van der Pol, E. Hooijberg, C. D. Dijkstra, and T. K. van den Berg. 2002. Signal-regulatory protein alpha-CD47 interactions are required for the transmigration of monocytes across cerebral endothelium. *J Immunol* 168:5832-5839.
51. Liu, Y., H. J. Buhring, K. Zen, S. L. Burst, F. J. Schnell, I. R. Williams, and C. A. Parkos. 2002. Signal regulatory protein (SIRPalpha), a cellular ligand for CD47, regulates neutrophil transmigration. *J Biol Chem* 277:10028-10036.
52. Lindberg, F. P., D. C. Bullard, T. E. Caver, H. D. Gresham, A. L. Beaudet, and E. J. Brown. 1996. Decreased resistance to bacterial infection and granulocyte defects in IAP-deficient mice. *Science* 274:795-798.
53. Oldenborg, P. A., A. Zheleznyak, Y. F. Fang, C. F. Lagenaur, H. D. Gresham, and F. P. Lindberg. 2000. Role of CD47 as a marker of self on red blood cells. *Science* 288:2051-2054.
54. Yamao, T., T. Noguchi, O. Takeuchi, U. Nishiyama, H. Morita, T. Hagiwara, H. Akahori, T. Kato, K. Inagaki, H. Okazawa, Y. Hayashi, T. Matozaki, K. Takeda, S. Akira, and M. Kasuga. 2002. Negative regulation of platelet clearance and of the macrophage phagocytic response by the transmembrane glycoprotein SHPS-1. *J Biol Chem* 277:39833-39839.

55. Ishikawa-Sekigami, T., Y. Kaneko, H. Okazawa, T. Tomizawa, J. Okajo, Y. Saito, C. Okuzawa, M. Sugawara-Yokoo, U. Nishiyama, H. Ohnishi, T. Matozaki, and Y. Nojima. 2006. SHPS-1 promotes the survival of circulating erythrocytes through inhibition of phagocytosis by splenic macrophages. *Blood* 107:341-348.
56. Ide, K., H. Wang, H. Tahara, J. Liu, X. Wang, T. Asahara, M. Sykes, Y. G. Yang, and H. Ohdan. 2007. Role for CD47-SIRPalpha signaling in xenograft rejection by macrophages. *Proc Natl Acad Sci U S A* 104:5062-5066.
57. Wang, H., J. VerHalen, M. L. Madariaga, S. Xiang, S. Wang, P. Lan, P. A. Oldenborg, M. Sykes, and Y. G. Yang. 2007. Attenuation of phagocytosis of xenogeneic cells by manipulating CD47. *Blood* 109:836-842.
58. Subramanian, S., E. T. Boder, and D. E. Discher. 2007. Phylogenetic divergence of CD47 interactions with human signal regulatory protein alpha reveals locus of species specificity. Implications for the binding site. *J Biol Chem* 282:1805-1818.
59. Takenaka, K., T. K. Prasolava, J. C. Wang, S. M. Mortin-Toth, S. Khalouei, O. I. Gan, J. E. Dick, and J. S. Danska. 2007. Polymorphism in Sirpa modulates engraftment of human hematopoietic stem cells. *Nat Immunol* 8:1313-1323.
60. van den Nieuwenhof, I. M., C. Renardel de Lavalette, N. Diaz, I. van Die, and T. K. van den Berg. 2001. Differential galactosylation of neuronal and haematopoietic signal regulatory protein-alpha determines its cellular binding-specificity. *J Cell Sci* 114:1321-1329.
61. Subramanian, S., R. Parthasarathy, S. Sen, E. T. Boder, and D. E. Discher. 2006. Species- and cell type-specific interactions between CD47 and human SIRPalpha. *Blood* 107:2548-2556.
62. Ogura, T., T. Noguchi, R. Murai-Takebe, T. Hosooka, N. Honma, and M. Kasuga. 2004. Resistance of B16 melanoma cells to CD47-induced negative regulation of motility as a result of aberrant N-glycosylation of SHPS-1. *J Biol Chem* 279:13711-13720.
63. Lee, W. Y., D. A. Weber, O. Laur, E. A. Severson, I. McCall, R. P. Jen, A. C. Chin, T. Wu, K. M. Gernert, and C. A. Parkos. 2007. Novel structural determinants on SIRP alpha that mediate binding to CD47. *J Immunol* 179:7741-7750.
64. Vernon-Wilson, E. F., W. J. Kee, A. C. Willis, A. N. Barclay, D. L. Simmons, and M. H. Brown. 2000. CD47 is a ligand for rat macrophage membrane signal regulatory protein SIRP (OX41) and human SIRPalpha 1. *Eur J Immunol* 30:2130-2137.
65. Seiffert, M., P. Brossart, C. Cant, M. Cella, M. Colonna, W. Brugger, L. Kanz, A. Ullrich, and H. J. Buhring. 2001. Signal-regulatory protein alpha (SIRPalpha) but not SIRPbeta is involved in T-cell activation, binds to CD47 with high affinity, and is expressed on immature CD34(+)CD38(-) hematopoietic cells. *Blood* 97:2741-2749.
66. Nakaishi, A., M. Hirose, M. Yoshimura, C. Oneyama, K. Saito, N. Kuki, M. Matsuda, N. Honma, H. Ohnishi, T. Matozaki, M. Okada, and A.

Nakagawa. 2008. Structural insight into the specific interaction between murine SHPS-1/SIRP alpha and its ligand CD47. *Journal of molecular biology* 375:650-660.

67. Hatherley, D., K. Harlos, D. C. Dunlop, D. I. Stuart, and A. N. Barclay. 2007. The structure of the macrophage signal regulatory protein alpha (SIRPalpha) inhibitory receptor reveals a binding face reminiscent of that used by T cell receptors. *J Biol Chem* 282:14567-14575.
68. Hatherley, D., S. C. Graham, J. Turner, K. Harlos, D. I. Stuart, and A. N. Barclay. 2008. Paired receptor specificity explained by structures of signal regulatory proteins alone and complexed with CD47. *Mol Cell* 31:266-277.
69. Liu, Y., Q. Tong, Y. Zhou, H. W. Lee, J. J. Yang, H. J. Buhring, Y. T. Chen, B. Ha, C. X. Chen, Y. Yang, and K. Zen. 2007. Functional elements on SIRPalpha IgV domain mediate cell surface binding to CD47. *Journal of molecular biology* 365:680-693.
70. Mawby, W. J., C. H. Holmes, D. J. Anstee, F. A. Spring, and M. J. Tanner. 1994. Isolation and characterization of CD47 glycoprotein: a multispanning membrane protein which is the same as integrin-associated protein (IAP) and the ovarian tumour marker OA3. *Biochem J* 304 (Pt 2):525-530.
71. Kong, X.-N., H.-X. Yan, L. Chen, L.-W. Dong, W. Yang, Q. Liu, L.-X. Yu, D.-D. Huang, S.-Q. Liu, H. Liu, M.-C. Wu, and H.-Y. Wang. 2007. LPS-induced down-regulation of signal regulatory protein {alpha} contributes to innate immune activation in macrophages. *J. Exp. Med.* 204:2719-2731.
72. Ohnishi, H., H. Kobayashi, H. Okazawa, Y. Ohe, K. Tomizawa, R. Sato, and T. Matozaki. 2004. Ectodomain shedding of SHPS-1 and its role in regulation of cell migration. *J Biol Chem* 279:27878-27887.
73. Tsai, R. K., and D. E. Discher. 2008. Inhibition of "self" engulfment through deactivation of myosin-II at the phagocytic synapse between human cells. *J Cell Biol* 180:989-1003.
74. Elkabetz, Y., A. Ofir, Y. Argon, and S. Bar-Nun. 2008. Alternative pathways of disulfide bond formation yield secretion-competent, stable and functional immunoglobulins. *Mol Immunol*.
75. Leitzgen, K., M. R. Knittler, and I. G. Haas. 1997. Assembly of immunoglobulin light chains as a prerequisite for secretion. A model for oligomerization-dependent subunit folding. *J Biol Chem* 272:3117-3123.
76. Chothia, C., J. Novotny, R. Bruccoleri, and M. Karplus. 1985. Domain association in immunoglobulin molecules. The packing of variable domains. *Journal of molecular biology* 186:651-663.
77. Chin, A. C., and C. A. Parkos. 2006. Neutrophil transepithelial migration and epithelial barrier function in IBD: potential targets for inhibiting neutrophil trafficking. *Ann N Y Acad Sci* 1072:276-287.
78. Parkos, C. A., S. P. Colgan, T. W. Liang, A. Nusrat, A. E. Bacarra, D. K. Carnes, and J. L. Madara. 1996. CD47 mediates post-adhesive events required for neutrophil migration across polarized intestinal epithelia. *J Cell Biol* 132:437-450.
79. Liu, Y., D. Merlin, S. L. Burst, M. Pochet, J. L. Madara, and C. A. Parkos. 2001. The role of CD47 in neutrophil transmigration. Increased rate of

migration correlates with increased cell surface expression of CD47. *J Biol Chem* 276:40156-40166.
80. Maile, L. A., J. Badley-Clarke, and D. R. Clemmons. 2003. The association between integrin-associated protein and SHPS-1 regulates insulin-like growth factor-I receptor signaling in vascular smooth muscle cells. *Mol Biol Cell* 14:3519-3528.
81. Oldenborg, P. A. 2004. Role of CD47 in erythroid cells and in autoimmunity. *Leukemia & lymphoma* 45:1319-1327.
82. Olsson, M., A. Nilsson, and P. A. Oldenborg. 2006. Target cell CD47 regulates macrophage activation and erythrophagocytosis. *Transfus Clin Biol* 13:39-43.
83. Olsson, M., P. Bruhns, W. A. Frazier, J. V. Ravetch, and P. A. Oldenborg. 2005. Platelet homeostasis is regulated by platelet expression of CD47 under normal conditions and in passive immune thrombocytopenia. *Blood* 105:3577-3582.
84. Liu, Y., A. Nusrat, F. J. Schnell, T. A. Reaves, S. Walsh, M. Pochet, and C. A. Parkos. 2000. Human junction adhesion molecule regulates tight junction resealing in epithelia. 2363-2374.
85. Horton, R. M., H. D. Hunt, S. N. Ho, J. K. Pullen, and L. R. Pease. 1989. Engineering hybrid genes without the use of restriction enzymes: gene splicing by overlap extension. *Gene* 77:61-68.
86. Weber, D. A., C. T. Dao, J. Jun, J. L. Wigal, and P. E. Jensen. 2001. Transmembrane Domain-Mediated Colocalization of HLA-DM and HLA-DR Is Required for Optimal HLA-DM Catalytic Activity. 5167-5174.
87. Marchler-Bauer, A., J. B. Anderson, P. F. Cherukuri, C. DeWeese-Scott, L. Y. Geer, M. Gwadz, S. He, D. I. Hurwitz, J. D. Jackson, Z. Ke, C. J. Lanczycki, C. A. Liebert, C. Liu, F. Lu, G. H. Marchler, M. Mullokandov, B. A. Shoemaker, V. Simonyan, J. S. Song, P. A. Thiessen, R. A. Yamashita, J. J. Yin, D. Zhang, and S. H. Bryant. 2005. CDD: a Conserved Domain Database for protein classification. *Nucleic Acids Res* 33:D192-196.
88. Zdanov, A., Y. Li, D. R. Bundle, S. Deng, C. R. MacKenzie, S. A. Narang, N. M. Young, and M. Cygler. 1994. Structure of a Single-Chain Antibody Variable Domain (Fv) Fragment Complexed with a Carbohydrate Antigen at 1.7-A Resolution. *PNAS* 91:6423-6427.
89. Fiser, A., and A. Sali. 2003. Modeller: generation and refinement of homology-based protein structure models. *Methods Enzymol* 374:461-491.
90. Shen, M. Y., and A. Sali. 2006. Statistical potential for assessment and prediction of protein structures. *Protein Sci* 15:2507-2524.
91. Pettersen, E. F., T. D. Goddard, C. C. Huang, G. S. Couch, D. M. Greenblatt, E. C. Meng, and T. E. Ferrin. 2004. UCSF Chimera--a visualization system for exploratory research and analysis. *Journal of computational chemistry* 25:1605-1612.
92. Meng, E. C., E. F. Pettersen, G. S. Couch, C. C. Huang, and T. E. Ferrin. 2006. Tools for integrated sequence-structure analysis with UCSF Chimera. *BMC bioinformatics* 7:339.

93. Thompson, J. D., D. G. Higgins, and T. J. Gibson. 1994. CLUSTAL W: improving the sensitivity of progressive multiple sequence alignment through sequence weighting, position-specific gap penalties and weight matrix choice. *Nucleic Acids Res* 22:4673-4680.
94. Viertlboeck, B. C., R. Schmitt, and T. W. Gobel. 2006. The chicken immunoregulatory receptor families SIRP, TREM, and CMRF35/CD300L. *Immunogenetics* 58:180-190.
95. van den Berg, T. K., J. A. Yoder, and G. W. Litman. 2004. On the origins of adaptive immunity: innate immune receptors join the tale. *Trends Immunol* 25:11-16.
96. Maile, L. A., B. E. Capps, E. C. Miller, A. W. Aday, and D. R. Clemmons. 2008. Integrin-associated protein association with SRC homology 2 domain containing tyrosine phosphatase substrate 1 regulates igf-I signaling in vivo. *Diabetes* 57:2637-2643.
97. Dong, L. W., X. N. Kong, H. X. Yan, L. X. Yu, L. Chen, W. Yang, Q. Liu, D. D. Huang, M. C. Wu, and H. Y. Wang. 2008. Signal regulatory protein alpha negatively regulates both TLR3 and cytoplasmic pathways in type I interferon induction. *Mol Immunol* 45:3025-3035.
98. Lee, W. Y., A. C. Chin, S. Voss, and C. A. Parkos. 2006. In vitro neutrophil transepithelial migration. *Methods Mol Biol* 341:205-215.
99. Mahoney, W. C., and D. Duksin. 1979. Biological activities of the two major components of tunicamycin. *J. Biol. Chem.* 254:6572-6576.
100. Dorner, A. J., D. G. Bole, and R. J. Kaufman. 1987. The relationship of N-linked glycosylation and heavy chain-binding protein association with the secretion of glycoproteins. *J. Cell Biol.* 105:2665-2674.
101. Elbein, A. D., J. E. Tropea, M. Mitchell, and G. P. Kaushal. 1990. Kifunensine, a potent inhibitor of the glycoprotein processing mannosidase I. *J. Biol. Chem.* 265:15599-15605.
102. Cummings, R. D., I. S. Trowbridge, and S. Kornfeld. 1982. A mouse lymphoma cell line resistant to the leukoagglutinating lectin from Phaseolus vulgaris is deficient in UDP-GlcNAc: alpha-D-mannoside beta 1,6 N-acetylglucosaminyltransferase. *J. Biol. Chem.* 257:13421-13427.
103. Demetriou, M., M. Granovsky, S. Quaggin, and J. W. Dennis. 2001. Negative regulation of T-cell activation and autoimmunity by Mgat5 N-glycosylation. *Nature* 409:733-739.
104. Feinberg, H., S. Park-Snyder, A. R. Kolatkar, C. T. Heise, M. E. Taylor, and W. I. Weis. 2000. Structure of a C-type carbohydrate recognition domain from the macrophage mannose receptor. *J Biol Chem* 275:21539-21548.
105. Stowell, S. R., C. M. Arthur, K. A. Slanina, J. R. Horton, D. F. Smith, and R. D. Cummings. 2008. Dimeric Galectin-8 induces phosphatidylserine exposure in leukocytes through polylactosamine recognition by the C-terminal domain. *J Biol Chem* 283:20547-20559.
106. Demotte, N., V. Stroobant, P. J. Courtoy, P. Van Der Smissen, D. Colau, I. F. Luescher, C. Hivroz, J. Nicaise, J. L. Squifflet, M. Mourad, D. Godelaine, T. Boon, and P. van der Bruggen. 2008. Restoring the association of the T

cell receptor with CD8 reverses anergy in human tumor-infiltrating lymphocytes. *Immunity* 28:414-424.
107. Nagayama, Y., H. Namba, N. Yokoyama, S. Yamashita, and M. Niwa. 1998. Role of Asparagine-linked Oligosaccharides in Protein Folding, Membrane Targeting, and Thyrotropin and Autoantibody Binding of the Human Thyrotropin Receptor. *J. Biol. Chem.* 273:33423-33428.
108. Finn, R. D., J. Tate, J. Mistry, P. C. Coggill, S. J. Sammut, H.-R. Hotz, G. Ceric, K. Forslund, S. R. Eddy, E. L. L. Sonnhammer, and A. Bateman. 2008. The Pfam protein families database. *Nucl. Acids Res.* 36:D281-288.
109. Lopez, M., M. Aoubala, F. Jordier, D. Isnardon, S. Gomez, and P. Dubreuil. 1998. The Human Poliovirus Receptor Related 2 Protein Is a New Hematopoietic/Endothelial Homophilic Adhesion Molecule. *Blood* 92:4602-4611.
110. Padlan, E. A. 1994. Anatomy of the antibody molecule. *Mol Immunol* 31:169-217.
111. Alzari, P. M., M. B. Lascombe, and R. J. Poljak. 1988. Three-dimensional structure of antibodies. *Annu Rev Immunol* 6:555-580.
112. Jimenez, D., P. Roda-Navarro, T. A. Springer, and J. M. Casasnovas. 2005. Contribution of N-Linked Glycans to the Conformation and Function of Intercellular Adhesion Molecules (ICAMs). *J. Biol. Chem.* 280:5854-5861.
113. Wyss, D. F., J. S. Choi, J. Li, M. H. Knoppers, K. J. Willis, A. R. Arulanandam, A. Smolyar, E. L. Reinherz, and G. Wagner. 1995. Conformation and function of the N-linked glycan in the adhesion domain of human CD2. *Science* 269:1273-1278.
114. Johansen, M. L., and E. J. Brown. 2007. Dual Regulation of SIRP{alpha} Phosphorylation by Integrins and CD47. *J. Biol. Chem.* 282:24219-24230.
115. Sharpe, A. H., and G. J. Freeman. 2002. The B7-CD28 superfamily. *Nat Rev Immunol* 2:116-126.
116. Smith, J. A. 1994. Neutrophils, host defense, and inflammation: a double-edged sword. *J Leukoc Biol* 56:672-686.
117. Binder, R., A. Kress, G. Kan, K. Herrmann, and M. Kirschfink. 1999. Neutrophil priming by cytokines and vitamin D binding protein (Gc-globulin): impact on C5a-mediated chemotaxis, degranulation and respiratory burst. *Mol Immunol* 36:885-892.
118. Binder, R., A. Kress, and M. Kirschfink. 1999. Modulation of C5a-mediated effector functions of human polymorphonuclear leukocytes by tumor necrosis factor alpha and granulocyte macrophage colony-stimulating factor. *Exp Clin Immunogenet* 16:212-225.
119. Snyderman, R., and M. C. Pike. 1984. Chemoattractant receptors on phagocytic cells. *Annu Rev Immunol* 2:257-281.
120. Brown, S., I. Heinisch, E. Ross, K. Shaw, C. D. Buckley, and J. Savill. 2002. Apoptosis disables CD31-mediated cell detachment from phagocytes promoting binding and engulfment. *Nature* 418:200-203.